



**Politecnico
di Torino**

Politecnico di Torino

Master's Degree in Civil Engineering

Master's Degree Thesis

The Design of GFRP Micropile

supervisor:
Prof. Alessandro Pasquale Fantilli.
Dott. Ing Renato Barra.

Candidate:
Omar Ahmed Mohammed Zeenelabdeen Sakr

Contents

1. Chapter 1: Introduction.	9
1.1 Objective of the thesis.....	13
1.2 Structure of the thesis.....	14
2. Chapter 2: The use of GFRP in substitution of steel in RC structures.	15
2.1 Steel Limitations	15
2.1.1 corrosion resistance.....	15
2.1.1.1 Corrosion Causes	15
2.1.1.2 Corrosion types.....	17
2.1.2 Production cost.....	17
2.1.3 Sustainability	18
2.1.4 Steel as a non-renewable material.....	18
2.2 Substitution of steel reinforcement.....	18
2.2.1 What is GFRP Reinforcement.....	19
2.2.2 GFRP bar properties.....	20
2.2.3 Structure elements reinforced with GFRP:.....	24
2.2.4 Projects with GFRP application.....	25
2.2.5 GFRP in Corrosion problem.....	28
2.2.6 GFRP Economic solution	28
2.2.7 Sustainability using GFRP.....	28
2.2.8 FRP reinforcement disadvantages.....	29
3. Chapter 3: Traditional micropiles design.	31
3.1 Advantages and uses of micropiles.....	31
3.2 Micropile types due to Grout Placement Techniques.....	32
3.3 Micropile design.....	33
3.4 Verification scheme.....	33
3.4.1 Load combinations.....	33
3.5 Micropile bearing capacity	35
3.5.1 Geotechnical design	37
3.5.1.1 Geotechnical investigation requirements.....	37
3.5.1.2 Geotechnical design procedure.....	37
3.5.2 Structural design.....	42
3.5.2.1 Evaluate allowable compression load for cased length	42
3.5.2.1.1 Strain compatibility between grout, casing, and reinforcing rod.	42
3.5.2.2 Evaluate allowable tension load for cased length	42
3.5.3 Evaluate combined axial and flexural strength:.....	42
4. Chapter 4: Elements design in glass fiber reinforced polymers.	45

4.1	GFRP micropiles geotechnical design.....	47
4.2	GFRP micropiles structural design.....	47
4.2.1	Evaluate allowable compression strength for GFRP Cased micropile	47
4.2.1.1	Strain compatibility between grout, casing.	47
4.2.2	Evaluate allowable tension strength of GFRP Cased micropiles	47
4.2.3	Evaluate combined axial compression and bending GFRP cased micropiles.....	48
5.	Chapter 5: study case.	49
5.1	Proposed solutions	52
5.1.1	Solution (1):	52
5.1.2	Solution (2):	53
5.1.3	Solution (3):	54
5.1.4	Solution (4)	55
5.1.5	Solution (5):	56
5.1.6	Solution (6):	57
5.2	Project description	59
5.3	Project materials	60
5.4	Applied loads	61
5.5	Loads combinations	66
5.5.1	Static analysis:.....	66
5.5.1.1	SLU approach [1] combination (A1+M1+R1).....	66
5.5.1.2	SLU approach [2] combination (A2+M2+R1).....	66
5.5.1.3	SLV combination (A=1+M=1+R1).....	67
5.6	Verification	68
5.6.1	Traditional steel micropile verification	69
5.6.1.1	Analysis of approach [1] combination.....	69
5.6.1.1.1	approach [1] Phase (1) results	69
5.6.1.1.2	Approach [1] Phase (2) results	73
5.6.1.1.3	Approach [1] internal actions envelope.....	77
5.6.1.2	Verification state approach [1] combination	79
5.6.1.2.1	Approach [1] verification Phase (1).....	79
5.6.1.2.2	Approach [1] verification Phase (2).....	82
5.6.1.3	Analysis of approach [2] combination.....	85
5.6.1.3.1	Approach [2] phase (1) results	85
5.6.1.3.2	Approach [2] phase (2) results	89
5.6.1.3.3	Approach [2] internal actions envelope.....	93
5.6.1.4	Verification state approach [2] combination	95
5.6.1.4.1	Approach [2] verification phase (1).....	95
5.6.1.4.2	Approach [2] verification Phase (2).....	98

5.6.1.5	Analysis SLV combination	101
5.6.1.5.1	SLV combination-Phase (1) results	101
5.6.1.5.2	SLV combination-Phase (2) results	105
5.6.1.5.3	SLV combination - internal actions envelope	109
5.6.1.6	Verification state SLV combination	111
5.6.1.6.1	SLV combination - verification Phase (1)	111
5.6.1.6.2	SLV combination - verification Phase (2)	114
5.6.2	GFRP micropile verification	117
5.6.2.1	Material properties definition	118
5.6.2.2	GFRP Approach [1] combination	119
5.6.2.2.1	GFRP Approach [1] - phase (1) verification	119
5.6.2.2.2	GFRP Approach [1] - phase (2) verification	119
5.6.2.3	GFRP micropile approach [2] combination	120
5.6.2.3.1	GFRP approach [2] - phase (1) verification.....	120
5.6.2.3.2	GFRP approach [2] - phase (2) verification.....	120
5.6.2.4	GFRP micropile SLV combination	121
5.6.2.4.1	GFRP SLV combination - phase (1) verification.....	121
5.6.2.4.2	GFRP SLV combination - phase (2) verification.....	121
5.6.2.4.3	GFRP micropile verification summery.....	122
5.7	Cost comparison:.....	122
6.	Chapter 6: Conclusion	125
	References	127

List of figures

Figure 1.1: Egyptian Pyramids constructed with rock blocks.	9
Figure 1.2 Wooden structure.....	10
Figure 1.3 Louvre Museum, Paris - glass structure.	10
Figure 1.4 Palazzo Carignano of Turin- masonry structure.....	11
Figure 1.5 Steel Structures	12
Figure 2.1 Reinforcement corrosion procedure (Chapter4 Corrosion and its Control - Advances in Civil Engineering Book).....	15
Figure 2.2: Comparison between GFRP bars with different surface types.....	20
Figure 2.3 GFRP variation of tensile strength with the bar diameter.....	21
Figure 2.4 Shear strength variation with the setting temperature.....	22
Figure 2.5 Samples prepared by Robert, Cousin and Benmokrane, (2009).....	23
Figure 2.6 The study results by Robert, Cousin and Benmokrane, (2009).....	24
Figure 2.7 Bored pile in GFRP The Jizan Flood Mitigation Channel in GFRP.....	24
Figure 2.8 Jizan Flood Mitigation Channel GFRP Reinforcement.....	25
Figure 2.9 Jizan Flood Mitigation Channel GFRP Reinforcement.....	25
Figure 2.10 Seawall Strengthening the iconic Burj Al Arab:	26
Figure 2.11 SHED concrete armor units	26
Figure 2.12 GFRP Reinforcement.....	26
Figure 2.13 GFRP piles reinforcement.	27
Figure 2.14 GFRP piles reinforcement.	27
Figure 2.15 Stress-strain curve	29
Figure 3.1 Uses of micropiles (FHWA – SA – 97 – 070)	31
Figure 3.2 Types of micropiles construction. (FHWA – SA – 97 – 070).....	32
Figure 3.3 Load Combinations NTC2018-Chap2.5.3.....	35
Figure 3.4 Pile load transfer mechanism.	36
Figure 3.5 injection diameter.	39
Figure 3.6 Micropile design flow.	43
Figure 4.1 Punching failure scheme under concentrated load.....	45
Figure 4.2 (Fam and Rizkalla, 2003) experiment.....	46
Figure 5.1 Location of the presented project.	49
Figure 5.2 Wall and pavement cracks.	50
Figure 5.3 The wall's Current situation	50
Figure 5.4 Monitoring systems.	51
Figure 5.5 Solution (1).....	52
Figure 5.6 Solution (2)	53
Figure 5.7 Solution (3)	54
Figure 5.8 Solution (4)	55
Figure 5.9 Solution (5).....	56
Figure 5.10 Solution 6.....	57
Figure 5.11 Solution (6) description.....	58
Figure 5.12 Cross section project scheme	59
Figure 5.13 plan Scheme of the project.....	59
Figure 5.14 Snow groups.	61
Figure 5.15 Spectrum accelerations.....	62
Figure 5.16 SLV spectrum graphs.	65
Figure 5.17 Scheme of phase (1).....	68
Figure 5.18 Scheme of phase 2	68
Figure 5.19 Approach (1)-Phase 1: Internal actions along the pile group	71
Figure 5.20 Approach (1) -Phase 2: Internal actions along the pile group	75

Figure 5.21 Approach 1- envelope: Internal actions along the pile group	77
Figure 5.22 Approach (1)-Stress verification phase 1	79
Figure 5.23 Properties definitions.....	81
Figure 5.24 Interaction domain verification.....	81
Figure 5.25 Approach (1)-Stress verification phase (2).....	82
Figure 5.26 Properties definitions.....	84
Figure 5.27 Interaction domain verification.....	84
Figure 5.28 Approach (2)-phase (1) internal actions.....	87
Figure 5.29 Approach (2)- phase (2) internal actions.....	91
Figure 5.30 Approach (2)- envelope of internal actions.	93
Figure 5.31 Approach (2)- Stress verification phase 1	95
Figure 5.32 Properties definitions.....	97
Figure 5.33 Interaction domain verification.....	97
Figure 5.34 Approach (2)-Stress verification phase 2.....	98
Figure 5.35 Properties definitions.....	100
Figure 5.36 Interaction domain verification.....	100
Figure 5.37 SLV-Phase (1) internal actions.	103
Figure 5.38 SLV-phase (2) internal actions.....	107
Figure 5.39 SLV envelope of internal actions.	109
Figure 5.40 SLV- Phase (1) Verification.....	111
Figure 5.41 Properties definitions.....	113
Figure 5.42 Interaction domain verification.....	113
Figure 5.43 SLV-phase (2) verification	114
Figure 5.44 properties definitions	116
Figure 5.45 Interaction domain verification.....	116
Figure 5.46 GFRP reinforcement properties.....	117
Figure 5.47 Material properties definition	118
Figure 5.48 Interaction domain verification approach [1] - phase (1).	119
Figure 5.49 Interaction domain verification approach [1] - phase (2).	119
Figure 5.50 Interaction domain verification approach [2] - phase (1).	120
Figure 5.51 Interaction domain verification approach [2] - phase (2).	120
Figure 5.52 Interaction domain verification approach [SLV] - phase (1).....	121
Figure 5.53 Interaction domain verification approach [SLV] - phase (2).....	121

List of tables

Table 2.1 Comparison between E-Glass and S-Glass	19
Table 3.1 A1 coefficient chapter (06) NTC2018	34
Table 3.2 M1 coefficient chapter 06 NTC2018.....	34
Table 3.3 Coefficient y for predominant loads.....	35
Table 3.4 Shear nominal strengths in FHWA-SA-97-070 (v00-06).....	38
Table 3.5 Values of (α)	40
Table 3.6 coefficients a, b, α, β of shear resistance.....	40
Table 3.7 C_s coefficient for clay.....	41
Table 3.8 C_s coefficient for sand	41
Table 5.1 Solutions comparison summery	58
Table 5.2 acceleration- return time calculations.....	62
Table 5.3 SLV spectrum values.	64
Table 5.4 Approach (1) - Phase 1 soil pressure.....	70
Table 5.5 Approach (1) - Phase 1 accumulative soil pressure	70
Table 5.6 Approach (1) - Phase 1 internal actions	72
Table 5.7 Approach (1) - Phase 2 soil pressure.....	74
Table 5.8 Approach (1) - Phase 2 accumulative soil pressure	74
Table 5.9 Approach (1) - Phase 2 internal actions	76
Table 5.10 Approach (1) Internal actions envelope along the pile group.....	78
Table 5.11 Approach (1) verification state phase 1	80
Table 5.12 Approach (1) verification state phase 2	83
Table 5.13 Approach (2) - Phase 1 soil pressure.....	86
Table 5.14 Approach (2) - Phase 1 accumulative soil pressure	86
Table 5.15 Approach (2) - Phase 1 internal actions	88
Table 5.16 Approach (2) - Phase 2 soil pressure.....	90
Table 5.17 Approach (2) - Phase 2 accumulative soil pressure	90
Table 5.18 Approach (2) - Phase 2 internal actions	92
Table 5.19 Approach (2) Internal actions envelope along the pile group.....	94
Table 5.20 Approach (2) verification state phase 1	96
Table 5.21 Approach (2) verification state phase 2	99
Table 5.22 SLV Approach - Phase 1 soil pressure.....	102
Table 5.23 SLV Approach - Phase 1 accumulative soil pressure	102
Table 5.24 SLV Approach - Phase 1 internal actions	104
Table 5.25 SLV Approach - Phase 2 soil pressure.....	106
Table 5.26 SLV Approach - Phase 2 accumulative soil pressure	106
Table 5.27 SLV Approach - Phase 2 internal actions	108
Table 5.28 SLV Approach - Internal actions envelope along the pile group.....	110
Table 5.29 SLV Approach - verification state phase 1.....	112
Table 5.30 SLV Approach - verification state phase 2.....	115
Table 5.31 GFRP micropiles verification summery	122
Table 5.32 Cost of traditional single micropile.	122
Table 5.33 Cost of GFRP single micropile.....	123

1. Chapter 1: Introduction.

The construction industry witnessed many materials and still in deep research for material enhancement and new materials. In the following paragraphs there is a summary of some of the materials the obtained an important role in the construction industry and some of their limitations.

Rock:

Since ancient ages homes or structures were just sculptured in mountains or constructed with heavy blocks of rocks. It can be clearly seen in the ancient civilizations. For example, the old Egyptian civilization where we can find the tombs were built in mountains as well as the great pyramids that were built with rock blocks thousands of years ago.



Figure 1.1: Egyptian Pyramids constructed with rock blocks.

The construction with rock blocks is full of limitations. It was the only possible option in old ages when there were no technologies and materials. The result structure has a very limited height and strength. If the structure is sculptured, there's no flexibility in design.

Timber:

Wood obtains huge importance in construction industry. It has been used since old ages as a construction material. The advantages of timber helped to obtain a remarkable role in the industry. Timber is energy-efficient material. It provides a decent heat isolation level. The light weight of wood was a result to obtain a good importance in seismic areas. Regarding sustainability, wood is a great material since it is a natural material. In this point we can have a different opinion. Some discuss that timber has no effect on the environment as a construction material, but some other discuss the environmental effect from the point of cutting down forests to get wood. The advantages extent to include strength, durability and recyclability of wood.

Although the mentioned advantages, wood suffers some important limitation. It has low fire resistance, low noise insulation and height limitations. These limitations lead to deep searches for different materials or a combination with other material to overcome the maximum possible defects in wood.



Figure 1.2 Wooden structure.

Glass:

Glass structures have been increasingly utilized in modern constructions for decades. It has been used as load-bearing walls or facades. The usage of glass is until now in deep research for development as a structural system, production facilities and processing methods for glass. (Publication-Article in E-Zbornik elektronički zbornik radova Građevinskog fakulteta · December 2019).

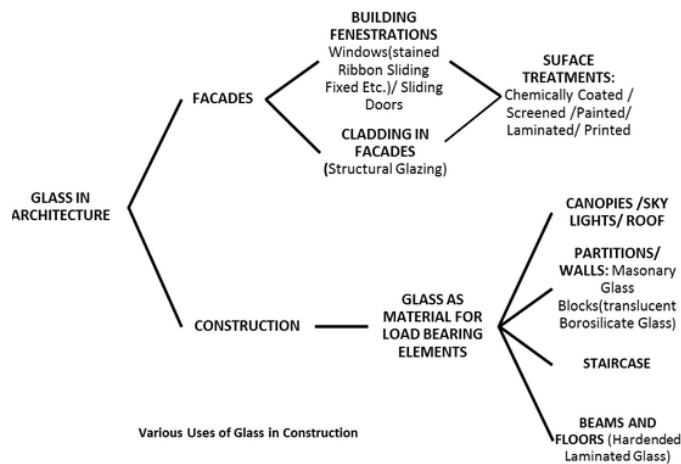


Figure 1 Glass Usage in construction (<https://www.understandconstruction.com/glass.html>).

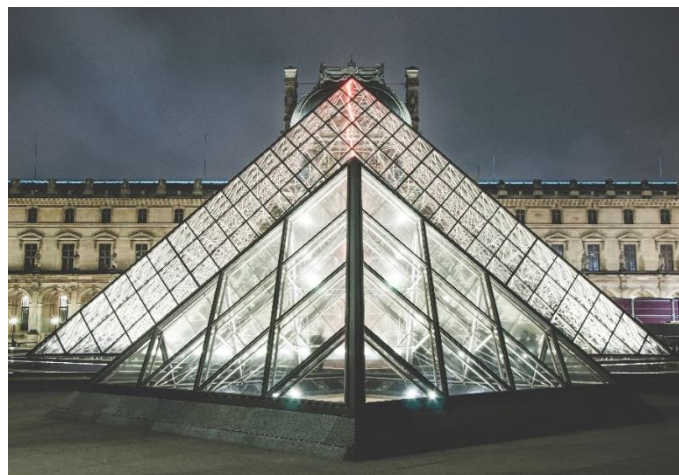


Figure 1.3 Louvre Museum, Paris - glass structure.

Glass maintains many advantages especially at the level of noise isolation and decoration, but it suffers a brittle failure. Deep researches are interested in mixing glass with other materials such as fibers to give it better ductile behavior.

Masonry:

Masonry buildings were widely common especially in Italy. The most famous churches and historic places in Italy are masonry structures. Masonry was one of the initial steps to move toward a better design. Masonry elements could be in bricks, stones and concrete masonry. Each type of these was introduced to overcome the limitations of the other types. The usage of masonry is not limited to residential, commercial, religious buildings. It extends to many other applications such as slope protection using masonry gabions and shore protection using stone masonry elements.



Figure 1.4 Palazzo Carignano of Turin- masonry structure.

Masonry helped the industry to obtain flexibility and better durability. It enjoys a better fire resistance and higher resistance. For a long period of time masonry structures were the most prevalent. It could be seen in different cultures and countries.

The extended need in construction industry showed many limitations in the usage of masonry. Low construction speed, low resistance seismic actions, brittle failure scheme are some of these limitations. In the sustainability point of view, masonry structures have very bad effects on the environment due to the gas amount emitted during fabrication process.

Steel:

Steel made a huge revolution in the construction industry. It has a great behavior in seismic zones. It is used almost in all the structures like high rise buildings, factories, bridges. It is due to the high strength, so we can have long spans without middle columns. Factory fabrication and site assembling take little time which leads to very fast construction process. Steel construction is world widely common.



Figure 1.5 Steel Structures

The usages of steel structures have some limitations such as the low fire resistance, the negative environmental effect and nonrenewable raw material. Regardless these limitations, steel is still one of the most important construction materials. Researchers are always in a deep search to overcome these limitations.

Concrete:

Though the Romans are generally credited as being the first concrete engineers, a form of concrete dating to 6500 B.C. has been discovered by archaeologists in Syria. From the Middle East, concrete technology spread and evolved, primarily in Europe. In 1871, the first Portland cement was produced in the United States at Coplay, Pennsylvania. (Prehistoric rubble mixes to Roman cement By Richard W. Steiger).

The durability, workability and high fire resistance are the most important characteristics of concrete.

The movement from one material to another is always due to the limitations in the material. The masonry structures have a general weak behavior. Plane concrete structures work efficiently in compression but have an unstable behavior in tension. Timber and glass structure have height limitation problems. The reinforced concrete structures were able to overcome many limitations faced by the other materials.

Although reinforced concrete was able to resolve many of the limitations of many other materials, they have some other limitations that drove researchers to investigate for an enhancement or replacement.

Concrete Structures are widespread for very long time all over the world, Concrete is well known for its good behavior in compression, and its weak behavior in tension fields. The problem of using just concrete is its failure mode "brittle" which is instant and comes without any warnings. Due to this, the first combination with steel took place in order to change the failure behavior from brittle failure to ductile failure, which gives a long failure period with many warning observations.

Steel reinforced concrete is used almost in all the structural elements starting from slab, beams, columns, stairs reaching foundations with all types as well as tanks, retaining structures and

seashore protection structures. It could be cast in place or prefabricated elements with various connection modes in order to satisfy the stability and safety requirements.

R.C elements could be used in all the environments such as regular buildings, marine structures, bridges, airports and nuclear plants. they also face different types of loads and could be exposed to all kinds of environments and chemicals.

Due to the diversity of the conditions where the R.C element is used, the construction philosophy as well as the design have been faced many challenges. It also leads to material properties limitations to overcome. This is why the researchers started to investigate for some improvements to the composite materials and also searching for new compositions such as fiber reinforced concrete.

The steel _ concrete combination suffers a limitation while is exposed to water due to the corrosion that takes place in steel. In particular, foundations are the most exposed elements to corrosion due to many factors, especially deep foundations since they usually reach the deep layers of soil as well the underground water. The exposure to chemicals would affect the resistance of the concrete. Wearing affects both concrete and steel reinforcement. The mentioned limitations are not the only limitations the combination faces. They might be the initial limitations that forced the researchers to investigate to modify the concrete characteristics to resist more chemicals and to investigate for a protection for steel reinforcement to avoid corrosion. The idea of replacing the steel reinforcement with other materials started to emerge lately not just due to the corrosion problem but for many other reasons that would be discussed in our study in chapter 2.

Corrosion in steel is the major cause of steel pile deterioration specially in foundations because of the fact of the existence of chemicals and ground water, The rate of corrosion in regular soils is about 0.03 mm/year and it increases significantly in splash zone to about 1.2 mm/year (Fleming et al. 1992).

1.1 Objective of the thesis

The objective of the study is to present:

- The reason why the construction industry is always in a deep search for new materials and the modifications of the material properties, in particular the steel reinforcement.
- The discussion of steel reinforcement drawback and the importance of finding a substitution.
- The definition of FRP reinforcement and the advantages of using it.
- The design procedure of the regular micropiles according to different codes.
- The design procedure of micropiles using the GFRP.
- The practical study case.

1.2 Structure of the thesis

This thesis has been developed in conventional format and the following seven chapters each address one of the objectives of the thesis as summarized below.

Chapter 1

It gives a short review of the materials used in the construction industry. Material limitations and the reason why the construction industry is always in search for material properties enhancement or new materials in particular the steel reinforcement. The particular situation of the deep search for new reinforcement generally, and particularly for micropiles.

Chapter 2

It discusses the steel problems in the construction industry, glass fiber reinforced polymer types, properties, forms of glass fiber polymers and the advantages of its use as a substitution of steel reinforcement in RC structures. The comparison between the use of steel reinforcement and glass fiber polymers in terms of durability, corrosion and pricing.

Chapter 3

reports the micropiles discovery, the different types of micropiles according to the construction procedure, the wide use of micropiles. It also summarizes the geotechnical and structural design procedure of regular steel reinforced micropiles according to FHWA code as well as in the Italian regulations highlighting the differences between them.

Chapter 4

It highlights different studies and experiments on elements in GFRP and the expectation of the differences in the design procedure in the case of micropiles.

Chapter 5

It studies a project case of the design of micropiles following both the procedures mentioned above with regular steel reinforcement and with glass fiber reinforced polymers.

Chapter 6

It gives a brief conclusion regarding both the design methods and the behavior.

Chapter 7

It presents all the references used in this case of study.

2. Chapter 2: The use of GFRP in substitution of steel in RC structures.

The continuing investigation in construction industry for new materials is not only for the instability and safety aspects. It is for many different aspects such as economic reasons, environmental effects, energy consumption, labor availability, complexity of application and time.

As mentioned before the limitation is not only related to steel, it is related to all the components of the R.C mix but our study would be limited to the steel reinforcement limitations and the current economic situations that pushed forward searching for alternatives.

In the following paragraphs, we are discussing some of the reasons related to steel reinforcement that forwarded us to search for an alternative to steel.

2.1 Steel Limitations

2.1.1 corrosion resistance

One of the most important limitations related to steel reinforcement is corrosion. It is highly probable since the concrete mix contains water. The concrete cover is not completely isolating, it means that the air (oxygen) can in many cases reach the reinforcing bars. It is not just a problem of porosity of concrete, if the concrete was well cast it would be cracked due to loading or thermal effects.

When steel rebars suffer corrosion, its cross section increases due to the interaction. The cross-section increase applies internal stresses on concrete. These stresses result in crack propagation which in its turn increases the exposure of steel to environmental corrosion factors. In addition, the corroded part strength is much lower than the steel strength, so it means decrease in the resisting reinforcement area. The problem of corrosion expands from one bar to the other which in return affects the total area of steel reinforcement and consequently the performance of the whole RC cross section.

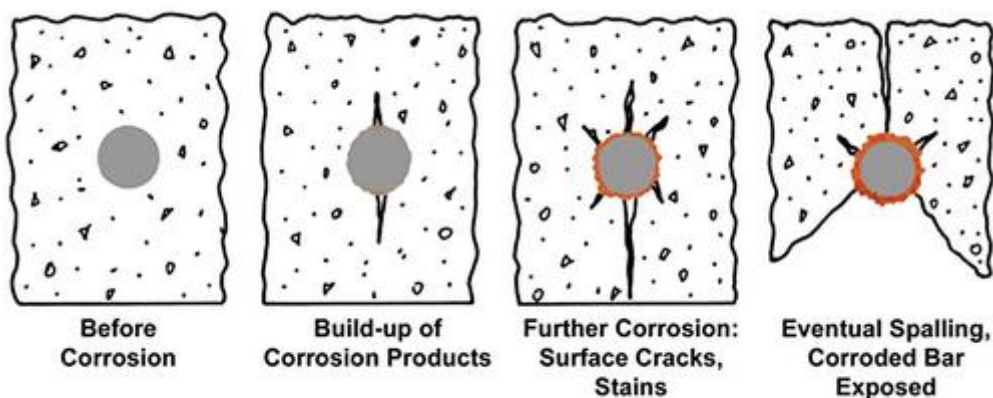


Figure 2.1 Reinforcement corrosion procedure (Chapter4 Corrosion and its Control - Advances in Civil Engineering Book).

2.1.1.1 Corrosion Causes

Generally, the alkaline environment provided by concrete provides the rebars with protection. This environment doesn't prevent corrosion, but it decreases the corrosion rates significantly.

For steel in concrete, the passive corrosion rate is typically $0.1 \mu\text{m}$ per year. Without the passive film, the steel would corrode at rates at least 1,000 times higher (ACI222 2001).

As a result, concrete provides steel with an important level of protection. The composition of steel concrete achieved success for ages, but once this protection is lost as a result of the loss of the concrete cover or other kinds of wearing in concrete, that would lead to having porous concrete cover. The steel would become vulnerable to corrosion agents.

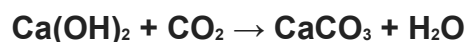
Chloride ions

Chloride ions are the primary cause of corrosion in steel. Chlorides dissolve in water that can easily penetrate inside the sound or cracked concrete and reach the steel (rebars) and causing corrosion, especially in the presence of water and oxygen to sustain the corrosion process. The mechanism of the chloride's corrosion is not entirely understood, but the most popular theory is that the chloride ions penetrate the protective oxide film easier than other ions, leaving steel vulnerable to corrosion. So, consequently the risk increases when the chloride content increases. The minimum amount of chloride ions to cause corrosion is called threshold. According to Federal Highway Administration (FHWA) studies, the threshold limit of 0.2% by weight of the cement could induce the corrosion only with the presence of water to sustain the corrosion. The chloride amounts trapped inside the aggregates don't participate in the corrosion procedure.

Although chlorides are mainly responsible for the initiation of corrosion, they appear to play only a secondary role in the corrosion rate after initiation. The primary rate-controlling factors are the availability of oxygen gas.

Carbonation

Carbonation occurs when carbon dioxide from the air penetrates inside the concrete and reacts with hydroxides, such as calcium hydroxide, to form carbonates. In the reaction with calcium hydroxide, calcium carbonate is formed:



This reaction reduces the alkaline environment (pH) the concrete protective layer. Carbonation of concrete also lowers the amount of chloride ions needed to promote corrosion. So, carbonation has a double negative effect. Firstly, it reduces the alkaline level of protection. Finally, makes steel reinforcement more vulnerable to corrosion due to chloride.

Carbonation is highly dependent on the level of humidity in concrete. Below 25 percent relative humidity, the degree of carbonation that takes place is considered insignificant. Above 75 percent relative humidity, moisture in the pores restricts CO₂ penetration. Carbonation occurs when the relative humidity is between 50 and 75 percent.

Compared with chloride ions, carbonation corrosion rate is slower.

Dissimilar Metal Corrosion

When two different metals, such as aluminum and steel, are in contact within concrete, corrosion can occur because each metal has a unique electrochemical potential. Dissimilar metal corrosion can occur in balconies where embedded aluminum railings are in contact with the reinforcing steel. (<https://www.cement.org/learn/concrete-technology/durability/corrosion-of-embedded-materials>)

Inadequacy of Concrete Cover:

Inadequacy of concrete cover could be the main and the summary of all the previous steel corrosion causes. Since all the corrosion causes are due to direct contact with steel surface, any agent that would decrease the concrete cover thickness or stiffness could be considered an initiative agent to steel corrosion.

2.1.1.2 Corrosion types

Electrochemical Corrosion:

Electrochemical corrosion is the most common form of attack in metals. It occurs when metal atoms lose electrons and become ions. It means that the metal is gradually getting consumed.

Electrochemical corrosion occurs frequently in a saturated medium, in which ions are present in water, soil, moist air or acids.

The Electrode Potential in Electrochemical cells:

When a metal is placed in an electrolyte (solution), an electrode potential develops that is related to the tendency of the material to give up its electrons.

2.1.2 Production cost

reinforcement is one of the major elements that defines the project's cost. Reinforcement could be considered the most expensive component in reinforced concrete production industry.

Steel prices are recently getting higher due to many reasons that could be shortly highlighted:

Covid 19 Pandemic

Starting with the pandemic covid situation that forced many countries to reduce the labors number and consequently the production rate of steel. Until now, all the countries and factories don't proceed the work at their full capacity. These situations affect steel production rates as well as prices, which in its turn affects the whole construction industry prices.

Wars

The steel production industry consumes a huge amount of energy yearly. Due to the current wars the European countries suffer a huge shortage in energy.

Transportation

Steel cost can't be considered only the raw material price plus the production. The total cost should also include the transportation prices. The cost of the transportation is a considerable cost because of the heavy weight of the steel. Transportation itself suffers the same previously mentioned problems due to Covid pandemic and the energy shortages which lead to increase the transportation cost.

Maintenance

Steel maintenance could be achieved if the steel element is an exterior element. It could be treated with some materials or galvanized to stop the corrosion spread. It could be treated by hot welding with other protective metals. If the rotten part is completely defected it could be cut and replaced.

Maintenance is rarely possible for the rebars inside the concrete, or we can say it would be very difficult to be accomplished since it would need to demolish the exterior concrete part to perform the maintenance and rebuild it one more time. It would be impossible to accomplish the maintenance of steel rebars inside the foundations.

Steel protection

There are many ways to protect steel from corrosion attacks. Coatings are the most common protections. Coatings prevent the propagation of oxygen and water that cause corrosion or oxidation.

There are many materials that could be used in coating steel such as Teflon or other plastic materials and zinc with all galvanization methods.

The protection ways are so expensive. They require additional energy, labor and time which result to an un-negligible cost. This at the end would increase the total cost of reinforcement and the construction process.

2.1.3 Sustainability

The construction industry is one of the most environmental costing industries. The production of all the materials emits huge amounts of gases that negatively affect the environment. The production of cement, masonry and steel cause the highest level of environmental harm.

The production of steel rebars emits a huge amount of pollution into the environment. The production has heavy waste that is difficult to be deposited. The effects of steel on the environment does not stop at this point, but its production consumes a huge amount of energy that can't be provided from a renewable resource. So, it consumes huge amount of petroleum fuel which in its turn is harmful to the environment. Steel is not a recyclable material when it suffers corrosion. So, Steel could not be considered a sustainable material.

2.1.4 Steel as a non-renewable material

The raw materials of steel (iron) are not renewable materials. This means that, one day due to this high amount of consumption it will suffer a shortage. It is clearly understood that the lower the availability of a material the higher the cost, so, in general there is no prediction to the cost decrease of reinforcement without finding a substitution.

2.2 Substitution of steel reinforcement

Due to all the previously mentioned disadvantages, economic situations and limitations of steel, the researchers were and still in deep research for a valid alternative of steel that is able to overcome many of the previously mentioned limitations and achieve an acceptable level of strength and durability.

There are many substitutions for steel rebars. Each alternative overcome some limitations of steel. The reason that there are many alternatives is that each alternative has its own characteristics.

FRP products are recently the most common alternative. The FRP products include CFRP (carbon fiber reinforced polymers), AFRP (aramid) and GFRP (glass fiber reinforced polymers). The properties of FRP products differ due to many factors such as fiber volume, type, orientation, resin type and quality control as well as dimensional effects (ACI Committee 440, 2006).

The following table is a comparison between mild steel, stainless steel, CFRP, AFRP and GFRP. It was reported in (ACI 440.1R-06, AS/NZS 4673: 2001, fib 2007).

	Mild Steel	Stainless Steel	CFRP	AFRP	GFRP
Nominal Yield Stress, MPa	276-517	250-450	-	-	-
Tensile Strength, MPa	483-690	380-680	600-3690	1720-2540	483-1600
Elastic Modulus, GPa	200	185-200	120-580	41-125	35-51
Yield Strain, %	0.14-0.25	0.2-0.3	-	-	-
Rupture Strain, %	6-20	15-20	0.5-1.7	1.9 to 4.4	1.2-3.1
Density, kg/m ³	7860	7480-8000	1430-1670	1300-1450	1730-2170

Table 2.1 Usual tensile properties of reinforcing bars (ACI 440.1R-06, AS/NZS 4673: 2001, fib 2007)

Glass fiber reinforced polymers is a valid option to be investigated. In the following paragraphs we will introduce the GFRP, its properties, show a short comparison between the steel rebars and GFRP and the limitations that GFRP could overcome.

2.2.1 What is GFRP Reinforcement

Glass fiber reinforced polymer is also known as glass fiber reinforced plastic. It is a composite of glass fibers and polyester material. In other words, it is a composition of many tiny continuous glass fibers enclosed inside a polymeric resin mold. Its tensile strength can range between 44-2358 MPa, and the compressive strength between 140-350 MPa while its weight is only a quarter of the weight of steel.

The properties of the mix depend on many aspects such as the type of the glass fibers, the fibers orientations, the resin material properties and the setting method. In the following paragraphs a short note on the properties of these components and the resultant mix.

Glass fibers

Here a short note about the types and the properties of the glass fibers. The glass fibers in GFRP can be made from various types of glass, including E-glass, S-glass, and others, each with distinct properties suitable for specific applications.

	S-Glass	E-Glass
	S-glass is a high-performance glass fiber, distinguished from E glass primarily by its higher silica content. S-glass typically contains the oxides of silicon, aluminum and magnesium.	E-glass is also known as electrical glass. It is the standard glass fibers. It is made from the oxides of silicon, aluminum, calcium, magnesium and boron.
Mechanical Properties		
Density	2.53 g/cm ³	2.54 g/cm ³
Tensile strength	4600 MPa	3400 MPa
Modulus of Elasticity	89 GPa	72 GPa
Elongation Percentage	5.2	4.7

Table 2.1 Comparison between E-Glass and S-Glass (<https://jpscm.com/products/e-glass-s-glass/>)

Resin matrix:

The properties as well depend on the resin matrix. The polymer resin matrix can consist of thermosetting or thermoplastic resins, which provide different characteristics like enhanced strength, flexibility, and chemical resistance.

The outcome mixture:

The final product's properties could be improved by modifying its texture and form. There are many attempts to increase the bond strength of the bars. A few different types of bar surface have been produced such as smooth bar surface, ribbing of the bar surface (similar to deformed mild steel), helical fiber wrapping of the bar (either simply bonded to the core or wrapped under tension to deform the bar slightly) and applying a rough coating with sand particles to the bar surface (Katz, 1998).

In the following figure there're three different surface types (a, b, c).

- (a) helical ribbed bar surface.
- (b) helical fiber wrapping of sand coated bar surface.
- (c) sand coated bar surface.

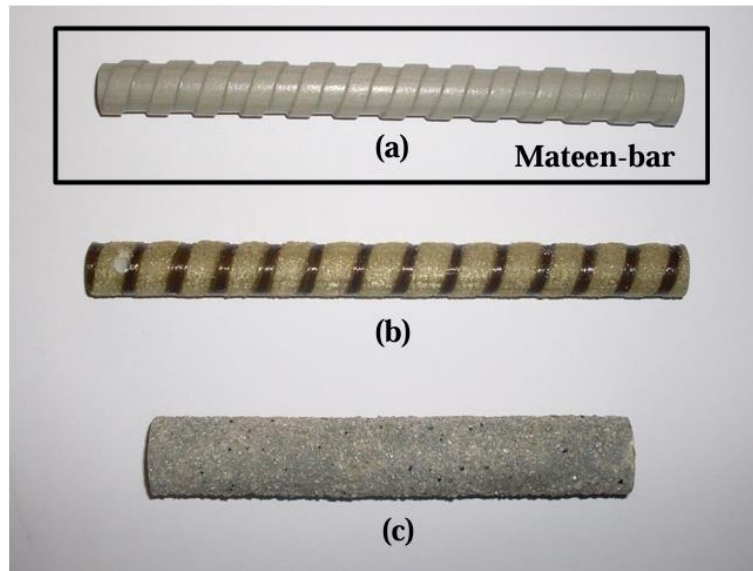


Figure 2.2: Comparison between GFRP bars with different surface types.

2.2.2 GFRP bar properties

Density:

GFRP bars have a unit weight of almost 2000.0 kg/m^3 , while the unit weight of steel reinforcing bars is almost 8000 kg/m^3 .

The lower density of GFRP reduces the weight which reduces transportation costs and makes handling the bars easier on the project site.

Thermal Properties:

The coefficient of thermal expansion for GFRP bars can vary greatly in the longitudinal and transverse directions. It depends on the type of glass fibers, their orientation, the resin type, the setting method and volume fraction of fiber. The longitudinal coefficient of thermal expansion is comparable to that of concrete which means that thermal incompatibility is unlikely to be a concern when designing GFRP reinforced concrete structures. The transverse coefficient of thermal expansion can be up to four times greater than the expansion in longitudinal direction which may lead to splitting cracks in cases where insufficient cover is provided. Here we can notice the importance of the concrete cover for GFRP reinforcement as the case of traditional steel reinforcement. It was found that a ratio of concrete cover thickness to bar diameter (C/Φ) of 2 or greater is sufficient to avoid cracking of concrete up to temperatures of $+80^\circ\text{C}$ (Masmoudi, Zaidi, & Gerard, 2005).

In the case of fire, GFRP bars embedded in concrete will not be burned, but the resin will soften due to the high temperatures. FRP composites have a glass transition temperature (T_g), above which the resin changes from its stiff state to a soft rubbery state. The value (T_g) depends on the resin type. Exceeding this temperature would affect many properties. The tensile properties of GFRP decrease above (T_g) due to a reduction in the bond between fibers since the matrix resin becomes less stiff. GFRP is not recommended where fire resistance is critical to maintaining structural integrity (fib, 2007).

Tensile Strength

The tensile strength of GFRP is much higher than the tensile strength of mild steel. However, its failure is brittle which means that it experiences a sudden failure at the ultimate loading point (Kocaoz, Samaranayake, & Nanni, 2005). The tensile strength of GFRP varies with the diameter change. It reduces by up to 40% proportionally as the diameter increases from 9.5mm to 22.2mm (ACI Committee 440, 2006). The following figure reports the variation of the tensile strength of GFRP with the diameter as a part of the publication Tensile Strength of GFRP Reinforcing Bars with Hollow Section by Young-Jun You, Ki-Tae Park, Dong-Woo Seo, and Ji-Hyun Hwang.

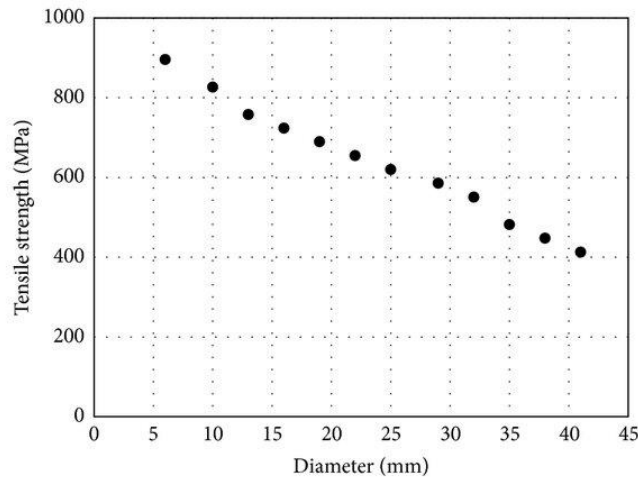


*Figure 2.3 GFRP variation of tensile strength with the bar diameter
(Tensile Strength of GFRP Reinforcing Bars with Hollow Section, Young-Jun You, Ki-Tae Park, Dong-Woo Seo, and Ji-Hyun Hwang)*

Compressive Strength

The compressive strength of GFRP reinforcement is much lower than its tensile strength. (ACI Committee 440, 2006). In general, compressive strengths of GFRP bars are higher for bars with higher tensile strengths, and the compressive modulus of elasticity lower than its tensile modulus of elasticity. Depending on the type of fiber, resin and fiber volume fraction, the compressive strength of a GFRP bar can reach up to 55% of its tensile strength. This shows the important fact that GFRP is a valid as tensile reinforcement. Since the concrete has a high compression strength but low tensile strength and GFRP has a high tensile strength but low compression strength the outcome mix would combine both the properties and would have high compression and tension strength.

Shear Strength

Shear properties of GFRP reinforcement are not yet well defined. There are many factors affect the shear strength such as the orientation of the fibers with respect to the longitudinal axis and the matrix setting temperature as reported in the publication (Study on the Mechanical Properties of Glass Fiber Reinforced Polyester Composites by Fazle Elahi, Milon Hossain, Shahida Afrin, Mubarak Ahmed Khan).

The following figure was extracted form the same study. It shows the effect of the temperature on different samples.

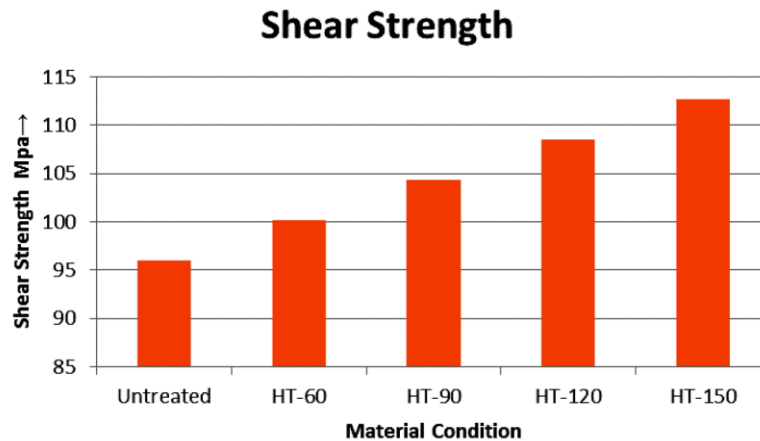


*Figure 2.4 Shear strength variation with the setting temperature
(Study on the Mechanical Properties of Glass Fiber Reinforced Polyester Composites by Fazle Elahi, Milon Hossain, Shahida Afrin, Mubarak Ahmed Khan).*

Temperature is directly proportional to shear strength. With the increase of heat, shear strength also increases and reaches its maximum value 112.742 MPa at 1500C. While all samples show shear strength greater than 100 MPa untreated sample shows only 96.04 MPa.

Bond Behavior:

Many experimental investigations have been done in order to understand the bond behavior of GFRP reinforcing bars. Experiments by Esani, Saadatmanesh and Tao (1996) lead to the authors modification of the ACI 318-71 formula for development length so that the formula for GFRP bar development length is the greater of:

$$l_{db} = 0.0022\left(\frac{A_b f_f}{f_c'}\right) \quad \text{and} \quad l_{db} = 0.0508 d_b f_f$$

Many studies show that the FRP-to-concrete bond behavior has shown that contrary to conventional steel bars, a GFRP bar has no standardization for surface preparation. Variable surface characteristics based on a sand-coated, ribbed surface with rope winding and a helically wrapped surface strongly affect the bond behavior between GFRP and concrete.

The research published under the name of “Bond behavior of GRFP bars to concrete in beam test” and was done by Renata Kotyniaa, Damian Szczech and Monika Kaszubskaa in 2017 shows the following results:

- The GFRP bars indicated good bond behavior to concrete, mainly due to the ribs on the bar surface. (Renata Kotyniaa, 2017)
- The increase in the bar diameter caused the decrease in the shear bond stress. (Renata Kotyniaa, 2017)
- The increase in the compressive concrete strength caused much better bar-to concrete bond behavior. (Renata Kotyniaa, 2017)
- The decrease in the concrete cover thickness led to the decrease in the shear bond stress. (Renata Kotyniaa, 2017)

Moisture Effect of GFRP Strength:

Moisture effect is a very important factor since its effect on the steel bars is critical. There are many investigations for the moisture effect on GFRP bars in concrete. We report here one of the most important studies performed by (Robert, Cousin and Benmokrane , 2009). 14 GFRP bar samples were embedded in concrete where were exposed to moisture at 23, 40 and 50°C to evaluate the effect of a moist concrete environment. The bars were then tested to determine the resulting reduction in tensile strength. The following figure shows the sample and the results.



*Figure 2.5 Samples prepared by Robert, Cousin and Benmokrane, (2009)
(JOURNAL OF COMPOSITES FOR CONSTRUCTION © ASCE / MARCH/APRIL 2009)*

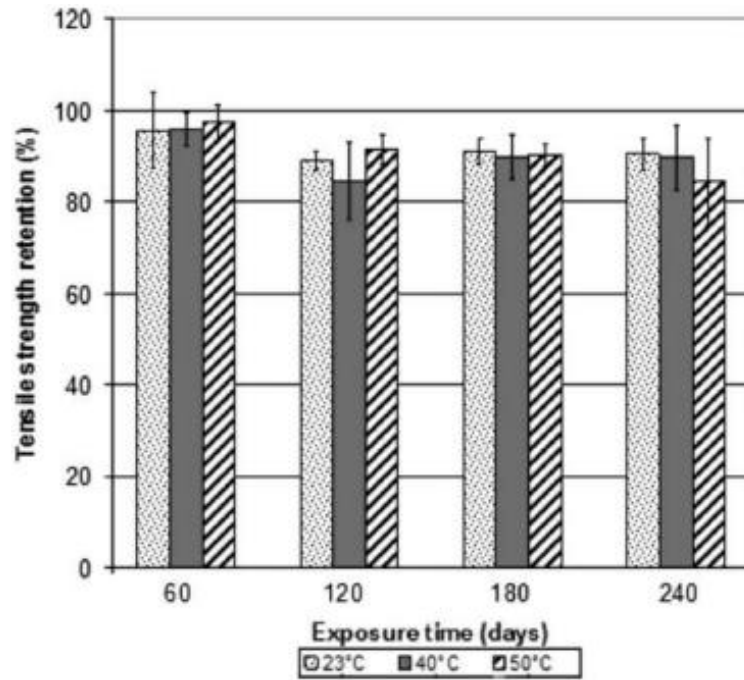


Figure 2.6 The study results by Robert, Cousin and Benmokrane, (2009)
 JOURNAL OF COMPOSITES FOR CONSTRUCTION © ASCE / MARCH/APRIL 2009

The experiment demonstrated that the effect of moisture on the tensile strength of the GFRP is very small even after a long period in moisture. It shows also that at high temperatures (increasing from 40 to 50°C over 240 days) the reduction of tensile strength was minor.

This is one of the most important limitations that steel bars suffer which GFRP can overcome.

2.2.3 Structure elements reinforced with GFRP:

GFRP bars can be used in reinforcing almost all the structure elements. Numerous studies have been conducted to date on different structural elements reinforced with GFRP reinforcement such as beams, columns, slabs, walls, piles and micropiles.



Figure 2.7 Bored pile in GFRP The Jizan Flood Mitigation Channel in GFRP

2.2.4 Projects with GFRP application.

Jizan Flood Mitigation Channel

Jizan project is the world's largest GFRP rebar project. It was completed in 2022. The procurement of the GFRP rebars was Mateenbar. They are one of the most popular GFRP suppliers. The main reason of using GFRP in the project is Corrosion and high chemical resistance provided by the GFRP rebars that can't be achieved by traditional steel reinforcement.

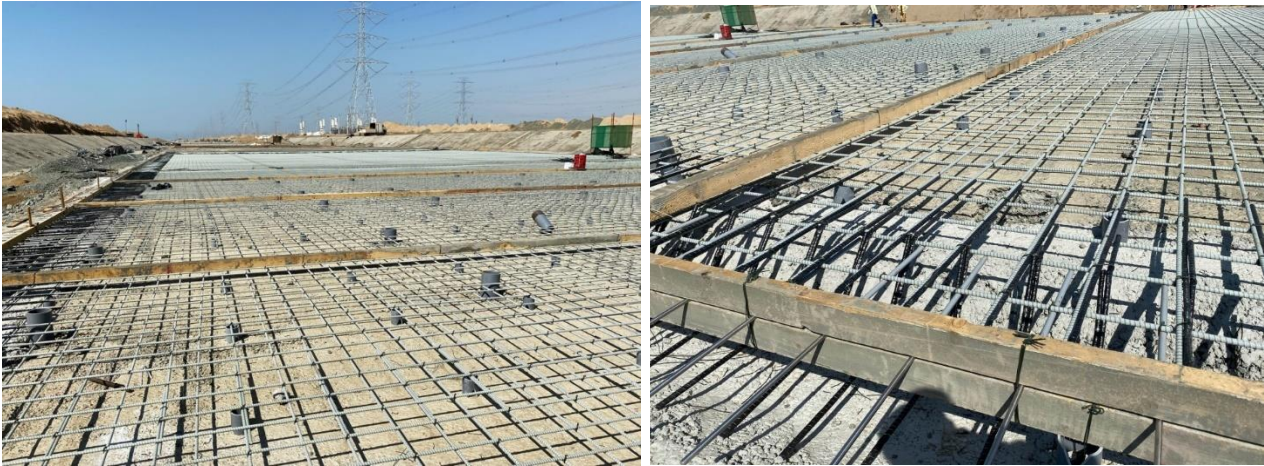


Figure 2.8 Jizan Flood Mitigation Channel GFRP Reinforcement.



Figure 2.9 Jizan Flood Mitigation Channel GFRP Reinforcement

Seawall Strengthening the iconic Burj Al Arab:

The Burj Al Arab is the iconic 7-star hotel located on a man-made island in Dubai. The project is considered as a shore protection structure. The reinforcement of 1,500 SHED concrete armor units protecting the Burj al Arab was required, as part of their maintenance program. These SHED are placed in the water where the corrosion problem is highly probable. The choice of GFRP was made to minimize the corrosion due to the exposure to water and chemicals inside. In the following figures the final project, the SHED position and the proposed GFRP reinforcement.



Figure 2.10 Seawall Strengthening the iconic Burj Al Arab:



Figure 2.11 SHED concrete armor units

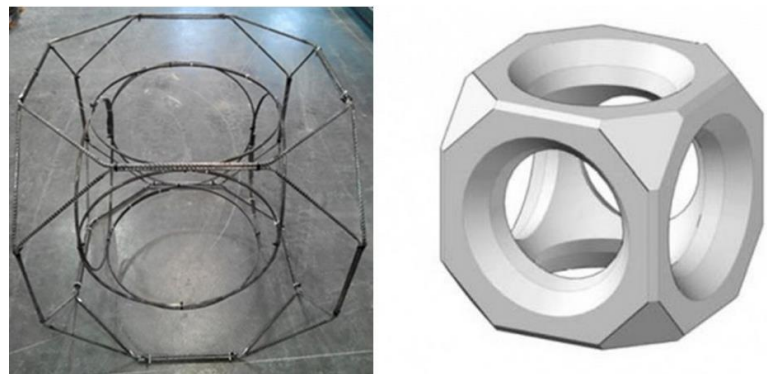


Figure 2.12 GFRP Reinforcement

Pile application for Mina Zayed Road

The circular design of pile was performed for the combination of moment and shear loads. Design safety and performance under combined loads were checked and approved. The use of GFRP rebar allowed for an economic and safe design.



Figure 2.13 GFRP piles reinforcement.

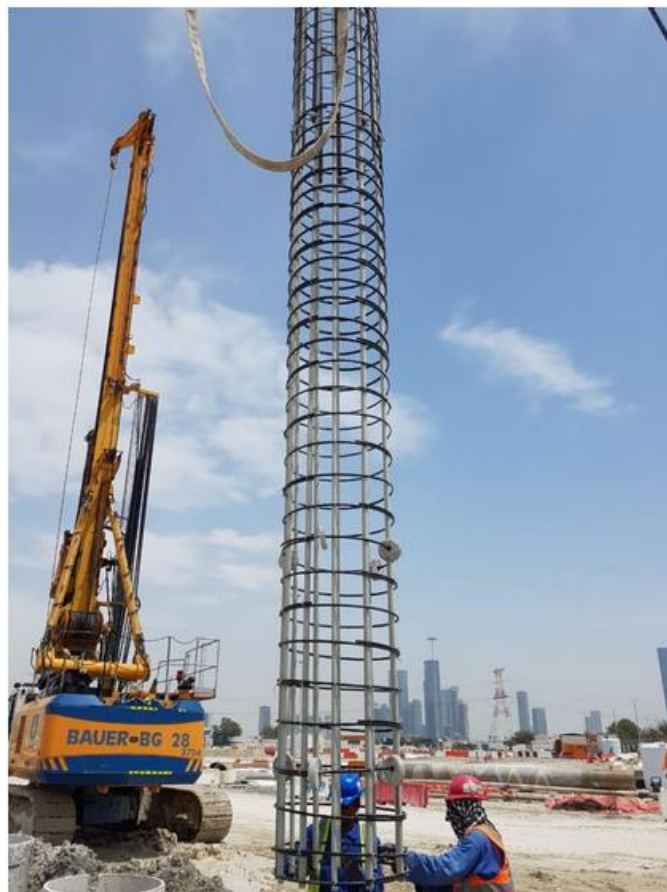


Figure 2.14 GFRP piles reinforcement.

2.2.5 GFRP in Corrosion problem

Since corrosion is the most important aspect of steel limitations, the comparison between the two materials can start from here. Polymers in general are not an active material so they don't suffer the electrochemical corrosion problem. They are not affected by the prosperity of the concrete or the exposure to water. The resistance of the material is not affected also with exposure to salty water. They are not metals, so the dissimilar metal corrosion doesn't happen as well as the Electrode Potential in Electrochemical cells problem. GFRP doesn't suffer from rust, rot or swelling. The life span of the FRP materials is longer than the steel life span without any protective agents. All the previously mentioned projects confirm the high resistance of GFRP rebars. They as well confirm validation of GFRP usage as an alternative to steel rebars.

2.2.6 GFRP Economic solution

As discussed previously, the continue rise of the steel reinforcement cost is one of the critical problems.

The production of the GFRP bars could be more expensive than the production of the steel bars, but as we have shown previously that the final cost is not just the production cost. Transportation, handling, protection and maintenance costs should be added to the production cost to have a valid comparison. GFRP doesn't suffer corrosion, so the protection cost is avoided as well as the maintenance cost. It is much lighter than steel, so the transportation cost is much lower that the steel reinforcement transportation cost. As explained previously that the cost of steel is in a daily increase due to the various reasons previously mentioned, The GFRP does not have the same situation since its uses are until now limited to some industries and thanks to the fact that it could be recycled.

In conclusion the total cost of an element reinforced by GFRP is lower than the cost of the same element reinforced with steel bars.

2.2.7 Sustainability using GFRP.

GFRP in a comparison of steel could be considered as a sustainable material thanks to the fact that it is made from recycled materials, and it can be recycled one more time and used so its production reduces the environmental waste. The production of GFRP doesn't consume the amount of energy consumed by steel production. GFRP production waste is not environmental harmful compared to steel production waste.

2.2.8 FRP reinforcement disadvantages

Despite all the previously described advantages of FRP reinforcement as a substitution of steel reinforcement, there are some disadvantages and drawback as well in using FRP. The following paragraph shortly reports some of the disadvantages of FRP reinforcement.

Brittle failure:

Generally, FRP reinforcing rebars have a linear stress-strain relationship up to its failure regardless the internal components. On the other hand, steel bars have an initially linear behavior followed by yielding phase and finally hardening at which the load is still in an increasing phase until failure.

The following figure reports the stress-strain curve of steel and different FRP bars:

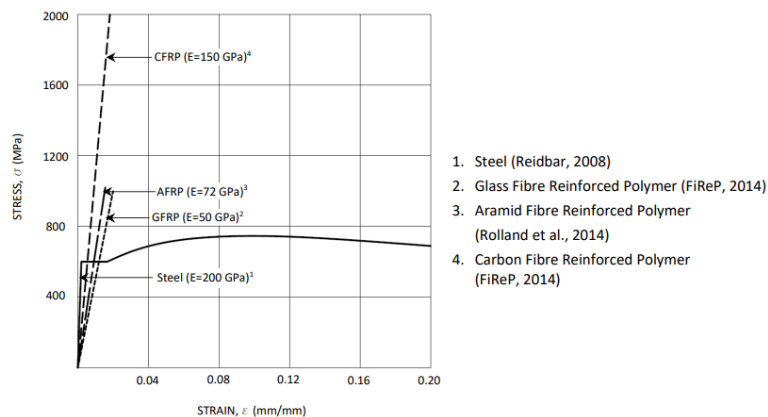


Figure 2.15 Stress-strain curve

Lower modulus of elasticity

One of the most important parameters in the structural design is the modulus of elasticity. FRP bars show a lower elastic modulus than steel bars. Which in return means higher deflections (deformations). Normally, for concrete reinforced elements higher deformations are not favorable for concrete since these deformations cause crushing in concrete.

Creep rupture failure

Under long-term, continuous, and cyclical loads, all materials are susceptible to creep. Creep is a function of time at a certain stress. It has been found that FRP reinforcing materials are more susceptible to creep than steel and may fail suddenly under sustained high loads and adverse environments.

3. Chapter 3: Traditional micropiles design.

Micropiles are piles with small diameter (150 to 250 mm). Micropiles are replacement piles that can be installed in almost any environment. Micropiles has obtained deep interest and have been used throughout the world since their development in Italy in 1952 as a means to underpin sensitive historic buildings. (FHWA, 1997)

The interest that micropiles obtained is due to their functionality in many different aspects of geotechnical engineering and the ease application in difficult ground conditions or with limited or difficult access places, like inside buildings to be underpinned.

3.1 Advantages and uses of micropiles

- A micropile is a small diameter (typically less than 300 mm), drilled, grouted and typically reinforced pile. It can withstand axial and or lateral loads thanks to the fact that they can be constructed at any angle below the horizontal. They are used in both fields of IN-SITU reinforcement and structural support.
- The installation procedure of the micropiles causes minimal vibrations and noise and are often used to underpin existing structures.
- Micropiles work as a structural support for new structures as a foundations system as well as for existing buildings as a seismic retrofitting system or underpinning system.
- The use of micropiles extended also for IN-SITU reinforcement, where micropiles are used as a slope stabilization. A group of vertical and inclined micropiles forms a stabilizations system of the ground slopes.
- In-situ requirements to improve the soil properties also can be achieved through applying driven micropile in different positions with designed spacing and diameter in order to decrease the soil particles' spacing and so decreasing the settlements.

The following graph was extracted from (FHWA–SA–97–070) . It gives a summary for the uses of micropiles in both fields (IN-SITU reinforcement and structural supports. The use of micropiles isn't limited to the different aspects we mentioned but it extends a way wider due to the construction ease, noise control, effective results and lower cost.

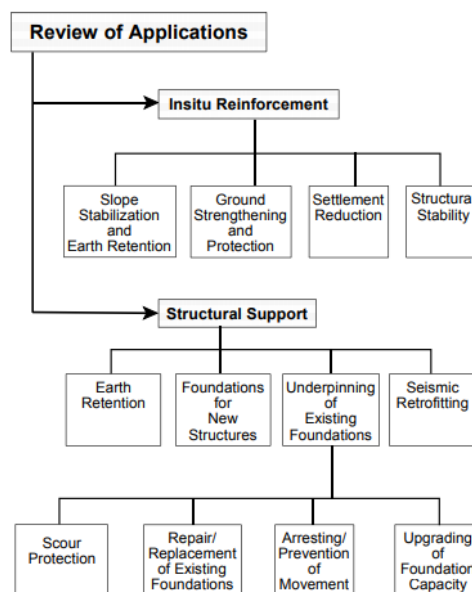


Figure 3.1 Uses of micropiles (FHWA – SA – 97 – 070)

3.2 Micropile types due to Grout Placement Techniques.

Type [A] (Gravity Fill).

Micropile type A are drilled piles at which the injection of concrete is done under gravity without and additional pressure.

Type [B] (Pressure Grouting Through the Casing).

The injection of the concrete in this case is mixed with additional pressure while removing the casing. The aim is to enhance the concrete/soil bond characteristics.

Type [C] (Mixed Technique).

This technique consists of two steps.

- 1) Cement grout is placed under gravity pressure exactly as mentioned in type (A).
- 2) Before hardening, Similar grout is injected one time through a sleeved grout pipe without the use of a packer at pressure of at least 1 MPa.

This pile type appears to be used only in France and is referred to as IGU (Injection Globale et Unitaire).

Type [D]:

This technique as well consists of two steps.

- 1) Cement grout is placed under gravity as in type A or pressured as in type B.
- 2) After the hardening of placed grout, additional grout would be injected with pressure of 2 to 8 MPa.

This pile type is used commonly worldwide and is referred to in France as the IRS (Injection Repetitive et Selective).

The following graph represents the four types mentioned.

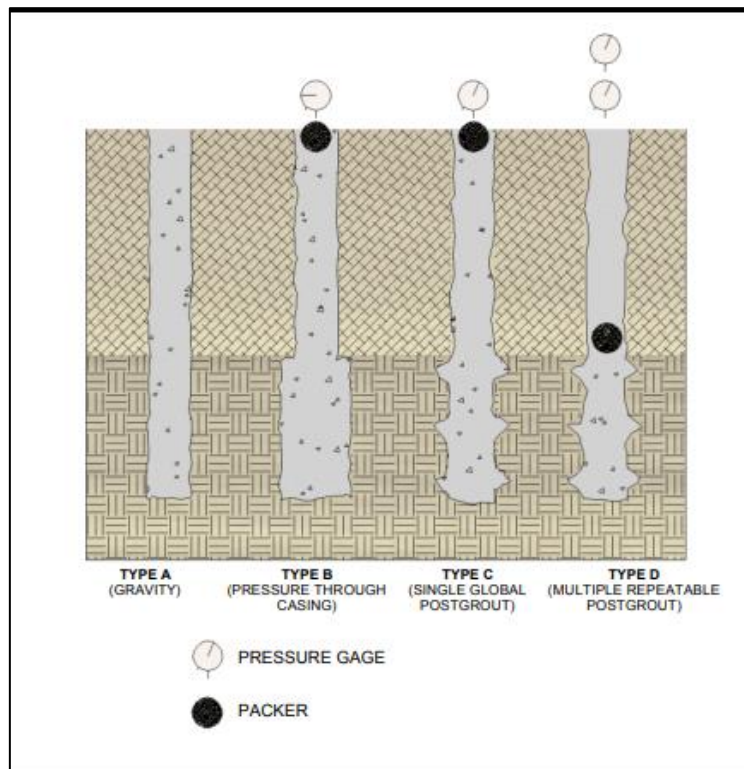


Figure 3.2 Types of micropiles construction. (FHWA – SA – 97 – 070)

3.3 Micropile design

Micropiles are most suited for the use where the primary loading is axial (compression or tension). Due to their small diameter, they are not efficient in resisting lateral loads, but when used in groups, they can efficiently support lateral loads (Abd Elaziz and El Nagggar, 2015; Long et al., 2004; Richards and Rothbauer, 2004). The tension or pull-out capacity of a micropile is a function of several parameters, such as the geometry of the micropile, embedment length, grouting and drilling characteristics and the soil's properties. Principles used in the design and analysis of micropiles are not different from those used for any the traditional piles. One point of difference in the design is that a conventional pile capacity is usually governed by geotechnical factors. Conversely, micropile design is governed by the structural parameters (reinforcing, grout bond). This is a consequence of the relatively small cross-section of micropiles and high grout-soil bond strength that can be achieved through the various available grouting techniques.

3.4 Verification scheme

The general way of any verification is the comparison between the expected applied load and the maximum load the element can withstand, in other words the maximum expected stress and the element strength. It is obvious that the element is verified when the strength is higher than the expected stress due to the different load applications.

Since construction operation is full of many uncertainties in terms of load application and material properties. Some loads are permanently present like the own weight, some others are occasionally present like variable loads, snow, wind and so on. The materials have some defects due to the site or factory construction process. These uncertainties obligate the use of safety factors. Safety factors should be applied to both loads and strength. It means to increase the applied loads by some coefficients and decrease the strength of the materials.

In the following paragraph we introduce the load combinations with the amplification factors according to the Italian standards NTC2018.

3.4.1 Load combinations

As well described in the regulation, the combination of loads should be applied for ultimate limit state, exercise limit state, seismic combination, extra. For the Piles design, the verification according to the Italian standard NTC2018 paragraph 6.5.3.1.2 about SLU verification. The reduction coefficients and safety factors follow the approach N.01 with combination N.01 (A1+M1+R1), approach N.02 with combination N.01 (A2+M2+R1) and the seismic combination SLV is reported in point 7.11.1 of the NTC2018.

(A1, A2) are amplification factors for the loads and it can be determined from the following table as reported in the regulations NTC2018:

Tab. 6.2.I – Coefficienti parziali per le azioni o per l'effetto delle azioni

	Effetto	Coefficiente Parziale γ_F (o γ_E)	EQU	(A1)	(A2)
Carichi permanenti G_1	Favorevole	γ_{G1}	0,9	1,0	1,0
	Sfavorevole		1,1	1,3	1,0
Carichi permanenti $G_2^{(1)}$	Favorevole	γ_{G2}	0,8	0,8	0,8
	Sfavorevole		1,5	1,5	1,3
Azioni variabili Q	Favorevole	γ_{Qi}	0,0	0,0	0,0
	Sfavorevole		1,5	1,5	1,3

Table 3.1 A1 coefficient chapter (06) NTC2018

(M1, M2) are the coefficients of the soil properties, it can be determined from the following table in chapter.06 of NTC2018.

Tab. 6.2.II – Coefficienti parziali per i parametri geotecnici del terreno

Parametro	Grandezza alla quale applicare il coefficiente parziale	Coefficiente parziale γ_M	(M1)	(M2)
Tangente dell'angolo di resistenza al taglio	$\tan \varphi'_k$	$\gamma_{\varphi'}$	1,0	1,25
Coesione efficace	c'_k	$\gamma_{c'}$	1,0	1,25
Resistenza non drenata	c_{uk}	γ_{cu}	1,0	1,4
Peso dell'unità di volume	γ_γ	γ_γ	1,0	1,0

Table 3.2 M1 coefficient chapter 06 NTC2018

(R1) equals 1, it is the coefficient of the verification which means that if the result stresses, using the combination factors A1, divided by the soil strength, determined using the coefficient M1, is equal of higher than the unit (1), the design is verified.

Since the presence of some loads are not always present, the linear addition of the loads would be unreasonable. Factors A1 and A2 are the load combination factor. These factors take into consideration the frequency and repetition of the load.

The application of A1, A2 values for the combination of loads should be applied according to the load combination scheme described in NTC2018 chapter 2 as reported below:

2.5.3. COMBINAZIONI DELLE AZIONI

Ai fini delle verifiche degli stati limite, si definiscono le seguenti combinazioni delle azioni.

- Combinazione fondamentale, generalmente impiegata per gli stati limite ultimi (SLU):

$$\gamma_{G1} \cdot G_1 + \gamma_{G2} \cdot G_2 + \gamma_P \cdot P + \gamma_{Q1} \cdot Q_{k1} + \gamma_{Q2} \cdot \psi_{02} \cdot Q_{k2} + \gamma_{Q3} \cdot \psi_{03} \cdot Q_{k3} + \dots \quad [2.5.1]$$

- Combinazione caratteristica, cosiddetta rara, generalmente impiegata per gli stati limite di esercizio (SLE) irreversibili:

$$G_1 + G_2 + P + Q_{k1} + \psi_{02} \cdot Q_{k2} + \psi_{03} \cdot Q_{k3} + \dots \quad [2.5.2]$$

- Combinazione frequente, generalmente impiegata per gli stati limite di esercizio (SLE) reversibili:

$$G_1 + G_2 + P + \psi_{11} \cdot Q_{k1} + \psi_{22} \cdot Q_{k2} + \psi_{23} \cdot Q_{k3} + \dots \quad [2.5.3]$$

- Combinazione quasi permanente (SLE), generalmente impiegata per gli effetti a lungo termine:

$$G_1 + G_2 + P + \psi_{21} \cdot Q_{k1} + \psi_{22} \cdot Q_{k2} + \psi_{23} \cdot Q_{k3} + \dots \quad [2.5.4]$$

- Combinazione sismica, impiegata per gli stati limite ultimi e di esercizio connessi all'azione sismica E:

$$E + G_1 + G_2 + P + \psi_{21} \cdot Q_{k1} + \psi_{22} \cdot Q_{k2} + \dots \quad [2.5.5]$$

- Combinazione eccezionale, impiegata per gli stati limite ultimi connessi alle azioni eccezionali A:

$$G_1 + G_2 + P + A_d + \psi_{21} \cdot Q_{k1} + \psi_{22} \cdot Q_{k2} + \dots \quad [2.5.6]$$

Gli effetti dell'azione sismica saranno valutati tenendo conto delle masse associate ai seguenti carichi gravitazionali:

$$G_1 + G_2 + \sum_j \psi_{2j} Q_{kj} \quad [2.5.7]$$

Figure 3.3 Load Combinations NTC2018-Chap2.5.3

Tab. 2.5.I – Valori dei coefficienti di combinazione

Categoria/Azione variabile	ψ_{0j}	ψ_{1j}	ψ_{2j}
Categoria A - Ambienti ad uso residenziale	0,7	0,5	0,3
Categoria B - Uffici	0,7	0,5	0,3
Categoria C - Ambienti suscettibili di affollamento	0,7	0,7	0,6
Categoria D - Ambienti ad uso commerciale	0,7	0,7	0,6
Categoria E – Aree per immagazzinamento, uso commerciale e uso industriale Biblioteche, archivi, magazzini e ambienti ad uso industriale	1,0	0,9	0,8
Categoria F - Rimesse , parcheggi ed aree per il traffico di veicoli (per autoveicoli di peso ≤ 30 kN)	0,7	0,7	0,6

Table 3.3 Coefficient ψ for predominant loads (NTC2018)

Using all the previously explained coefficients we are able to find the final applied load due to the different limit states SLU, SLV, SLE, extra. In the following paragraph the evaluation of the strength or the capacity of the piles will be studied. At this point the verification would simply follow the reported equation:

$$F. s = \frac{\text{Applied load}}{\text{resistant load}} \geq 1 \text{ the element is verified.}$$

3.5 Micropile bearing capacity

Vertical load is by far the most common and relevant load condition for pile foundations. The load Q applied to the pile head is transmitted to the soil partially by normal stress (p) at the pile base, and partially by shear stress (skin friction) (S) at the lateral pile–soil interface.

$$Q = P + S = (\pi d^2/4) \cdot P + \sum \pi \cdot d \cdot L_i \cdot \tau \quad (\text{Eq-3.1})$$

Where Q is vertical axial load.

d the diameter.

L_i the length of the pile for each soil layer.

P is total point load.

S the total side resistance (or side friction or shaft resistance).

τ shear bond between pile shaft and soil.

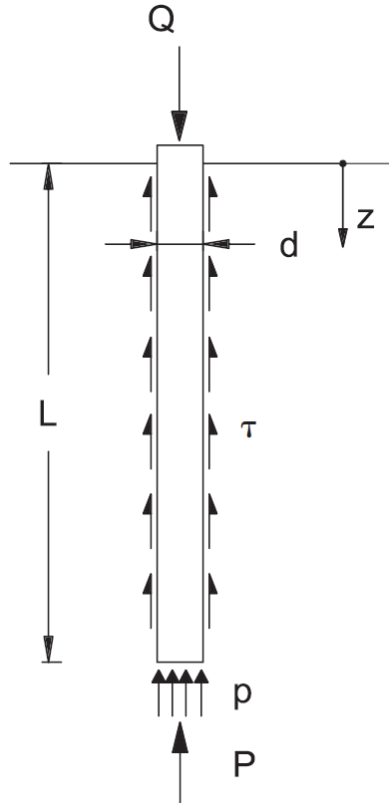


Figure 3.4 Pile load transfer mechanism.

Micropiles design doesn't differ a lot from the general design approach of the traditional piles. (Salgado 2008) suggest evaluating the bearing capacity of micropiles in accordance with the suggestions given for replacement piles of the CFA type.

The system must be capable of sustaining the loading conditions with the pile components at safe stress levels and displacements falling within acceptable limits. For conventional piling systems, where the large cross-sectional area results in high structural capacity and stiffness, the design is normally governed by the geotechnical load carrying capacity. With a micropile's smaller cross-sectional area, the pile design is more frequently governed by structural and stiffness considerations. The structural pile design is further increased by the high grout-to-ground bond capacities that can be obtained using the pressure grouting techniques. The major difference is the base resistance (P). Since the diameter of the micropiles is so small compared with the diameter of the traditional piles, the base resistance is also so small. It is advised in different design codes to calculate the base resistance as a percentage of the shaft resistance or to be neglected, which is a very conservative approach. According to the Italian regulations, the base resistance of micropiles is usually calculated as 15% of the shaft resistance. So, the Q_{ult} for micropiles can be written as following.

$$Q_{ult} = 1.15 \cdot S = 1.15 \cdot (\sum \pi \cdot d_s \cdot L_i \cdot \tau) \quad (\text{Eq-3.2})$$

Where Q is vertical axial load.

S the total side resistance (or side friction or shaft resistance).

d_s the increased diameter.

L_i the length of the pile for each soil layer.

τ shear bond between pile shaft and soil.

So, shortly we can divide the design of the micropiles into two main parts.

- 1- The evaluation of the geotechnical load capacity of the micropile, which requires appropriate estimation of the grout-ground bond which is the result of pressure grouting.
In this part the parameters to be estimated are:
 - a- Estimate load transfer parameters (grout-to-ground bond) for the different soil layers and determine the pile bond length required to support the loading.
 - b- Evaluate pile spacing for impact to geotechnical capacity from group effects.
- 2- The structural load capacity and stiffness performance of the micropile section depends mainly on the area of the composite reinforced micropile and the strength of the materials.
In this part the parameters to be estimated are:
 - A- Pile cased length structural capacity (bar and/or pipe reinforcement with grout)
 - B- Pile uncased length structural capacity (bar reinforcement with grout).
 - C- Grout to steel bond capacity.
 - D- Transition between reinforcement types (cased to uncased section).
 - E- Strain compatibility between structural components/ductility.
 - F- Reinforcement splice connections (bar and/or pipe reinforcement).
 - G- Pile to footing connection.

3.5.1 Geotechnical design

3.5.1.1 Geotechnical investigation requirements

The subsurface investigations required for the geotechnical design of micropiles are the same for any other type of deep foundation element such as drilled shafts or driven piles. The following investigations are necessary for a proper micropile design:

- General geology.
- Site history
- Description of geologic processes or modes of deposition of soil layers.
- Logs of soil borings completed in close proximity to the structure with the required number according to the Italian regulations (NTC2018). It includes description and classification of the soil strata encountered, unit weights, moisture contents, standard penetration tests (SPT) or cone penetrometer test (CPT) values, and description of groundwater conditions.
- An estimation of soil shear strength parameters. Determination of liquid and plastic limits for cohesive soils, and determination of the grain size distribution for granular soils.
- If rock is encountered, logs with rock classifications, penetration rates, degree of weathering and fracturing, recovery and RQD measurements, unconfined compressive strength, and driller's observations should be provided.
- Determination and discussion of the presence of hazardous and/or corrosive conditions if applicable. This may include resistivity, pH, and the presence of lead, sulfates, and chloride content.

3.5.1.2 Geotechnical design procedure

As mentioned previously, the geotechnical design includes the grout-ground bond and the length of bond length of the pile. It could be divided into some main design parameters:

1- **Selection of Micropile Spacing**

In all cases, the center-to-center spacing between individual micropiles should be at least 760 mm or 3 times the micropile diameter, whichever is greater. This spacing criterion was originally developed for driven piles, and it allows for potential deviations in drilling over significant depths and reduces group effects between adjacent micropiles.

The spacing of micropiles for structural foundation support will also depend on each specific application. It is a flexible parameter which can vary from an application to another as long as the number of the micropiles transfer safely the required load.

2- Selection of Micropile Cross Section:

To carry required axial loads, it is common for up to one half of the cross-sectional area of the micropile to comprise steel casing and/or steel reinforcing rod (s). The use of common casing sizes is preferred to avoid delays associated with material availability. In other words, the micropile diameter (cross section) is usually assumed based on the availability of the reinforcing system.

3- Selection of Micropile Length:

The total length of an individual micropile will be selected to satisfy the required geotechnical capacity by skin friction (shaft resistance) between the grout and the ground over a suitable depth in the soil variable layers.

The total length will also be checked to resist uplift forces and to provide additional lateral resistance where other sources of lateral load need to be considered in the design.

The maximum length of a micropile that can be achieved using common drilling equipments is up to 90 m, but the construction of such piles would have many economic and construction considerations and difficulties. It also considers the stability of the piles itself not to suffer buckling. So, usually the length limit of a micropile is around 30 m.

The grout to ground bond mainly depends on the construction procedure as explained before in micropiles construction types (A, B, C and D) as well as the soil characteristics.

The nominal bond strength for the four types of micropiles and all soil types are reported in the following table as mentioned in (FHWA-SA-97-070) (v00-06) of the design manual of micropiles.

Soil / Rock Description	Typical Range of Grout-to-Ground Bond Nominal Strengths (kPa)			
	Type A	Type B	Type C	Type D
Silt & Clay (some sand) (soft, medium plastic)	35-70	35-95	50-120	50-145
Silt & Clay (some sand) (stiff, dense to very dense)	50-120	70-190	95-190	95-190
Sand (some silt) (fine, loose-medium dense)	70-145	70-190	95-190	95-240
Sand (some silt, gravel) (fine-coarse, med.-very dense)	95-215	120-360	145-360	145-385
Gravel (some sand) (medium-very dense)	95-265	120-360	145-360	145-385
Glacial Till (silt, sand, gravel) (medium-very dense, cemented)	95-190	95-310	120-310	102-335
Soft Shales (fresh-moderate fracturing, little to no weathering)	205-550	N/A	N/A	N/A
Slates and Hard Shales (fresh-moderate fracturing, little to no weathering)	515-1380	N/A	N/A	N/A
Limestone (fresh-moderate fracturing, little to no weathering)	1035-2072	N/A	N/A	N/A
Sandstone (fresh-moderate fracturing, little to no weathering)	520-1725	N/A	N/A	N/A
Granite and Basalt (fresh-moderate fracturing, little to no weathering)	1380-4200	N/A	N/A	N/A

Table 3.4 Shear nominal strengths in FHWA-SA-97-070 (v00-06).

From the reported table we are able to define Shear nominal strength (τ) or as described the grout to ground bond, remembering the main design equation (Eq-3.2) of micropiles.

$$Q_{ult} = 1.15 \cdot S = 1.15 \cdot (\sum \pi \cdot d_s \cdot L_i \cdot \tau) \quad (\text{Eq-3.2}).$$

By assuming the pile diameter between (150-250) mm, obtaining (τ) from the table and determining the ultimate required loading level Q_{ult} by the means of load combinations on the structure, we are able to evaluate the pile length.

We must pay attention that d_s represents the expanded diameter due to the injection pressure.

$$d_s = \alpha d \quad (\text{Eq-3.3}).$$

Where d is the pile diameter.

α expansion coefficient due to injection pressure. Its value depends on the soil type. The values of are reported in the following table as reported in the book piles and pile foundations by Carlo Viggiani, Alessandro Mandolini, Gianpiero Russo.

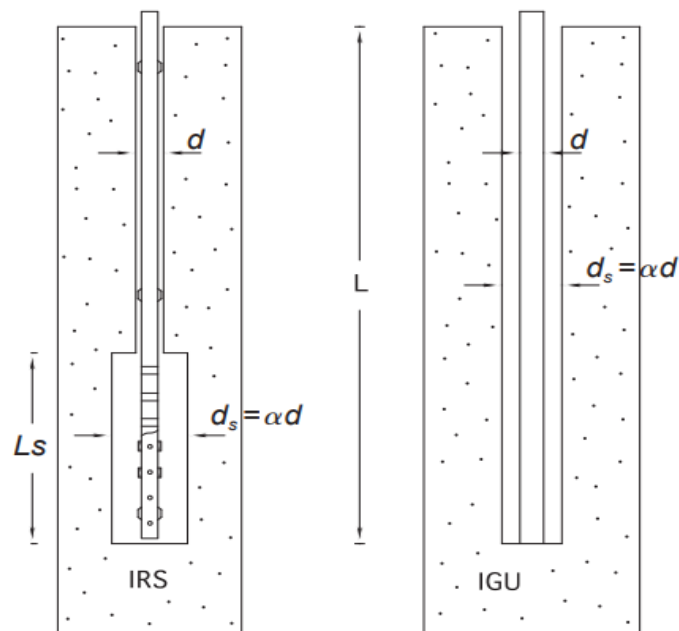


Figure 3.5 injection diameter.

pile Type of soil	Values of α		Minimum suggested grout volume*
	IRS	IGU	
Gravel	1.8	1.3–1.4	$1.5 V_s$
Sandy gravel	1.6–1.8	1.2–1.4	$1.5 V_s$
Gravelly sand	1.5–1.6	1.2–1.3	$1.5 V_s$
Coarse sand	1.4–1.5	1.1–1.2	$1.5 V_s$
Medium sand	1.4–1.5	1.1–1.2	$1.5 V_s$
Fine sand	1.4–1.5	1.1–1.2	$1.5 V_s$
Silty sand	1.4–1.5	1.1–1.2	IRS: $(1.5-2)V_s$; IGU: $1.5 V_s$
Silt	1.4–1.6	1.1–1.2	IRS: $2 V_s$; IGU: $1.5 V_s$
Clay	1.8–2.0	1.2	IRS: $(2.5-3)V_s$; IGU: $(1.5-2)V_s$
Marl	1.8	1.1–1.2	$(1.5-2)V_s$ for stiff layers
Marly limestone			
Weathered or fractured limestone	1.8	1.1–1.2	$(2-6)V_s$ or more for fractured layers
Weathered and/or fractured rock	1.2	1.1	$(1.1-1.5)V_s$ for slightly fractured layers $2 V_s$ or more for fractured layers

Table 3.5 Values of (α)

Since defining the characteristics of soil is misleading with just soil description so soil investigations should be done such as standard penetration test N_{SPT} and cone penetration test N_{CPT} . The values of (τ) the nominal shear resistance (nominal skin friction) is to be evaluated based on soil investigation results N_{SPT} and P_L as reported in the following equations. Piles and pile foundations (Viggiani, Mandolini, & Russo).

$$\tau = a + b \cdot P_L \quad (\text{Eq-3.4}).$$

$$\tau = \alpha + \beta \cdot N_{SPT} \quad (\text{Eq-3.5}).$$

$$\tau = c_{si} + q_{ci} \quad (\text{Eq-3.6}).$$

- q_{ci} is the cone resistance representative of the layer.

- c_{si} are empirical coefficient.

The values of the Coefficients a , b , α , β are given in the next table (Piles and pile foundations by Carlo Viggiani, Alessandro Mandolini, Gianpiero Russo (Viggiani, Mandolini, & Russo)).

Soil type	Micropile type	a (MPa)	b	α (MPa)	β (MPa)
Sand and gravel	IGU	0	0.10	0	0.005
	IRS	0.05	0.10	0.05	0.005
Silt and clay	IGU	0.04	0.06	0.04	0.004
	IRS	0.10	0.084	0.1	0.006
Weathered and fractured rock	IGU	0.04	0.10	–	–
	IRS	0.04	0.13	–	–

Table 3.6 coefficients a , b , α , β of shear resistance.

c_s	Source
0.074 ÷ 0.086 for sensitive clay 0.046 ÷ 0.056 for soft clay 0.021 ÷ 0.028 for silty clay or stiff clay Driven piles This method uses a corrected value of cone resistance $q_c - u$, where u is the pore pressure at the depth considered	Eslami and Fellenius (1997)
0.025 Displacement piles	Thorburn and MacVicar (1971)
0.017 for pure clay 0.011 for silty clay 0.0086 for silty clay with sand 0.0080 for sandy clay with silt 0.0069 for sandy clay Driven piles: for Franki piles: multiply number above by 0.7 For drilled shafts: multiply number above by 0.5	Aoki and Velloso (1975) Aoki <i>et al.</i> (1978)
0.012 for pure clay 0.011 for silty clay 0.010 for silty clay with sand 0.0087 for sandy clay with silt 0.0077 for sandy clay Non displacement piles	Lopes and Laprovitera (1988)

Table 3.7 C_s coefficient for clay

c_s	Source
0.008 for open ended steel pipe piles 0.012 for precast concrete and closed-ended steel pipe piles	Schmertmann (1978)
0.004 ÷ 0.006 per $D_R \leq 50\%$ 0.004 ÷ 0.007 per $50\% < D_R \leq 70\%$ 0.004 ÷ 0.009 per $70\% < D_R \leq 90\%$ Closed-ended pipe piles	Lee <i>et al.</i> (2003)
0.0040 for clean sand 0.0057 for silty sand 0.0069 for silty sand with clay 0.0080 for clayey sand with silt 0.0086 for clayey sand Driven piles: for Franki piles: multiply number above by 0.7 For drilled shafts: multiply number above by 0.5	Aoki and Velloso (1975) Aoki <i>et al.</i> (1978)
0.0027 for clean sand 0.0037 for silty sand 0.0046 for silty sand with clay 0.0054 for clayey sand with silt 0.0058 for clayey sand Replacement piles	Lopes and Laprovitera (1988)
0.0034 ÷ 0.006 This method uses a corrected value of cone resistance $q_c - u$, where u is the pore pressure at the depth considered	Eslami and Fellenius (1997)

Table 3.8 C_s coefficient for sand

3.5.2 Structural design

3.5.2.1 Evaluate allowable compression load for cased length

The allowable compression load for the cased length of a micropile is given as:

$$P_{c-allowable} = [0.4 f_{c-grout} \times A_{grout} + 0.47 F_{y-steel} (A_{bar} + A_{casing})] \quad (\text{Eq-3.7}).$$

Where.

$P_{c-allowable}$ = allowable compression load.

f_c = unconfined compressive strength of grout (typically a 28-day strength).

A_{grout} = area of grout in micropile cross section (inside casing only, discount grout outside the casing).

$F_{y-steel}$ = yield stress of steel.

A_{bar} = cross sectional area of steel reinforcing bar (if used).

A_{casing} = cross sectional area of steel casing.

3.5.2.1.1 Strain compatibility between grout, casing, and reinforcing rod.

It means that the design of the micropiles should be limited to a single strain for all the components steel casing, steel bars and grout. This strain obviously the lower strain of the components. To understand these limitations, we refer to (Section 8.16.2.3 of AASHTO, 2002) it reports that the maximum usable strain at the extreme concrete compression fiber is equal to 0.003". so, if the grout is limited to a compression strain of 0.003, the steel components must also be limited to this value. The stress in the steel at this strain level is equal to the Young's modulus of steel, E, multiplied by strain (i.e., 0.003). For a typical E for steel of 200,000 MPa, the allowable steel yield stress is then $200,000 \text{ MPa} \times 0.003 = 600 \text{ MPa}$. Therefore, the maximum stress based on considerations of grout failure is 600 MPa.

3.5.2.2 Evaluate allowable tension load for cased length

For projects in which the micropiles will be subject to tensile loads, the allowable tension load

$P_{t-allowable}$ for the cased length of a micropile can be calculated as neglecting any contribution of concrete in tension:

$$P_{t-allowable} = 0.55 F_{y-steel} (A_{bar} + A_{casing}) \quad (\text{Eq-3.8}).$$

where $F_{y-steel}$ is the minimum yield stress of the bar and casing.

3.5.3 Evaluate combined axial and flexural strength:

The application of lateral loads or overturning moments which could be a result of eccentricity, lateral loading as in the case of soil stabilization or many other factors at the ground surface create bending stresses in the micropile. These bending stresses cause additional compressive stresses other than those from vertical compression loads in the micropile. Allowable stresses in the cased length of the micropile are evaluated using a combined stress evaluation.

The applied bending moments in the micropile are calculated as a result of the different loads on the whole structure for sure considering all the load combinations previously discussed. The determination of the maximum bending moment can be calculated with the help of many finite element software. The following paragraph reports the evaluation of the structural capacity of the micropile in the bending case.

$$\frac{f_a}{F_a} + \frac{f_b}{\left(1 - \frac{f_a}{F'_e}\right) F_b} \quad (\text{Eq-3.9}).$$

Where

- (f_a) is the axial stress = $\frac{pc}{A_{\text{casing}}}$.
- (f_b) is the bending stress = $\frac{Mm}{S}$ where S is the elastic section modulus of the steel casing.
- (F_a) is the allowable axial stress as if axial force alone existed = $0.47 \times F_{y\text{-casing}}$.
- (F_b) is the allowable bending stress that would be permitted if bending moment alone existed = $0.55 F_{y\text{-casing}}$.
- (F'_e) is the Euler buckling stress.

$$F'_e = \frac{\pi^2 E}{F_s (Kl/r)^2} \quad (\text{Eq-3.10}).$$

- (E) is the elastic modulus of the steel casing.
- (F_s) is a factor of safety equal to 2.12.
- (K) is the effective length factor (assumed equal to 1.0)
- (l) is the unsupported length of the micropile.
- (r) is radius of gyration of the steel casing = $(I_{\text{casing}}/A_{\text{casing}})^{1/2}$

The contribution of a central reinforcing bar to bending strength is small compared to that of the casing, so, its effects on bending strength could be neglected. This approach is conservative by assuming that the maximum axial compression load, P_c , is carried by the steel casing only and the yield stress of the steel casing is used.

It is noted that a combined stress evaluation is not performed for the uncased length since micropiles are designed so that bending stresses are negligible within the uncased portion of the micropile. In other words, the steel casing will be placed to a sufficient depth so that bending moments below that depth tends to zero.

The following flow chart summarize the design flow of traditional micropiles.

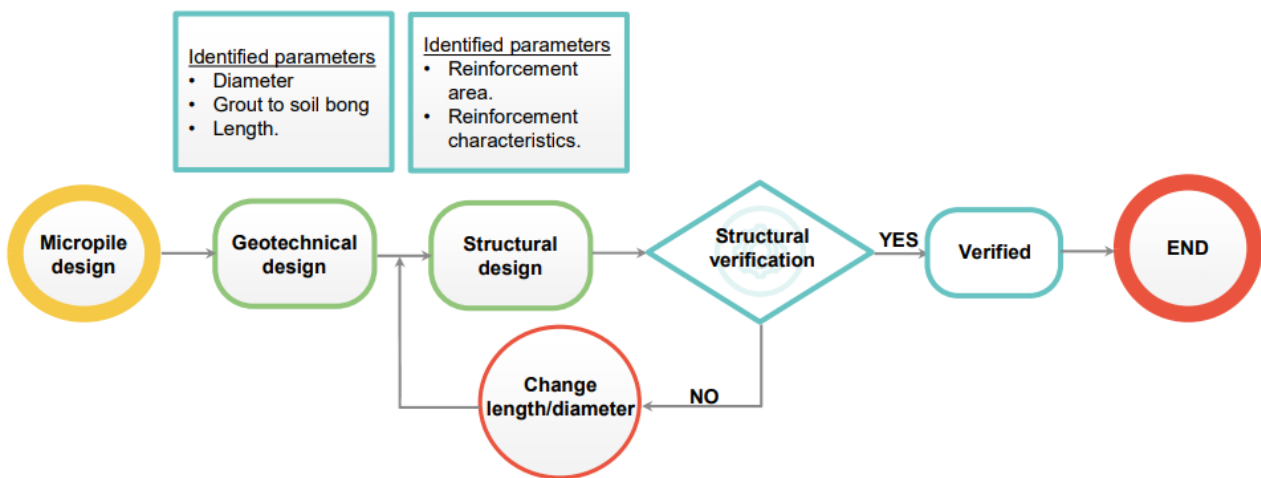


Figure 3.6 Micropile design flow.

4. Chapter 4: Elements design in glass fiber reinforced polymers.

Elements in bending and Shear

In the past decade many experiments have been made to understand the behavior of GFRP reinforced elements. It has been found that a GFRP reinforced beam compared with a steel reinforced beam designed for the same target load will behave in a different way due to differences in properties of the reinforcement. For the same area of reinforcement, a GFRP reinforced element was found to exhibit more deflection than a steel reinforced beam due to the much lower modulus of elasticity of GFRP compared with steel. It means that more strain will take place in GFRP and since concrete suffers cracks due to tension, so, the cracks in the case of GFRP are longer.

It has been reported that beams subjected to bending moments, GFRP reinforced concrete beams behave linearly up until cracking, and then linearly with reduced stiffness (Abdalla, 2002).

Several empirical design formulas have been developed through experiments of the flexural behavior of GFRP reinforced elements (beams, one-way Slabs).

Regarding the shear design of elements, Through the continue experiments, it has been found that the shear failure modes for GFRP beams are similar to that of steel reinforced beams. So, it has been assumed that summing the contributions of shear reinforcement and concrete is valid in the GFRP case (Guadagnini, Pilakoutas, & Waldron, 2003). This turns out to be conservative following the guides described by ACI 440 and underestimating following the guides described by ACI 318 (Yost, Gross, & Dinehart, 2001) (Deitz, Harik, & Gesund, 1999). Finally, these results forced to evaluate several empirical equations to move more accurately toward the prediction of the shear capacity of a GFRP reinforced element.

Two-way slabs

Investigations have found that punching shear will typically govern as a failure mechanism over bending for a GFRP reinforced slab under concentrated loading (El-Gamal, El-Salakawy, & Benmokrane, 2007) (Ospina, Alexander, & Cheng, 2003) (El-Ghandour, Pilakoutas, & Waldron, 2003) (Hassan, Ahmed, & Benmokrane, 2013) (Dulude, Hassan, Ahmed, & Benmokrane, 2013) (Bouguerra, Ahmed, El-Gamal, & Benmokrane, 2011).

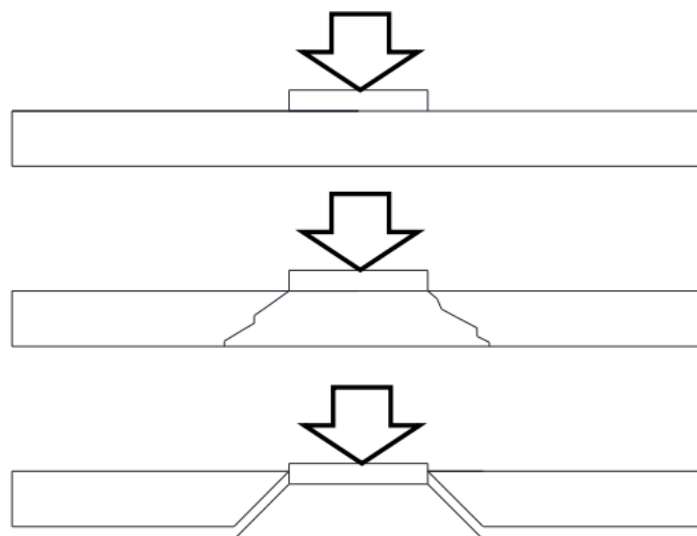


Figure 4.1 Punching failure scheme under concentrated load.

The previously reported figure shows the punching failure of slabs. It starts with inclined cracks under the loaded area. These cracks propagate to reach the other side of the loading area and finally a complete separation takes place.

Behavior under Flexural Load

Piles are one of the foundation types. They are structural members that support and transfer loads from the structure to the ground. Practically, pile can be considered as a special type of column that carries axial and flexural loads but with different cases of boundary conditions.

As previously explained that the urgent need for a substitution of steel leads to the application of the FRP tubes confined concrete technique. It is a new and rapidly increasing technique in the field of civil engineering structures. Although the beneficial effects of confinement of concrete are less in flexural as compared to axially loaded members, other advantages such as utilization of the FRP tubes as stay-in-place framework, ease of fabrication and speed of erection still makes this system attractive. The FRP tubes can be used successfully for different flexural structural members such as beams, columns, piles, bridge girders, pipes and tunnels. One of the earliest attempts to produce FRP/concrete beam elements was done by (Fardis and Khalili 1981) They proposed pouring concrete into FRP boxes. They also pointed out the mechanical role of FRP and concrete as follows:

1. FRP carries the tensile forces in the tension zone. This is the as in the steel reinforcement case which indicates that GFRP reinforcement is valid in tension.
2. It provides partial confinement of concrete in the compression zone, improving strength and ductility.
3. The concrete core provides compressive strength and rigidity and prevents local buckling of the FRP casing.

One of the most important experiments on the flexure behavior of beams made of FRP tubes was done by (Fam and Rizkalla, 2002) The diameter of these beams varies from 89 to 942 mm and the spans varies from 1.07 to 10.4 m. The study investigated the effects of concrete filling, cross-sectional configurations including tubes with a central hole, tube-in-tube with concrete filling in between, and different structures of the GFRP tubes. The study demonstrated that the flexural behavior was highly dependent on the stiffness and diameter-to-thickness ratio of the tube. Test results suggested that the contribution of concrete confinement to the flexural strength was insignificant; however, the ductility of the member was improved. It was found that in bending, the filling (grout) is more efficient for thin-walled tubes than it is for thick tubes. They also reported that the flexural strength can be increased by increasing the wall thickness. However, the failure mode could change to compression (brittle).



Figure 4.2 (Fam and Rizkalla, 2003) experiment

The continue research in the field is wide to stabilize a procedure of design and to have available commercial GFRP reinforcement with several diameters and applications.

In the following paragraphs the demonstration of the design procedure of micropiles in GFRP. The following chapter a practical case study applied using a commercial GFRP tube.

The design of micropiles as previously mentioned is divided into two steps. Firstly, the geotechnical design which mainly depends on the soil and concrete characteristics and the bond strength between them. Through the geotechnical design, the main parameters to be define are the length of the micropile and the number of micropiles in the case of having a pile group. Secondly, the structural design which mainly define the resisting structure of the pile. Through the structural design the role of the reinforcement with all its forms comes to light.

4.1 GFRP micropiles geotechnical design

Since the geotechnical design of micropiles does not include any parameters of the reinforcement, the geotechnical design is identically the same in all the cases regardless the type or the characteristics of the reinforcement. So, the geotechnical design would follow the same procedure reported in the previous chapter (3) point 3.5.1.1.2 with the following equations.

$$Q_{ult} = 1.15 \cdot S = 1.15 \cdot (\sum \pi \cdot d_s \cdot L_i \cdot \tau) \quad (\text{Eq-3.2}).$$

4.2 GFRP micropiles structural design

4.2.1 Evaluate allowable compression strength for GFRP Cased micropile

The allowable compression load for the cased length of a micropile with GFRP tube is the same in the case of steel rebars, replacing the strength properties of the steel with the GFRP properties as given:

$$P_{c-allowable} = [0.4 f_{c-grout} \times A_{grout} + 0.47 F_{u-GFRP} \times A_{casing}] \quad (\text{Eq:4.1})$$

Where;

$P_{c-allowable}$ = allowable compression load.

f_c = unconfined compressive strength of grout (typically a 28-day strength).

A_{grout} = area of grout in micropile cross section (inside casing only, discount grout outside the casing).

F_{u-GFRP} = ultimate stress of GFRP tube.

A_{casing} = cross sectional area of GFRP casing tube.

4.2.1.1 Strain compatibility between grout, casing.

The previously mentioned consideration of the strain limitation remains valid in the GRFP reinforcement case. It means that the design of the micropiles should be limited to a single strain for all the components GFRP casing and grout. This strain obviously the lower strain of the components. To understand these limitations. It limits the strain of the GFRP to the concrete strain which would decrease the (F_u) The strength of the reinforcing tube.

4.2.2 Evaluate allowable tension strength of GFRP Cased micropiles

For projects in which the micropiles will be subject to tensile loads, the allowable tension load $P_{t-allowable}$ for the cased length of a micropile can be calculated as:

$$P_{t-allowable} = 0.55 F_{u-GFRP} \times A_{casing} \quad (\text{Eq:4.2})$$

Where; F_{u-GFRP} is the strength of the casing.

4.2.3 Evaluate combined axial compression and bending GFRP cased micropiles

The application of lateral loads or overturning moments which could be a result of the eccentricity, lateral loading (soil stabilization) or many other factors at the ground surface create bending stresses in the micropile. The verification equation is the same reported before but using strength properties of GFRP reinforcement.

$$\frac{f_a}{F_a} + \frac{f_b}{\left(1 - \frac{f_a}{F'_e}\right) F_b} \quad (\text{Eq:4.3})$$

Where;

(f_a) is the axial stress = $\frac{P_c}{A_{\text{casing}}}$.

(f_b) is the bending stress = $\frac{M_m}{S}$ where S is the elastic section modulus of the casing.

(F_a) is the allowable axial stress as if axial force alone existed = $0.47Xf_{u\text{-GFRP}}$.

(F_b) is the allowable bending stress that would be permitted if bending moment alone existed = $0.55 F_{u\text{-GFRP}}$.

(F'_e) is the Euler buckling stress.

$$F'_e = \frac{\pi^2 E}{F_s (Kl/r)^2} \quad (\text{Eq:4.4})$$

(E) is the elastic modulus of the GFRP casing.

(F_s) is a factor of safety equal to 2.12.

(K) is the effective length factor (assumed equal to 1.0)

(l) is the unsupported length of the micropile.

(r) is radius of gyration of the steel casing = $(I_{\text{casing}}/A_{\text{casing}})^{1/2}$

5. Chapter 5: study case.

In our thesis we are reporting a practical project of the society ESSEBI Ingegneria (The designer) to the property of FERRERO (The client). The project is a structural system to reinforce an existing wall between two properties. The following figure reports the Location of the wall:



Figure 5.1 Location of the presented project.

The previously mentioned wall suffers multiple cracks, as well as the adjacent pavement as it could be seen in the following photographic pictures taken at the site visit:



Figure 5.2 Wall and pavement cracks.

These reported cracks could be a result of many factors such as:

- A) Un completed compaction works at the construction time.
- B) Differential settlement due to the loss of ground water level absorbed by the adjacent trees as reported in the following scheme:

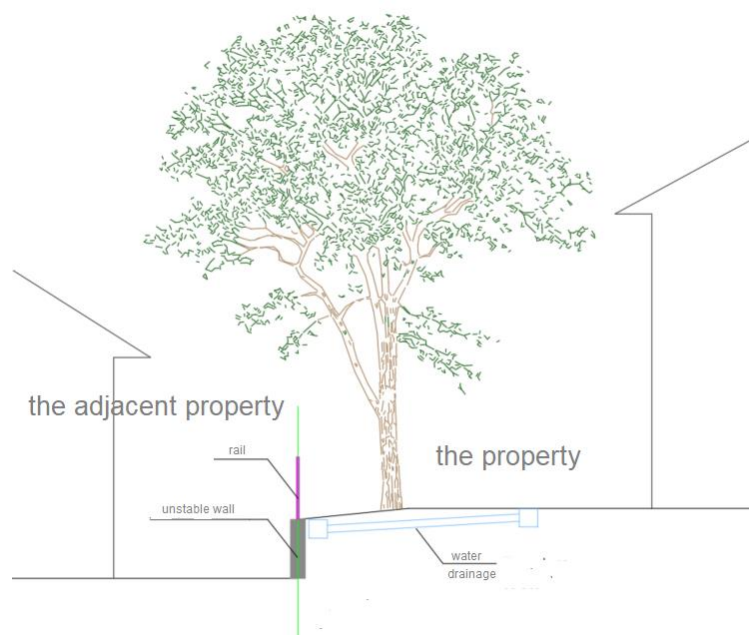


Figure 5.3 The wall's Current situation

Monitoring works have been performed to determine the criticality of the situation. These cracks could be passive cracks which means they do not expand, or active cracks which means its thickness expands. The critical situation is when the cracks are active. This requires immediate suitable actions. The monitoring system has been fixed on the cracks as reported in the following figure:



Figure 5.4 Monitoring systems.

Many alternatives have been studied to determine the best action to be performed. The study of alternatives structural systems was done based on multiple factors such as the accessibility of the machines, the minimum possibility of the adjacent property, economical factors and timing. The following paragraph reports a short description of the studied alternatives.

5.1 Proposed solutions

5.1.1 Solution (1):

The first solution is the realization of a completely new retaining wall positioned in the adjacent property. It could be considered as a replacement of the old-cracked wall with the new wall without the elimination of the existing cracked wall. This will help to avoid the collapse of the soil. The new predicted retaining wall will have the horizontal feet at sight as it could be seen in the following scheme:

Solution 1

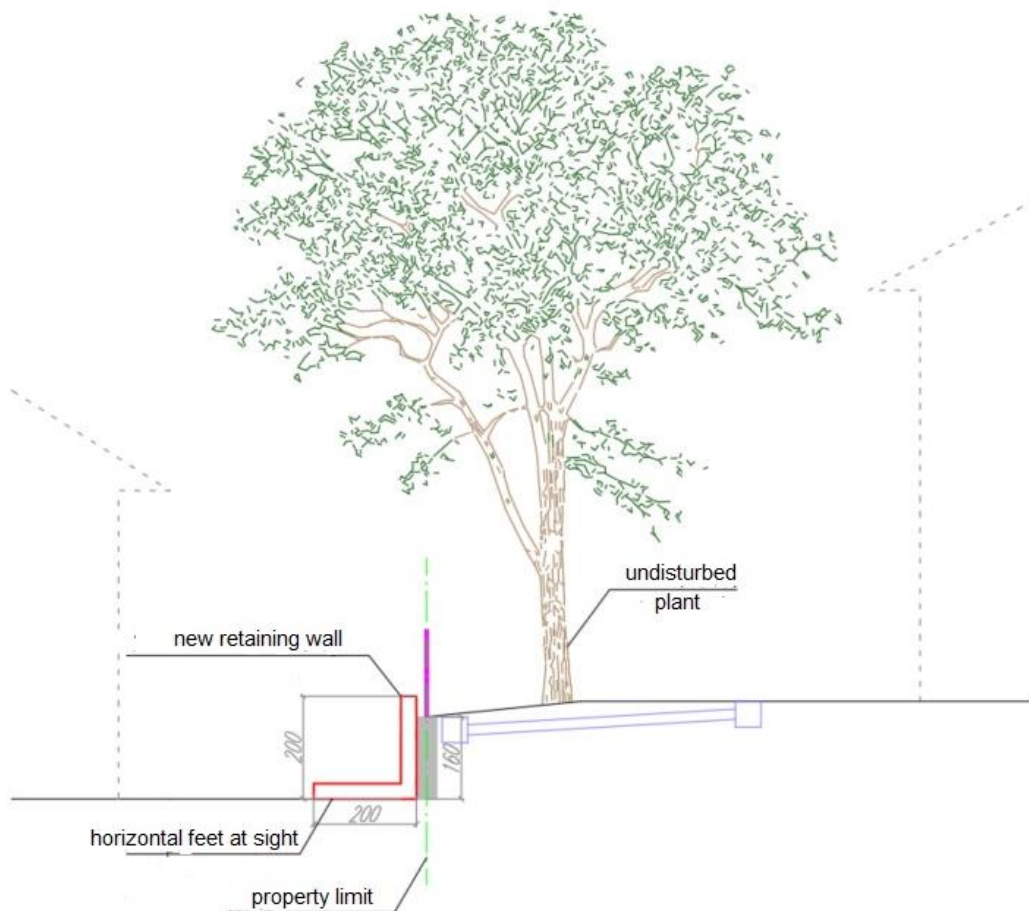


Figure 5.5 Solution (1).

In this case we also can avoid the excavation which will result in the fall of the existing trees. There is a permanent occupation of space in the adjacent property. There is no use of special machines.

5.1.2 Solution (2):

In order to avoid works in the adjacent property, the demolishing of the existing wall will take place. It will be followed by excavation with an inclination of 45° in order to avoid soil collapse. The excavation will result in the elimination of the trees. The same retaining wall will be constructed without the occupation of the adjacent property. the construction of a new retaining wall is reported in the following figure:

Solution 2

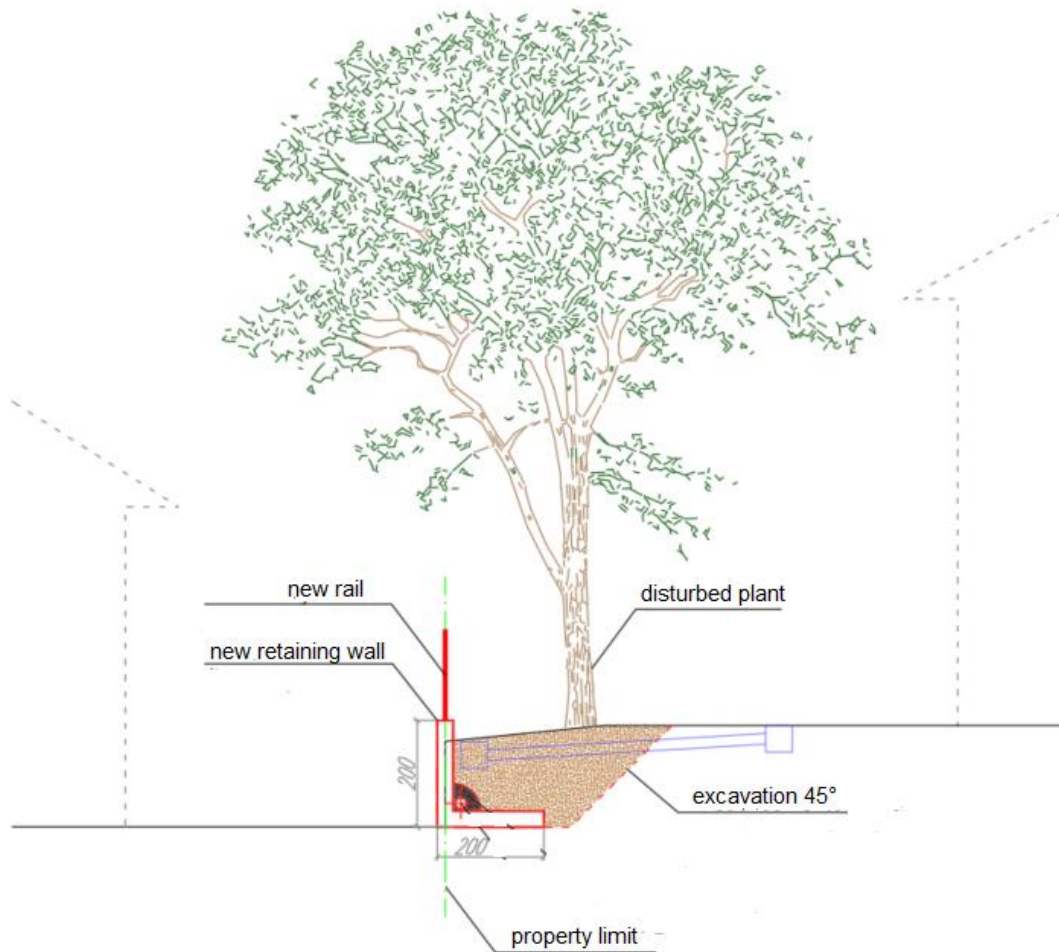


Figure 5.6 Solution (2)

In this case we also can avoid the permanent occupation of space in the adjacent property. The excavation will result in the elimination of the existing trees. There is no use of special machines.

5.1.3 Solution (3):

It is planned to install a plate on the downstream side of the existing wall and to hold it with several ties with an interval of 4 m. The drilling operations, necessary for the creation of the tie rod, must be carried out by positioning the machine in the adjacent property (as proposed in Figure). During this phase it will be necessary to ensure the stability of the wall to avoid its possible collapse. Once the drilling has been carried out, the insertion of the tie rod, the injection of the anchor bulb and its traction would be done using a special distribution plate.

Solution 3

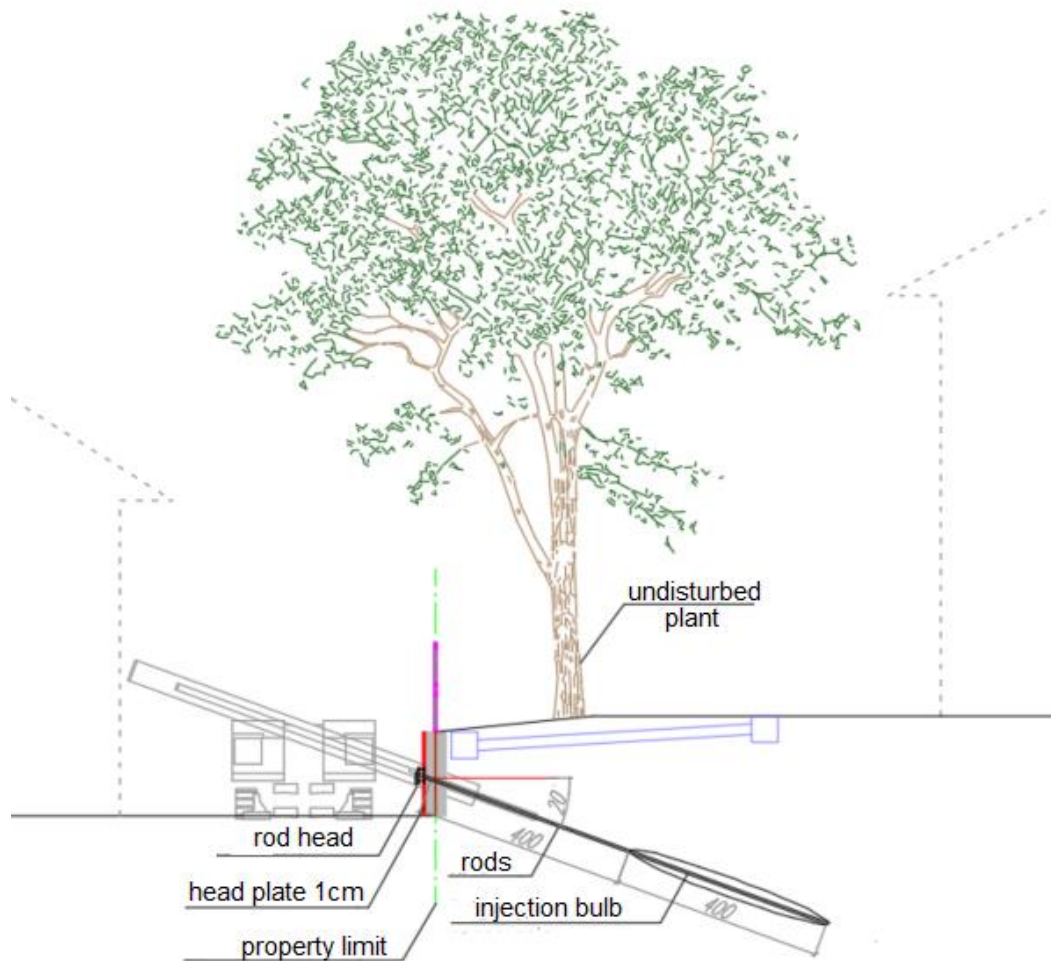


Figure 5.7 Solution (3)

This solution would occupy a minimal portion of the adjacent property and avoid excavation and felling of tall trees. The use of special machines is necessary in order to apply the tie rod without destroying the green area.

5.1.4 Solution (4)

The realization of a wall of micropiles positioned to the east of the tall trees. These would be made with an interval of 2.00 m.

For each of the micropiles, a trench at depth of 0.80 m would be excavated with an Air-spade compressed air system. The excavation is carried out thanks to a supersonic jet of compressed air (~2000 km/h) which penetrates the macropores of the soil creating fractures in the soil. The roots, which do not have this type of structure, remain completely unharmed. At this point, the trench would allow the insertion of a bar which, after having been made integral with the structure of the micropile by means of an anchoring handle, will be put under tension with a specific distribution plate. Also, in this case it will be necessary to place a Corten plate downstream of the wall.

Solution 4

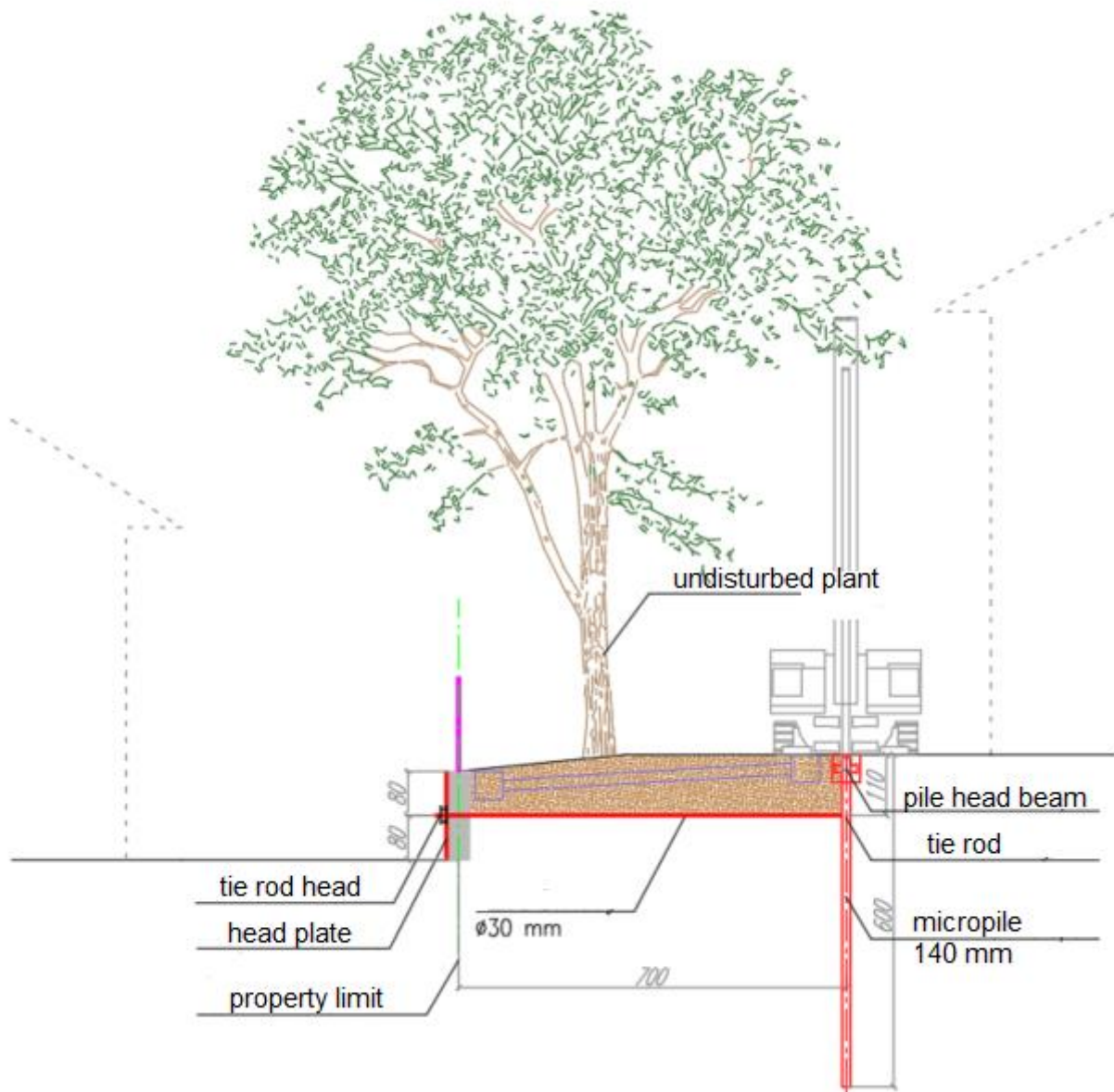


Figure 5.8 Solution (4)

5.1.5 Solution (5):

The construction of micropiles with a center distance of 0.50 m is planned behind the existing wall. During this phase it will be necessary to ensure the stability of the wall to avoid its possible collapse. A post head beam will be created which will result in a buried curb immediately upstream of the wall, as proposed in the Figure. This solution would avoid excavation, cutting down the plants and taking up space on the adjacent property.

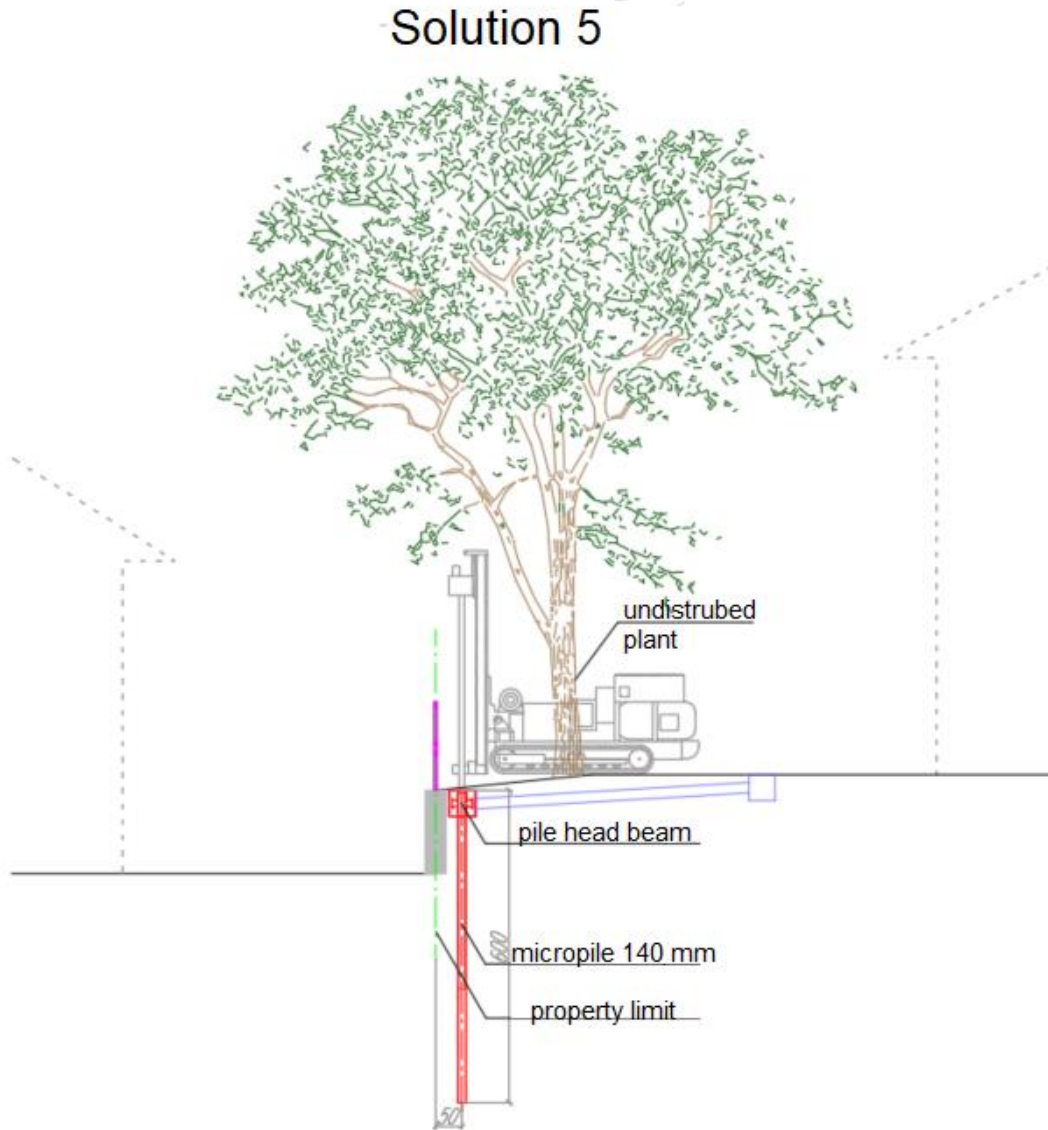


Figure 5.9 Solution (5).

5.1.6 Solution (6):

This solution incorporates what was proposed in solution 5, in addition to the demolition of the existing wall. The existing wall will be replaced by cladding wall downstream of the micropiles, as proposed in figure. In this case, the intervention would not occupy the adjacent property since by knocking down the existing wall, it will be possible to rebuild it in the same position.

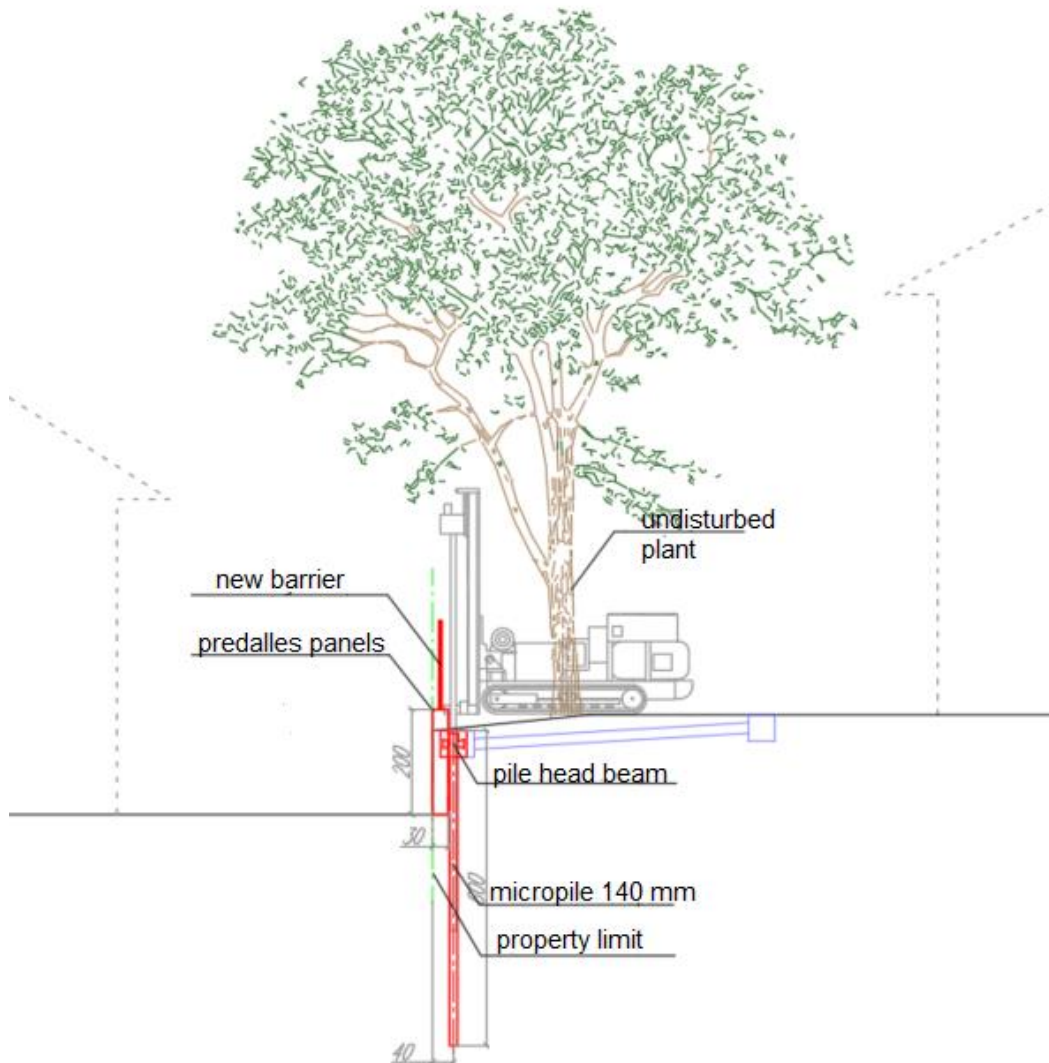


Figure 5.10 Solution 6

This solution results in no occupation of the adjacent property. By replacing the damaged wall, the safety factors are much higher as well as the visual situation.

The previous paragraphs report all the studied solutions. All these solutions at the structural level are valid at all the security and safety levels. The other important factors of the comparison are the occupation of the adjacent property temporarily or permanently, the demolition of the existing wall, the usage of heavy or particular machines, excavation, reduction of the green area and also economical level. The next table summarizes the comparison:

Solution Number	Adjacent property occupation	Demolition of the existing wall	Usage of heavy or particular machines	Excavation	Reduction of the green area	Economical
1	Yes (permanently)	No	No	No	No	25000 €
2	No	Yes	Yes	Yes	Yes	45000 €
3	Yes (temporarily)	No	Yes	No	No	36000 €
4	Yes (temporarily)	No	Yes	No	No	36000 €
5	No	No	Yes	No	No	37000 €
6	Yes (temporarily)	Yes	Yes	No	No	47000 €

Table 5.1 Solutions comparison summary

The economic calculations were done applying the regional price lists published by the country. Since the occupation permanently of the other property is not possible the first solution was excluded. The other solutions at the economic level are similar. The previously reported table shows that the solutions of the micropiles could cost a little more but have more advantages. These advantages could be avoiding the occupation of the other property permanently, avoiding the reduction of the green areas and avoiding the extended excavation.

At last, it was decided to apply solution n (6), which consists of the construction of micropiles behind the cracked existing wall then it would be followed by the demolition of the existing wall and finally construct a cladding wall of the type (Predalles). The new cladding walls would be connected to the piles' cap beam as reported in the following figure:

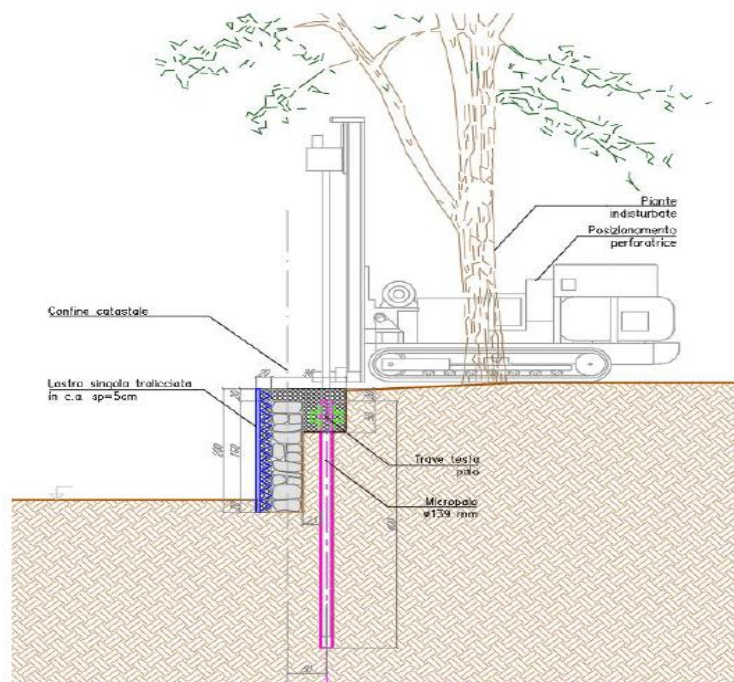


Figure 5.11 Solution (6) description

The following paragraphs would show the complete design of the steel reinforced micropiles with the use of the software Dolmen. Dolmen software gives a complete analysis report and a complete verification. The verification was also checked by the software VCASLU. The internal actions were extracted from the software Dolmen and applied directly on VCASLU after a complete definition of a micropile geometrical and material properties.

5.2 Project description

The project is considered a wall of micropiles with spacing of 50 cm. Each micropile has a diameter of 140 mm and the diameter of the reinforcement 114.30 mm. The reinforcement is considered a steel tube of a thickness = 8.00 mm of steel S355. The length of the micropiles is 5.00 m. The piles' cap is a beam of a cross section 55.00X70.00 cm².

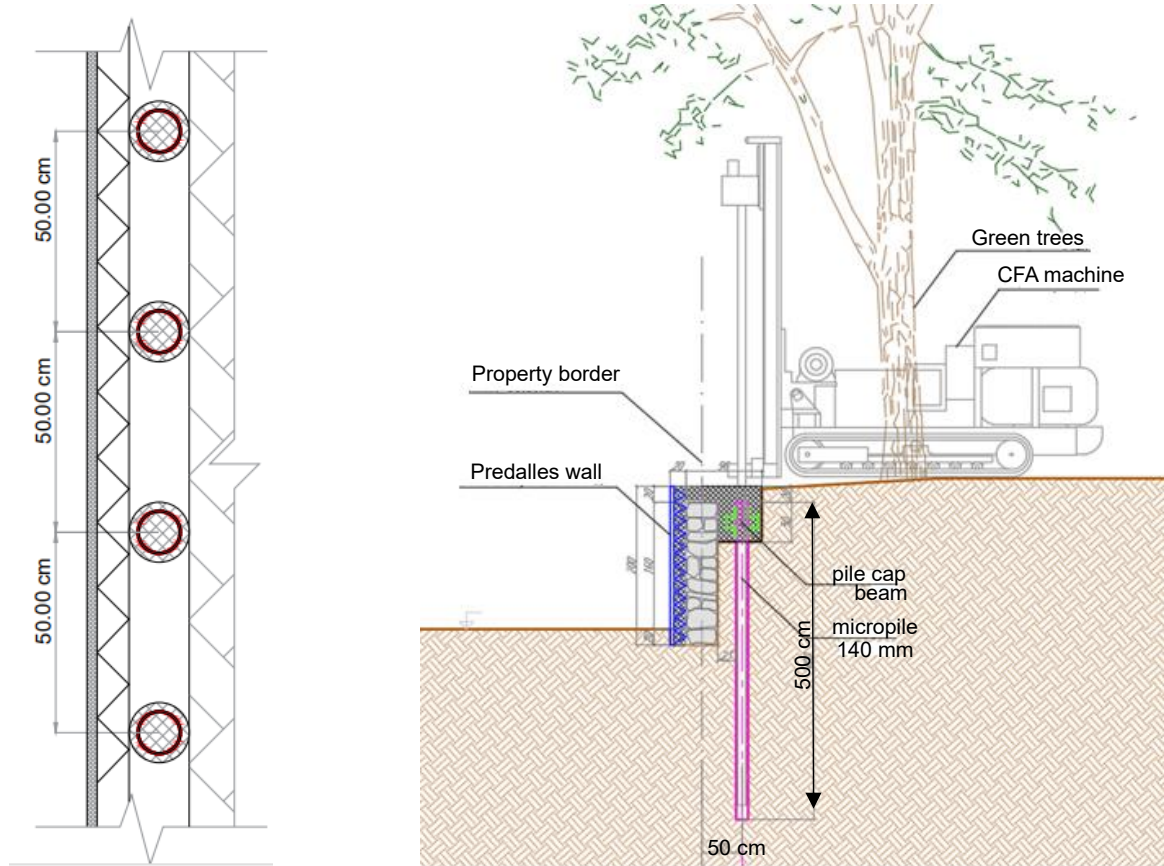


Figure 5.12 Cross section project scheme

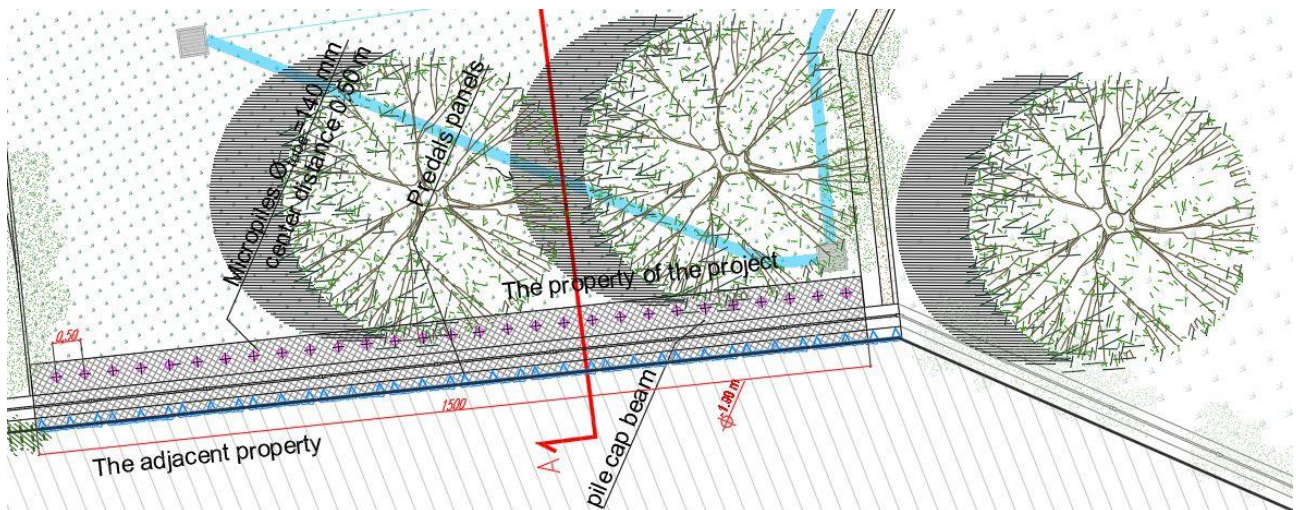


Figure 5.13 plan Scheme of the project

5.3 Project materials

The following materials are initially assumed with the previously mentioned dimensions to be used in the verifications, if the calculations are verified so we can definitively consider the following materials properties, otherwise the assumed dimensions should be modified and/or the materials properties.

The up following materials properties follow the Italian construction regulations (NTC2018).

Reinforced Concrete

Characteristic resistance C25/30	$f_{ck} = 25 \text{ N/mm}^2$ $f_{cd} = 14.17 \text{ N/mm}^2$ $\gamma_c = 25 \text{ kN/m}^3$
The minimum concrete cover 5 cm	5 cm
Exposure class	XC2
Consistency class	S4
Water//cement ratio	<0.45
Maximum aggregate diameter	25 mm

Steel reinforcement (cap beam)

Steel bars reinforcement B450C	$f_{tk} \geq 540 \text{ N/mm}^2$ $f_{yk} \geq 450 \text{ N/mm}^2$ $f_{yd} = 391 \text{ N/mm}^2$ $\gamma_s = 78.5 \text{ kN/m}^3$
--------------------------------	---

Micropiles

Steel pipe of type S355 (UNI EN 10025-2)	$f_{tk} = 510 \text{ N/mm}^2$ $f_{yd} = 355 \text{ N/mm}^2$ $\gamma = 78.5 \text{ kN/m}^3$
--	--

Soil layers

Soil composite of a single layer with the following properties:

	Layer 1
Description	Sand
Friction angle (ϕ') [°]	30
cohesion (c') [daN/cm ²]	0
Undrained resistance (s_u) [daN/cm ²]	0
Permeability (m) [cm/s]	0.001
Unit weight above water level (γ_d) [daN/cm ³]	0.0018
Unit weight under water level (γ_d) [daN/cm ³]	0.002

5.4 Applied loads

A) The own weight of the structure elements.

The own weight of the elements would be calculated automatically by the software by defining the unit weight of all the materials as follow:

Unit weight of reinforced concrete.

$$\gamma = 25 \text{ kN/m}^3$$

Unit weight of Steel reinforcement.

$$\gamma = 78.5 \text{ kN/m}^3$$

B) Variable Loads.

Variable load of the transitional and definitive construction phases.

$$q = 4 \text{ kN/m}^2$$

Variable load of trees' roots

$$q = 10 \text{ kN}$$

C) Soil Pressure Loads.

Soil unit weight.

$$\gamma = 18 \text{ kN/m}^3$$

Soil friction angle.

$$\phi_k = 30^\circ$$

Cohesion.

$$c' k = 0.0 \text{ kPa}$$

D) Snow.

The snow load is calculated as follows according to (D.M. 17/01/2018) paragraph. 3.4.

Due to the variability of snowfall from area to area, to determine the snow load on the ground q_{sk} , it is necessary to refer to the local climate and exposure conditions; for this purpose, the standard divides the national territory into three different groups according to the frequency of snowfall and for each area identifies the possibility that the building may be located at different heights above sea level.

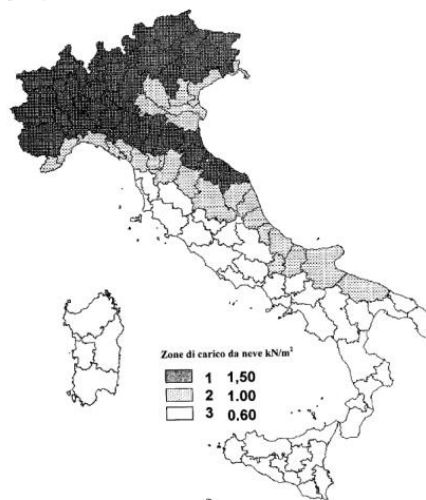


Figura 3.4.1 – Zone di carico da neve

Figure 5.14 Snow groups.

$$q_s = \mu_i * q_{sk} * C_E * C_t = 1.62 \text{ kN/m}^2$$

where;

(q_{sk}) for the area is: $q_{sk} = 2.032 \text{ kN/m}^2$

assuming $\mu_i = 0.80$ valid for single-pitch roofs with an inclination of less than 30° - where $\alpha = 0^\circ$

exposure coefficient $C_E = 1$

thermal coefficient $C_t = 1$

(In the modelling the snow load is not reduced as it is directly applied to the road surface, therefore the q_{sk} value equal to 2.03 kN/m^2 is directly considered.)

E) Seismic

The seismic action is evaluated only for the definitive phase as the response spectrum of the structure as described in the Ministerial Decree 17/01/18 Technical standards on constructions. In terms of acceleration the expression is:

$$\begin{aligned}
 S_u(T) &= a_g \cdot S \cdot \frac{F_0}{q} \left[\frac{T}{T_B} + q \left(1 - \frac{T}{T_B} \right) \right] & \alpha < T < T_B \\
 S_u(T) &= a_g \cdot \frac{S F_0}{q} & T_B < T < T_C \\
 S_u(T) &= a_g \cdot \frac{S F_0}{q} \left(\frac{T_C}{T} \right) & T_C < T < T_D \\
 S_u(T) &= a_g \cdot \frac{S F_0}{q} \left(\frac{T_C \cdot T_D}{T} \right) & T_B < T
 \end{aligned}$$

Figure 5.15 Spectrum accelerations

The spectrum can be defined numerically once the following parameters are known:

- a_g = Maximum horizontal acceleration on category A of ground soil.
- F_0 = maximum value of the spectrum amplification factor of horizontal acceleration.
- T_C^* = period of the constant velocity portion of the horizontal acceleration spectrum.

The structure in question can be classified in Class II (constructions whose use involves normal crowding) as point 2.4.2 of the NTC while it can be assumed that the nominal life V_N must be ≥ 50 years (table 2.4.I), it follows that the reference period for the seismic action is $V_R = V_N \cdot C_U = 50$ years, having assumed the use coefficient C_U equal to 1.0 from (table 2.4. II.). The seismic vulnerability checks for the ultimate limit state of safeguarding human lives (SLV) are reported below. The design earthquake (SLV) corresponds to a probability of exceeding in the reference period of the structure of 10% (return period T_R of the seismic action of 475 years).

All the previously defined coefficients are applied as well as the project location (latitude, longitude) are applied on the provided software of the Italian national standards to evaluate the response spectrum.

The coordinates of the project is in **Comune di Pino Torinese** with:

Longitude: 7.78026

Latitude: 45.04002

SLATO LIMITE	T_R [anni]	a_g [g]	F_0 [-]	T_C^* [s]
SLO	30	0.021	2.605	0.172
SLD	50	0.026	2.602	0.189
SLV	475	0.049	2.755	0.272
SLC	975	0.058	2.803	0.294

Table 5.2 acceleration- return time calculations

The other parameters necessary for the definition of the maximum acceleration expected at the site are:

S= factor that considers the stratigraphic profile of the foundation soil and the topographic conditions through the relationship:

$$S = S_s \cdot S_t$$

Where S_s the stratigraphic amplification coefficient (Tab. 3.2.IV D.M. 17/01/18) for category C of soil assumed to be equal to 1,50.

S_T the topographic amplification coefficient (Tab. 3.2.V D.M. 17/01/18) assumed to be equal to 1.0 valid for topographic category T1.

The maximum acceleration value expected at the site is evaluated with the following relation:

$$a_{\max} = S_s * S_T * a_g = 0,0735g$$

The design spectrum used for the verification of reinforced concrete structures provides for a structure factor $q=1.0$.

Parametri e punti dello spettro di risposta orizzontale per lo stato SLV

Parametri indipendenti

STATO LIMITE	SLV
a_g	0.049 g
F_o	2.755
T_c	0.272 s
S_s	1.500
C_c	1.614
S_T	1.000
q	1.000

Parametri dipendenti

S	1.500
η	1.000
T_B	0.146 s
T_C	0.438 s
T_D	1.797 s

Espressioni dei parametri dipendenti

$$S = S_s \cdot S_T \quad (\text{NTC-08 Eq. 3.2.5})$$

$$\eta = \sqrt{10/(5+\xi)} \geq 0,55; \quad \eta = 1/q \quad (\text{NTC-08 Eq. 3.2.6; §. 3.2.3.5})$$

$$T_B = T_c / 3 \quad (\text{NTC-07 Eq. 3.2.8})$$

$$T_C = C_c \cdot T_c \quad (\text{NTC-07 Eq. 3.2.7})$$

$$T_D = 4,0 \cdot a_g / g + 1,6 \quad (\text{NTC-07 Eq. 3.2.9})$$

Espressioni dello spettro di risposta (NTC-08 Eq. 3.2.4)

$$0 \leq T < T_B \quad S_c(T) = a_g \cdot S \cdot \eta \cdot F_o \cdot \left[\frac{T}{T_B} + \frac{1}{\eta \cdot F_o} \left(1 - \frac{T}{T_B} \right) \right]$$

$$T_B \leq T < T_C \quad S_c(T) = a_g \cdot S \cdot \eta \cdot F_o$$

$$T_C \leq T < T_D \quad S_c(T) = a_g \cdot S \cdot \eta \cdot F_o \cdot \left(\frac{T_C}{T} \right)$$

$$T_D \leq T \quad S_c(T) = a_g \cdot S \cdot \eta \cdot F_o \cdot \left(\frac{T_C \cdot T_D}{T^2} \right)$$

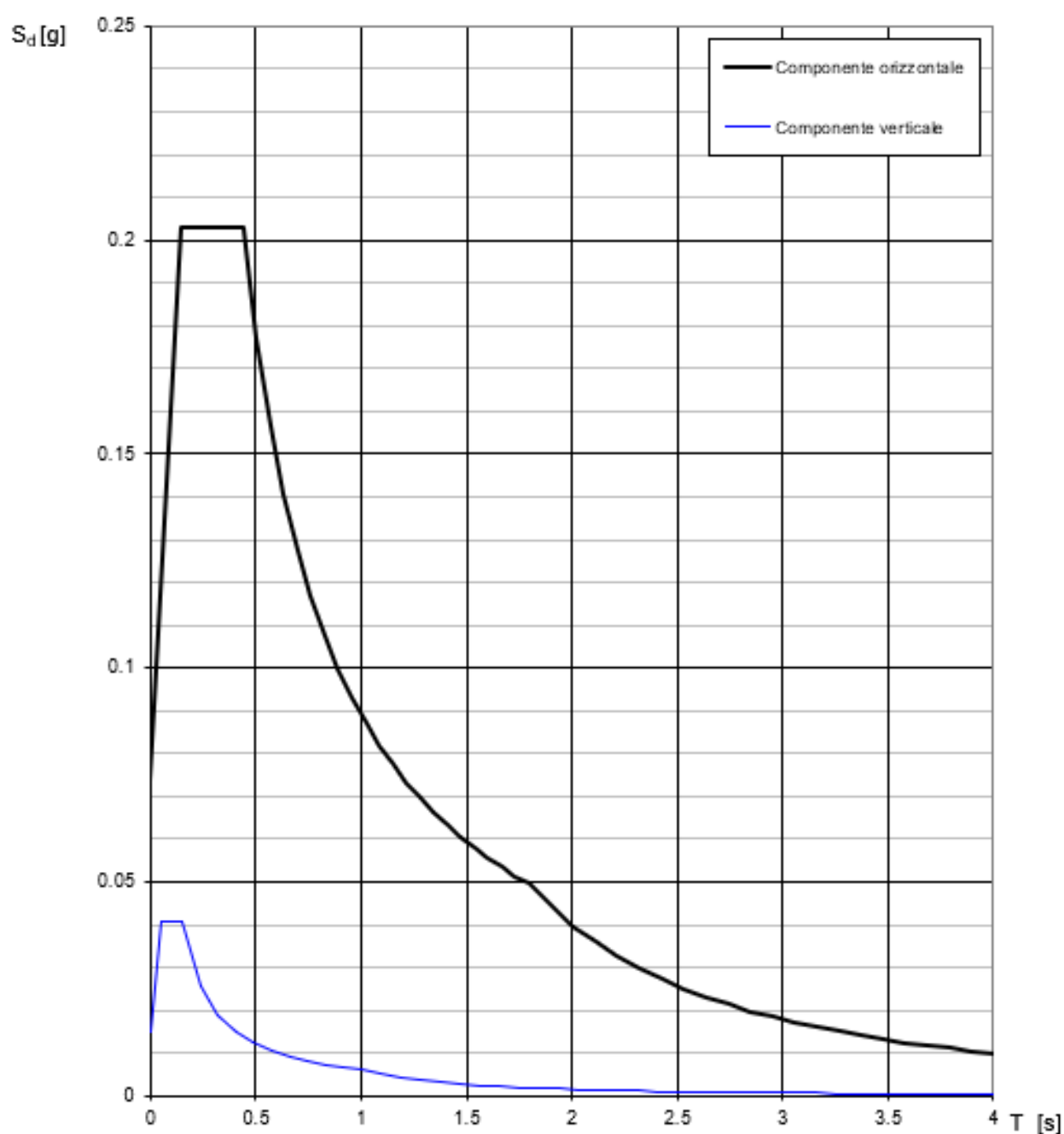
Lo spettro di progetto $S_d(T)$ per le verifiche agli Stati Limite Ultimi è ottenuto dalle espressioni dello spettro elastico $S_e(T)$ sostituendo η con $1/q$, dove q è il fattore di struttura. (NTC-08 § 3.2.3.5)

Punti dello spettro di risposta

	T [s]	Se [g]
	0.000	0.074
T_B	0.146	0.203
T_C	0.438	0.203
	0.503	0.177
	0.568	0.157
	0.633	0.141
	0.697	0.128
	0.762	0.117
	0.827	0.108
	0.891	0.100
	0.956	0.093
	1.021	0.087
	1.085	0.082
	1.150	0.077
	1.215	0.073
	1.279	0.070
	1.344	0.066
	1.409	0.063
	1.473	0.060
	1.538	0.058
	1.603	0.056
	1.667	0.053
	1.732	0.051
T_D	1.797	0.050
	1.902	0.044
	2.006	0.040
	2.111	0.036
	2.216	0.033
	2.321	0.030
	2.426	0.027
	2.531	0.025
	2.636	0.023
	2.741	0.021
	2.846	0.020
	2.951	0.018
	3.056	0.017
	3.161	0.016
	3.266	0.015
	3.370	0.014
	3.475	0.013
	3.580	0.012
	3.685	0.012
	3.790	0.011
	3.895	0.011
	4.000	0.010

Table 5.3 SLV spectrum values.

Spettri di risposta (componenti orizz. e vert.) per lo stato li SLV



La verifica dell' idoneità del programma, l' utilizzo dei risultati da esso ottenuti sono onere e responsabilità esclusiva dell' utente. Il Consiglio Superiore dei Lavori Pubblici non potrà essere ritenuto responsabile dei danni risultanti dall' utilizzo dello stesso.

Figure 5.16 SLV spectrum graphs.

5.5 Loads combinations

The load conditions considered for the purposes of verifying the load-bearing structural elements are those provided for by the current Italian standards NTC2018 C.2.5.3 knowing the following action forces:

- Own weight.
- Permanent loads.
- Variable loads.
- Seismic load.

The next previously described combinations in chapter 3 are directly identified on the used software dolmen.

5.5.1 Static analysis:

The static analysis in the study is evaluated as reported in the next paragraph.

5.5.1.1 SLU approach [1] combination (A1+M1+R1)

Load combination

The intensity of the actions, or the effect of the actions, is amplified by applying the following partial safety coefficients at loads:

$$\gamma_{G1} = 1.30$$

$$\gamma_{G2} = 1.50$$

$$\gamma_{Qi} = 1.50$$

Soil pressure

The partial safety coefficients applied to the mechanical characteristics of the soil:

$$\gamma_j = 1.30$$

$$\gamma_c = 1.50$$

$$\gamma_{su} = 1.50$$

$$\gamma_g = 1$$

Coefficients for the pull-out resistance:

The safety coefficients listed below apply to the pull-out resistance, obtained with an analytical method:

Active tie rod, permanent: $\gamma_R = 2.16$

Passive, permanent tie: $\gamma_R = 2.16$

5.5.1.2 SLU approach [2] combination (A2+M2+R1)

Load combination

The intensity of the actions, or the effect of the actions, is amplified by applying the following partial safety coefficients at loads:

$$\gamma_{G1} = 1.00$$

$$\gamma_{G2} = 1.30$$

$$\gamma_{Qi} = 1.30$$

Soil pressure

The partial safety coefficients applied to the mechanical characteristics of the soil:

$$\gamma_j = 1.25$$

$$\gamma_c = 1.25$$

$$\gamma_{su} = 1.40$$

$$\gamma_g = 1$$

Coefficients for the pull-out resistance:

The safety coefficients listed below apply to the pull-out resistance, obtained with an analytical method:

Active tie rod, permanent: $\gamma_R = 2.00$

Passive, permanent tie: $\gamma_R = 2.20$

5.5.1.3 SLV combination (A=1+M=1+R1)

Seismic combination coefficients

The intensity of the actions, or the effect of the actions, is amplified by applying the following partial safety coefficients at loads:

$$\gamma_{G1} = 1.00$$

$$\gamma_{G2} = 1.00$$

$$\gamma_{Qi} = 1.00$$

Soil pressure

The partial safety coefficients applied to the mechanical characteristics of the soil:

$$\gamma_j = 1.00$$

$$\gamma_c = 1.00$$

$$\gamma_{su} = 1.00$$

$$\gamma_g = 1.00$$

Coefficients for the pull-out resistance:

The safety coefficients listed below apply to the pull-out resistance, obtained with an analytical method:

Active tie rod, permanent: $\gamma_R = 2.16$

Passive, permanent tie: $\gamma_R = 2.10$

5.6 Verification

The verification of the piles in the project has been done applying different construction phases since the load application varies in both phases.

Phase (1) description:

Phase (1) describes the initial phase, where the installation of the required micropiles take place. The retaining wall of micropiles would be place where the soil at both sides at the same level. The following figure describes the scheme of the phase.

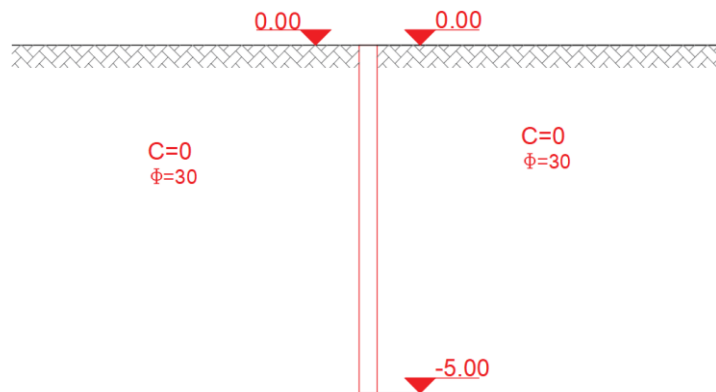


Figure 5.17 Scheme of phase (1)

Phase (2) description:

Phase (2) describes the following final situation, where the installation of the micropiles has been completed, and effectively resist the conditions of the previous phase. Demolition of the damaged wall would take place until an elevation of -2.00 from the soil surface. This demolition would be followed by the construction of the Predalles.

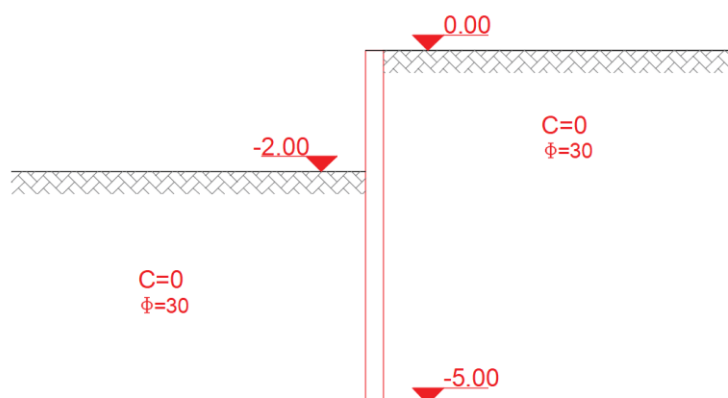


Figure 5.18 Scheme of phase 2

5.6.1 Traditional steel micropile verification

5.6.1.1 Analysis of approach [1] combination

5.6.1.1.1 approach [1] Phase (1) results

The phase results are obtained Using the Software (DOLMEN). The software calculates the soil pressure along the structure as well as the combination of load and gives finally the internal action results. These results are reported in terms of stresses, deformations, constraint reactions, pressures in the ground and results of the thrusts.

The following figures are extracted from the software design report which report the respectively soil pressure along the micropile, the accumulative pressure results and moment arm and internal actions (bending moment, shear force, axial forces) along the pile group (retaining wall of micropiles) and deformation resulted in phase (1).

Soil pressure along the micropiles results:

Soil pressure												
Elevation [cm]	Active pressure [daN/cm ²]						Passive pressure [daN/cm ²]					
	σ_v	σ_h	U	σ'_v	σ'_h	τ	σ_v	σ_h	U	σ'_v	σ'_h	τ
0	0.005	0.002	0	0.005	0.002	0	0.005	0.002	0	0.005	0.002	0
-8.33	0.02	0.009	0	0.02	0.009	0	0.02	0.009	0	0.02	0.009	0
-16.67	0.039	0.017	0	0.039	0.017	0	0.039	0.017	0	0.039	0.017	0
-25	0.058	0.026	0	0.058	0.026	0	0.058	0.026	0	0.058	0.026	0
-33.33	0.078	0.034	0	0.078	0.034	0	0.078	0.034	0	0.078	0.034	0
-41.67	0.098	0.043	0	0.098	0.043	0	0.098	0.043	0	0.098	0.043	0
-50	0.117	0.051	0	0.117	0.051	0	0.117	0.052	0	0.117	0.052	0
-58.33	0.136	0.06	0	0.136	0.06	0	0.136	0.06	0	0.136	0.06	0
-66.67	0.156	0.068	0	0.156	0.068	0	0.156	0.069	0	0.156	0.069	0
-75	0.176	0.077	0	0.176	0.077	0	0.176	0.078	0	0.176	0.078	0
-83.33	0.195	0.085	0	0.195	0.085	0	0.195	0.086	0	0.195	0.086	0
-91.67	0.215	0.094	0	0.215	0.094	0	0.215	0.095	0	0.215	0.095	0
-100	0.234	0.103	0	0.234	0.103	0	0.234	0.103	0	0.234	0.103	0
-108.33	0.254	0.111	0	0.254	0.111	0	0.254	0.112	0	0.254	0.112	0
-116.67	0.273	0.12	0	0.273	0.12	0	0.273	0.121	0	0.273	0.121	0
-125	0.292	0.128	0	0.292	0.128	0	0.292	0.129	0	0.292	0.129	0
-133.33	0.312	0.137	0	0.312	0.137	0	0.312	0.138	0	0.312	0.138	0
-141.67	0.331	0.145	0	0.331	0.145	0	0.331	0.146	0	0.331	0.146	0
-150	0.351	0.154	0	0.351	0.154	0	0.351	0.155	0	0.351	0.155	0
-158.33	0.371	0.162	0	0.371	0.162	0	0.371	0.164	0	0.371	0.164	0
-166.67	0.39	0.171	0	0.39	0.171	0	0.39	0.172	0	0.39	0.172	0
-175	0.41	0.18	0	0.41	0.18	0	0.41	0.181	0	0.41	0.181	0
-183.33	0.429	0.188	0	0.429	0.188	0	0.429	0.189	0	0.429	0.189	0
-191.67	0.449	0.197	0	0.449	0.197	0	0.449	0.198	0	0.449	0.198	0
-200	0.468	0.205	0	0.468	0.205	0	0.468	0.207	0	0.468	0.207	0
-208.82	0.489	0.214	0	0.489	0.214	0	0.489	0.216	0	0.489	0.216	0
-217.65	0.509	0.223	0	0.509	0.223	0	0.509	0.225	0	0.509	0.225	0
-226.47	0.53	0.232	0	0.53	0.232	0	0.53	0.234	0	0.53	0.234	0

-235.29	0.551	0.241	0	0.551	0.241	0	0.551	0.243	0	0.551	0.243	0
-244.12	0.571	0.25	0	0.571	0.25	0	0.571	0.252	0	0.571	0.252	0
-252.94	0.592	0.259	0	0.592	0.259	0	0.592	0.261	0	0.592	0.261	0
-261.76	0.613	0.269	0	0.613	0.269	0	0.613	0.271	0	0.613	0.271	0
-270.59	0.633	0.278	0	0.633	0.278	0	0.633	0.28	0	0.633	0.28	0
-279.41	0.654	0.287	0	0.654	0.287	0	0.654	0.289	0	0.654	0.289	0
-288.24	0.674	0.296	0	0.674	0.296	0	0.674	0.298	0	0.674	0.298	0
-297.06	0.695	0.305	0	0.695	0.305	0	0.695	0.307	0	0.695	0.307	0
-305.88	0.716	0.314	0	0.716	0.314	0	0.716	0.316	0	0.716	0.316	0
-314.71	0.736	0.323	0	0.736	0.323	0	0.736	0.325	0	0.736	0.325	0
-323.53	0.757	0.332	0	0.757	0.332	0	0.757	0.334	0	0.757	0.334	0
-332.35	0.778	0.341	0	0.778	0.341	0	0.778	0.343	0	0.778	0.343	0
-341.18	0.798	0.35	0	0.798	0.35	0	0.798	0.353	0	0.798	0.353	0
-350	0.819	0.359	0	0.819	0.359	0	0.819	0.362	0	0.819	0.362	0
-358.82	0.84	0.368	0	0.84	0.368	0	0.84	0.371	0	0.84	0.371	0
-367.65	0.86	0.377	0	0.86	0.377	0	0.86	0.38	0	0.86	0.38	0
-376.47	0.881	0.386	0	0.881	0.386	0	0.881	0.389	0	0.881	0.389	0
-385.29	0.902	0.395	0	0.902	0.395	0	0.902	0.398	0	0.902	0.398	0
-394.12	0.922	0.404	0	0.922	0.404	0	0.922	0.407	0	0.922	0.407	0
-402.94	0.943	0.413	0	0.943	0.413	0	0.943	0.416	0	0.943	0.416	0
-411.76	0.964	0.422	0	0.964	0.422	0	0.964	0.426	0	0.964	0.426	0
-420.59	0.984	0.431	0	0.984	0.431	0	0.984	0.435	0	0.984	0.435	0
-429.41	1.005	0.44	0	1.005	0.44	0	1.005	0.444	0	1.005	0.444	0
-438.24	1.025	0.45	0	1.025	0.45	0	1.025	0.453	0	1.025	0.453	0
-447.06	1.046	0.459	0	1.046	0.459	0	1.046	0.462	0	1.046	0.462	0
-455.88	1.067	0.468	0	1.067	0.468	0	1.067	0.471	0	1.067	0.471	0
-464.71	1.087	0.477	0	1.087	0.477	0	1.087	0.48	0	1.087	0.48	0
-473.53	1.108	0.486	0	1.108	0.486	0	1.108	0.489	0	1.108	0.489	0
-482.35	1.129	0.495	0	1.129	0.495	0	1.129	0.498	0	1.129	0.498	0
-491.18	1.149	0.504	0	1.149	0.504	0	1.149	0.508	0	1.149	0.508	0
-500	1.165	0.511	0	1.165	0.511	0	1.165	0.514	0	1.165	0.514	0

σ_v = total vertical tension
 σ_h = total horizontal tension
 u = neutral pressure
 σ'_v = effective vertical tension
 σ'_h = effective horizontal tension

Table 5.4 Approach (1) - Phase 1 soil pressure

The accumulative pressure and the corresponding moment arm:

Results of pressures [daN] and arms [cm], Bulkhead PAR_1							
Active				Passive			
R_h	-12822.6	b_h	333.3	R_h	12917.4	b_h	333.3
R'_h	-12822.6	b'_h	333.3	R'_h	12917.4	b'_h	333.3
R_u	0	b_u	0	R_u	0	b_u	0

R = results of the thrusts, b = arms with respect to the head of the micropile.
subscript h = resulting from the total pressures on the micropile.
subscript $'h$ = resulting from the effective pressures on the micropile.
subscript u = resultant of the neutral pressures on the micropile.

Table 5.5 Approach (1) - Phase 1 accumulative soil pressure

Internal actions:

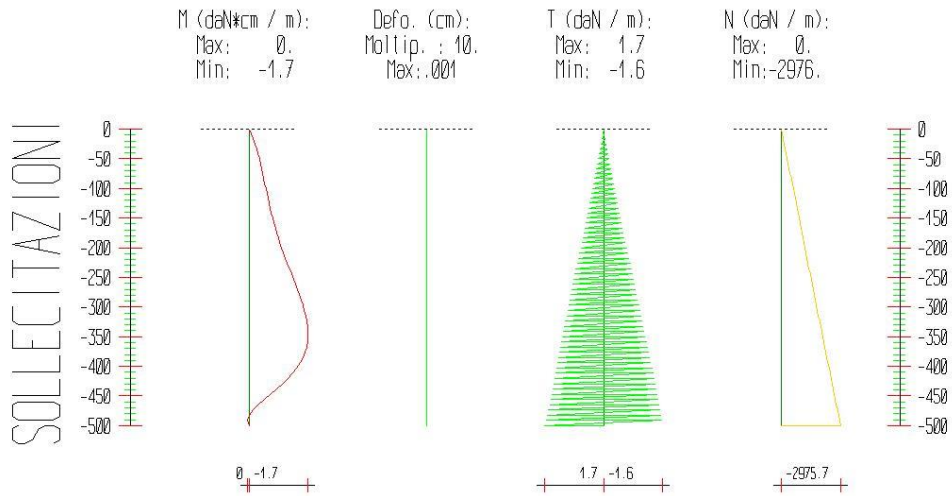


Figure 5.19 Approach (1)-Phase 1: Internal actions along the pile group

Phase 1: Internal actions					
Elevation [cm]	Horizontal Deformation [cm]	Vertical Deformation [cm]	Bending Moment [daN cm]	Shear Forces [daN]	Axial Forces [daN]
-8.3	0	-0.001	-0.068	0	-49
-16.7	0	-0.001	-0.128	0.1	-98.1
-25	0	-0.001	-0.18	0.1	-147.1
-33.3	0	-0.001	-0.226	0.1	-196.2
-41.7	0	-0.001	-0.268	0.1	-245.3
-50	0	-0.001	-0.305	0.2	-294.5
-58.3	0	-0.001	-0.339	0.2	-343.6
-66.7	-0.0001	-0.001	-0.372	0.2	-392.8
-75	-0.0001	-0.001	-0.403	0.2	-442
-83.3	-0.0001	-0.001	-0.433	0.3	-491.2
-91.7	-0.0001	-0.001	-0.462	0.3	-540.4
-100	-0.0001	-0.001	-0.492	0.3	-589.6
-108.3	-0.0001	-0.001	-0.523	0.3	-638.9
-116.7	-0.0001	-0.001	-0.554	0.4	-688.2
-125	-0.0001	-0.001	-0.586	0.4	-737.5
-133.3	-0.0001	-0.001	-0.62	0.4	-786.8
-141.7	-0.0001	-0.001	-0.655	0.4	-836.1
-150	-0.0001	-0.001	-0.692	0.5	-885.5
-158.3	-0.0001	-0.001	-0.73	0.5	-934.9
-166.7	-0.0001	-0.001	-0.769	0.5	-984.2
-175	-0.0001	-0.001	-0.811	0.5	-1033.7
-183.3	-0.0001	-0.001	-0.853	0.6	-1083.1
-191.7	-0.0001	-0.001	-0.898	0.6	-1132.5
-200	-0.0002	-0.001	-0.943	0.6	-1182
-208.8	-0.0002	-0.001	-1.001	0.7	-1234.4
-217.6	-0.0002	-0.001	-1.06	0.7	-1286.8
-226.5	-0.0002	-0.001	-1.119	0.8	-1339.3

-235.3	-0.0002	-0.001	-1.179	0.8	-1391.8
-244.1	-0.0002	-0.001	-1.238	0.8	-1444.2
-252.9	-0.0002	-0.001	-1.297	0.8	-1496.8
-261.8	-0.0002	-0.001	-1.354	0.9	-1549.3
-270.6	-0.0002	-0.001	-1.411	0.9	-1601.8
-279.4	-0.0002	-0.001	-1.465	0.9	-1654.4
-288.2	-0.0002	-0.001	-1.517	1	-1707
-297.1	-0.0002	-0.001	-1.566	1	-1759.6
-305.9	-0.0002	-0.001	-1.61	1	-1812.3
-314.7	-0.0002	-0.001	-1.648	1	-1864.9
-323.5	-0.0002	-0.001	-1.68	1.1	-1917.6
-332.4	-0.0003	-0.001	-1.703	1.1	-1970.3
-341.2	-0.0003	-0.001	-1.716	1.1	-2023
-350	-0.0003	-0.001	-1.718	1.2	-2075.8
-358.8	-0.0003	-0.001	-1.706	1.2	-2128.5
-367.6	-0.0003	-0.001	-1.679	1.2	-2181.3
-376.5	-0.0003	-0.001	-1.635	1.2	-2234.1
-385.3	-0.0003	-0.001	-1.572	1.3	-2287
-394.1	-0.0003	0	-1.49	1.3	-2339.8
-402.9	-0.0003	0	-1.388	1.3	-2392.7
-411.8	-0.0003	0	-1.266	1.4	-2445.6
-420.6	-0.0003	0	-1.125	1.4	-2498.5
-429.4	-0.0003	0	-0.967	1.4	-2551.5
-438.2	-0.0003	0	-0.796	1.4	-2604.4
-447.1	-0.0003	0	-0.617	1.5	-2657.4
-455.9	-0.0003	0	-0.438	1.5	-2710.4
-464.7	-0.0004	0	-0.269	1.5	-2763.4
-473.5	-0.0004	0	-0.123	1.6	-2816.5
-482.4	-0.0004	0	-0.016	1.6	-2869.5
-491.2	-0.0004	0	0.033	1.6	-2922.6
-500	-0.0004	0	0	1.7	-2975.7

Table 5.6 Approach (1) - Phase 1 internal actions

5.6.1.1.2 Approach [1] Phase (2) results

Soil pressure along the micropiles results:

Soil pressure												
Elevation [cm]	Active pressure [daN/cm ²]						Passive pressure [daN/cm ²]					
Z	σ_v	σ_h	u	σ'_v	σ'_h	τ	σ_v	σ_h	u	σ'_v	σ'_h	τ
0	0.065	0.017	0	0.065	0.017	0	0	0	0	0	0	0
-8.33	0.08	0.021	0	0.08	0.021	0	0	0	0	0	0	0
-16.67	0.099	0.026	0	0.099	0.026	0	0	0	0	0	0	0
-25	0.118	0.031	0	0.118	0.031	0	0	0	0	0	0	0
-33.33	0.138	0.036	0	0.138	0.036	0	0	0	0	0	0	0
-41.67	0.158	0.041	0	0.158	0.041	0	0	0	0	0	0	0
-50	0.177	0.046	0	0.177	0.046	0	0	0	0	0	0	0
-58.33	0.196	0.051	0	0.196	0.051	0	0	0	0	0	0	0
-66.67	0.216	0.056	0	0.216	0.056	0	0	0	0	0	0	0
-75	0.236	0.061	0	0.236	0.061	0	0	0	0	0	0	0
-83.33	0.255	0.066	0	0.255	0.066	0	0	0	0	0	0	0
-91.67	0.274	0.071	0	0.274	0.071	0	0	0	0	0	0	0
-100	0.294	0.076	0	0.294	0.076	0	0	0	0	0	0	0
-108.33	0.314	0.082	0	0.314	0.082	0	0	0	0	0	0	0
-116.67	0.333	0.087	0	0.333	0.087	0	0	0	0	0	0	0
-125	0.352	0.092	0	0.352	0.092	0	0	0	0	0	0	0
-133.33	0.372	0.097	0	0.372	0.097	0	0	0	0	0	0	0
-141.67	0.391	0.102	0	0.391	0.102	0	0	0	0	0	0	0
-150	0.411	0.107	0	0.411	0.107	0	0	0	0	0	0	0
-158.33	0.431	0.112	0	0.431	0.112	0	0	0	0	0	0	0
-166.67	0.45	0.117	0	0.45	0.117	0	0	0	0	0	0	0
-175	0.47	0.122	0	0.47	0.122	0	0	0	0	0	0	0
-183.33	0.489	0.127	0	0.489	0.127	0	0	0	0	0	0	0
-191.67	0.509	0.132	0	0.509	0.132	0	0	0	0	0	0	0
-200	0.528	0.137	0	0.528	0.137	0	0	0.001	0	0	0.001	0
-208.82	0.549	0.143	0	0.549	0.143	0	0.021	0.107	0	0.021	0.107	0
-217.65	0.569	0.148	0	0.569	0.148	0	0.041	0.215	0	0.041	0.215	0
-226.47	0.59	0.153	0	0.59	0.153	0	0.062	0.322	0	0.062	0.322	0
-235.29	0.611	0.159	0	0.611	0.159	0	0.083	0.429	0	0.083	0.429	0
-244.12	0.631	0.164	0	0.631	0.164	0	0.103	0.537	0	0.103	0.537	0
-252.94	0.652	0.169	0	0.652	0.169	0	0.124	0.644	0	0.124	0.644	0
-261.76	0.673	0.175	0	0.673	0.175	0	0.145	0.752	0	0.145	0.752	0
-270.59	0.693	0.18	0	0.693	0.18	0	0.165	0.859	0	0.165	0.859	0
-279.41	0.714	0.186	0	0.714	0.186	0	0.186	0.966	0	0.186	0.966	0
-288.24	0.734	0.191	0	0.734	0.191	0	0.206	1.074	0	0.206	1.074	0
-297.06	0.755	0.196	0	0.755	0.196	0	0.227	1.181	0	0.227	1.181	0
-305.88	0.776	0.202	0	0.776	0.202	0	0.248	1.258	0	0.248	1.258	0
-314.71	0.796	0.207	0	0.796	0.207	0	0.268	0.993	0	0.268	0.993	0
-323.53	0.817	0.212	0	0.817	0.212	0	0.289	0.77	0	0.289	0.77	0
-332.35	0.838	0.218	0	0.838	0.218	0	0.31	0.586	0	0.31	0.586	0
-341.18	0.858	0.223	0	0.858	0.223	0	0.33	0.437	0	0.33	0.437	0
-350	0.879	0.229	0	0.879	0.229	0	0.351	0.321	0	0.351	0.321	0

-358.82	0.9	0.327	0	0.9	0.327	0	0.372	0.233	0	0.372	0.233	0
-367.65	0.92	0.408	0	0.92	0.408	0	0.392	0.169	0	0.392	0.169	0
-376.47	0.941	0.468	0	0.941	0.468	0	0.413	0.128	0	0.413	0.128	0
-385.29	0.962	0.51	0	0.962	0.51	0	0.434	0.113	0	0.434	0.113	0
-394.12	0.982	0.537	0	0.982	0.537	0	0.454	0.118	0	0.454	0.118	0
-402.94	1.003	0.553	0	1.003	0.553	0	0.475	0.123	0	0.475	0.123	0
-411.76	1.024	0.559	0	1.024	0.559	0	0.496	0.129	0	0.496	0.129	0
-420.59	1.044	0.557	0	1.044	0.557	0	0.516	0.134	0	0.516	0.134	0
-429.41	1.065	0.551	0	1.065	0.551	0	0.537	0.154	0	0.537	0.154	0
-438.24	1.085	0.541	0	1.085	0.541	0	0.557	0.182	0	0.557	0.182	0
-447.06	1.106	0.528	0	1.106	0.528	0	0.578	0.213	0	0.578	0.213	0
-455.88	1.127	0.513	0	1.127	0.513	0	0.599	0.246	0	0.599	0.246	0
-464.71	1.147	0.497	0	1.147	0.497	0	0.619	0.28	0	0.619	0.28	0
-473.53	1.168	0.481	0	1.168	0.481	0	0.64	0.314	0	0.64	0.314	0
-482.35	1.189	0.465	0	1.189	0.465	0	0.661	0.349	0	0.661	0.349	0
-491.18	1.209	0.448	0	1.209	0.448	0	0.681	0.383	0	0.681	0.383	0
-500	1.225	0.43	0	1.225	0.43	0	0.697	0.416	0	0.697	0.416	0

σ_v = total vertical tension
 σ_h = total horizontal tension
 u = neutral pressure
 σ'_v = effective vertical tension
 σ'_h = effective horizontal tension

Table 5.7 Approach (1) - Phase 2 soil pressure

The accumulative pressure and the corresponding moment arm:

Results of pressures [daN] and arms [cm], micropile							
Active				Passive			
R_h	-11572.1	b_h	352.8	R_h	13173.4	b_h	323.9
R'_h	-11572.1	b'_h	352.8	R'_h	13173.4	b'_h	323.9
R_u	0	b_u	0	R_u	0	b_u	0

R = results of the thrusts, b = arms with respect to the head of the micropile.
subscript h = resulting from the total pressures on the micropile.
subscript $'h$ = resulting from the effective pressures on the micropile.
subscript u = resultant of the neutral pressures on the micropile.

Table 5.8 Approach (1) - Phase 2 accumulative soil pressure

Internal actions:

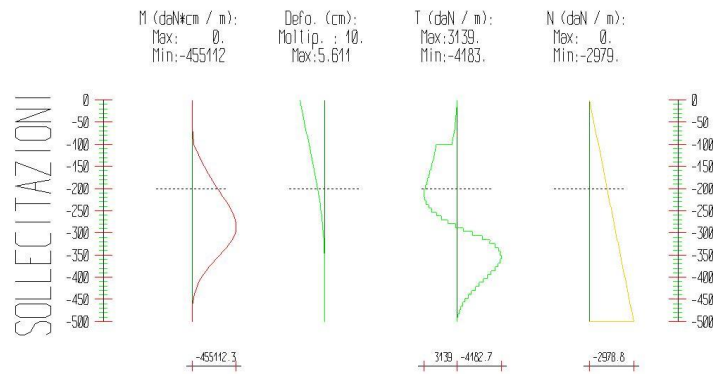


Figure 5.20 Approach (1) -Phase 2: Internal actions along the pile group

Phase 2: Internal actions					
Elevation [cm]	Horizontal deformation [cm]	Vertical deformation [cm]	Bending moment [daN cm]	Shear forces [daN]	Axial forces [daN]
-8.3	-5.4364	-0.001	-58.668	7.1	-49
-16.7	-5.2618	-0.001	-261.398	24.4	-98.1
-25	-5.0872	-0.001	-643.878	46	-147.2
-33.3	-4.9126	-0.001	-1241.796	71.9	-196.3
-41.7	-4.738	-0.001	-2090.839	102	-245.4
-50	-4.5635	-0.001	-3226.693	136.5	-294.5
-58.3	-4.389	-0.001	-4685.045	175.2	-343.7
-66.7	-4.2146	-0.001	-6501.58	218.2	-392.8
-75	-4.0404	-0.001	-8711.981	265.5	-442
-83.3	-3.8662	-0.001	-11351.932	317.1	-491.3
-91.7	-3.6923	-0.001	-14457.11	372.9	-540.5
-100	-3.5187	-0.001	-18063.194	433.1	-589.8
-108.3	-3.3454	-0.001	-34705.856	1997.5	-639
-116.7	-3.1727	-0.001	-51920.765	2066.2	-688.3
-125	-3.001	-0.001	-69743.587	2139.2	-737.7
-133.3	-2.8305	-0.001	-88209.98	2216.4	-787
-141.7	-2.6616	-0.001	-107355.597	2298	-836.4
-150	-2.4946	-0.001	-127216.085	2383.8	-885.8
-158.3	-2.3299	-0.001	-147827.083	2473.9	-935.2
-166.7	-2.1678	-0.001	-169224.224	2568.2	-984.6
-175	-2.0087	-0.001	-191443.133	2666.9	-1034
-183.3	-1.8531	-0.001	-214519.428	2769.8	-1083.5
-191.7	-1.7013	-0.001	-238488.72	2877	-1133
-200	-1.5538	-0.001	-263386.613	2988.4	-1182.5
-208.8	-1.4028	-0.001	-290789.325	3106.4	-1235
-217.6	-1.2576	-0.001	-318479.387	3139	-1287.4
-226.5	-1.1187	-0.001	-345663.173	3081.6	-1339.9
-235.3	-0.9868	-0.001	-371547.066	2934.4	-1392.4
-244.1	-0.8623	-0.001	-395337.46	2697.1	-1445

-252.9	-0.7458	-0.001	-416240.768	2370	-1497.5
-261.8	-0.6375	-0.001	-433463.43	1952.8	-1550.1
-270.6	-0.538	-0.001	-446211.91	1445.8	-1602.7
-279.4	-0.4473	-0.001	-453692.702	848.8	-1655.4
-288.2	-0.3658	-0.001	-455112.323	161.9	-1708
-297.1	-0.2933	-0.001	-449677.31	-614.9	-1760.7
-305.9	-0.2298	-0.001	-436594.22	-1481.6	-1813.4
-314.7	-0.1751	-0.001	-415305.515	-2411.6	-1866.1
-323.5	-0.1286	-0.001	-387914.519	-3103.1	-1918.9
-332.4	-0.0899	-0.001	-356201.364	-3593	-1971.7
-341.2	-0.0583	-0.001	-321644.125	-3915.3	-2024.5
-350	-0.0332	-0.001	-285443.361	-4101.5	-2077.3
-358.8	-0.0138	-0.001	-248548.922	-4180.1	-2130.1
-367.6	0.0006	-0.001	-212411.699	-4094.2	-2183
-376.5	0.0108	-0.001	-178155.439	-3881	-2235.9
-385.3	0.0174	-0.001	-146571.988	-3578.1	-2288.8
-394.1	0.021	0	-118105.828	-3224.7	-2341.7
-402.9	0.0223	0	-92928.046	-2852	-2394.7
-411.8	0.0217	0	-71117.161	-2470.4	-2447.7
-420.6	0.0196	0	-52678.759	-2088.2	-2500.7
-429.4	0.0165	0	-37562.505	-1711.6	-2553.7
-438.2	0.0126	0	-25565.892	-1358	-2606.8
-447.1	0.0082	0	-16387.324	-1038.6	-2659.8
-455.9	0.0035	0	-9684.583	-758	-2713
-464.7	-0.0015	0	-5089.245	-519.1	-2766.1
-473.5	-0.0065	0	-2217.232	-323.8	-2819.2
-482.4	-0.0116	0	-676.08	-172.9	-2872.4
-491.2	-0.0167	0	-69.522	-67	-2925.6
-500	-0.0219	0	0	-6.1	-2978.8

Table 5.9 Approach (1) - Phase 2 internal actions

5.6.1.1.3 Approach [1] internal actions envelope

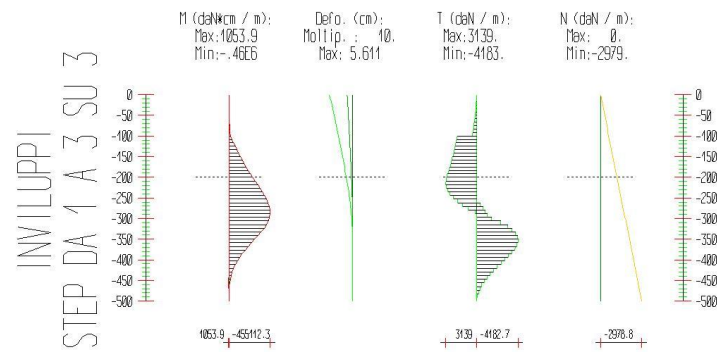


Figure 5.21 Approach 1- envelope: Internal actions along the pile group

Internal actions envelope						
Elevation [cm]	Bending moment [daN cm]		Shear forces [daN]		Axial forces [daN]	
	Min.	Max	Min.	Max	Min.	Max
z						
-8.3	-58.7	-0.1	0.	7.1	-49.	-49.
-16.7	-261.4	-0.1	0.1	24.4	-98.1	-98.1
-25.	-643.9	-0.2	0.1	46.	-147.2	-147.1
-33.3	-1242.	-0.2	0.1	71.9	-196.3	-196.2
-41.7	-2091.	-0.3	0.1	102.	-245.4	-245.3
-50.	-3227.	-0.3	0.2	136.5	-294.5	-294.5
-58.3	-4685.	-0.3	0.2	175.2	-343.7	-343.6
-66.7	-6502.	-0.4	0.2	218.2	-392.8	-392.8
-75.	-8712.	-0.4	0.2	265.5	-442.	-442.
-83.3	-11352	-0.4	0.3	317.1	-491.3	-491.2
-91.7	-14457	-0.5	0.3	372.9	-540.5	-540.4
-100.	-18063	-0.5	0.3	433.1	-589.8	-589.6
-108.3	-34706	-0.5	0.3	1997.5	-639.	-638.9
-116.7	-51921	-0.6	0.4	2066.2	-688.3	-688.2
-125.	-69744	-0.6	0.4	2139.2	-737.7	-737.5
-133.3	-88210	-0.6	0.4	2216.4	-787.	-786.8
-141.7	-.11E6	-0.7	0.4	2298.	-836.4	-836.1
-150.	-.13E6	-0.7	0.5	2383.8	-885.8	-885.5
-158.3	-.15E6	-0.7	0.5	2473.9	-935.2	-934.9
-166.7	-.17E6	-0.8	0.5	2568.2	-984.6	-984.2
-175.	-.19E6	-0.8	0.5	2666.9	-1034.	-1034.
-183.3	-.21E6	-0.9	0.6	2769.8	-1084.	-1083.
-191.7	-.24E6	-0.9	0.6	2877.	-1133.	-1133.
-200.	-.26E6	-0.9	0.6	2988.4	-1183.	-1182.
-208.8	-.29E6	-1.0	0.7	3106.4	-1235.	-1234.
-217.6	-.32E6	-1.1	0.7	3139.	-1287.	-1287.
-226.5	-.35E6	-1.1	0.8	3081.6	-1340.	-1339.
-235.3	-.37E6	-1.2	0.8	2934.4	-1392.	-1392.
-244.1	-.4E6	-1.2	0.8	2697.1	-1445.	-1444.
-252.9	-.42E6	-1.3	0.8	2370.	-1498.	-1497.
-261.8	-.43E6	-1.4	0.9	1952.8	-1550.	-1549.

-270.6	-.45E6	-1.4	-341.5	1445.8	-1603.	-1602.
-279.4	-.45E6	-1.5	-647.5	848.8	-1655.	-1654.
-288.2	-.46E6	-1.5	-880.4	161.9	-1708.	-1707.
-297.1	-.45E6	-1.6	-1051.	1.	-1761.	-1760.
-305.9	-.44E6	-1.6	-1482.	1.	-1813.	-1812.
-314.7	-.42E6	-1.6	-2412.	1.	-1866.	-1865.
-323.5	-.39E6	-1.7	-3103.	1.1	-1919.	-1918.
-332.4	-.36E6	-1.7	-3593.	1.1	-1972.	-1970.
-341.2	-.32E6	-1.7	-3915.	1.1	-2025.	-2023.
-350.	-.29E6	-1.7	-4102.	1.2	-2077.	-2076.
-358.8	-.25E6	-1.7	-4180.	1.2	-2130.	-2129.
-367.6	-.21E6	-1.7	-4094.	1.2	-2183.	-2181.
-376.5	-.18E6	-1.6	-3881.	1.2	-2236.	-2234.
-385.3	-.15E6	-1.6	-3578.	1.3	-2289.	-2287.
-394.1	-.12E6	-1.5	-3225.	1.3	-2342.	-2340.
-402.9	-92928	-1.4	-2852.	1.3	-2395.	-2393.
-411.8	-71117	-1.3	-2470.	1.4	-2448.	-2446.
-420.6	-52679	-1.1	-2088.	1.4	-2501.	-2499.
-429.4	-37563	-1.	-1712.	1.4	-2554.	-2552.
-438.2	-25566	357.5	-1358.	1.4	-2607.	-2604.
-447.1	-16387	889.1	-1039.	1.5	-2660.	-2657.
-455.9	-9685.	1053.9	-758.	1.5	-2713.	-2710.
-464.7	-5089.	956.9	-519.1	12.5	-2766.	-2763.
-473.5	-2217.	701.6	-323.8	30.5	-2819.	-2817.
-482.4	-676.1	389.8	-172.9	36.9	-2872.	-2870.
-491.2	-69.5	122.5	-67.	31.9	-2926.	-2923.
-500.	0.	0.	-6.1	15.5	-2979.	-2976.

Table 5.10 Approach (1) Internal actions envelope along the pile group

5.6.1.2 Verification state approach [1] combination

5.6.1.2.1 Approach [1] verification Phase (1)

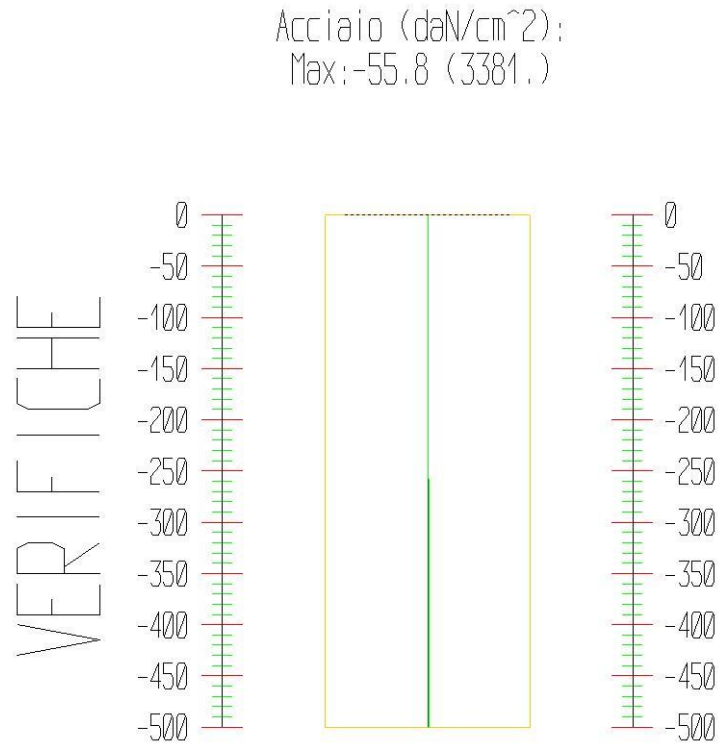


Figure 5.22 Approach (1)-Stress verification phase 1

Phase 1 Verification							
σ max = max compression stress, σ max2 = max tensile stress, ε max = max compression strain, ε max2 = max tensile strain.							
Elevation [cm]	M [daN.cm]	N [daN]	σ max [daN/cm ²]	σ max2 [daN/cm ²]	ε max [%]	ε max2 [%]	Verification
0	0	0	0	0	0	0	Satisfied
-8.3	0	-24.5	-0.9	-0.9	0	0	Satisfied
-16.7	-0.1	-49	-1.8	-1.8	0	0	Satisfied
-25	-0.1	-73.6	-2.8	-2.8	0	0	Satisfied
-33.3	-0.1	-98.1	-3.7	-3.7	0	0	Satisfied
-41.7	-0.1	-122.7	-4.6	-4.6	0	0	Satisfied
-50	-0.2	-147.2	-5.5	-5.5	0	0	Satisfied
-58.3	-0.2	-171.8	-6.4	-6.4	0	0	Satisfied
-66.7	-0.2	-196.4	-7.4	-7.4	0	0	Satisfied
-75	-0.2	-221	-8.3	-8.3	0	0	Satisfied
-83.3	-0.2	-245.6	-9.2	-9.2	0	0	Satisfied
-91.7	-0.2	-270.2	-10.1	-10.1	0	0	Satisfied
-100	-0.2	-294.8	-11.1	-11	0	0	Satisfied
-108.3	-0.3	-319.4	-12	-12	0	0	Satisfied
-116.7	-0.3	-344.1	-12.9	-12.9	0	0	Satisfied
-125	-0.3	-368.7	-13.8	-13.8	0	0	Satisfied

-133.3	-0.3	-393.4	-14.7	-14.7	0	0	Satisfied
-141.7	-0.3	-418.1	-15.7	-15.7	0	0	Satisfied
-150	-0.3	-442.7	-16.6	-16.6	0	0	Satisfied
-158.3	-0.4	-467.4	-17.5	-17.5	0	0	Satisfied
-166.7	-0.4	-492.1	-18.4	-18.4	0	0	Satisfied
-175	-0.4	-516.8	-19.4	-19.4	0	0	Satisfied
-183.3	-0.4	-541.5	-20.3	-20.3	0	0	Satisfied
-191.7	-0.4	-566.3	-21.2	-21.2	0	0	Satisfied
-200	-0.5	-591	-22.2	-22.1	0	0	Satisfied
-208.8	-0.5	-617.2	-23.1	-23.1	0	0	Satisfied
-217.6	-0.5	-643.4	-24.1	-24.1	0	0	Satisfied
-226.5	-0.6	-669.6	-25.1	-25.1	0	0	Satisfied
-235.3	-0.6	-695.9	-26.1	-26.1	0	0	Satisfied
-244.1	-0.6	-722.1	-27.1	-27.1	0	0	Satisfied
-252.9	-0.6	-748.4	-28.1	-28	0	0	Satisfied
-261.8	-0.7	-774.6	-29	-29	0	0	Satisfied
-270.6	-0.7	-800.9	-30	-30	0	0	Satisfied
-279.4	-0.7	-827.2	-31	-31	0	0	Satisfied
-288.2	-0.8	-853.5	-32	-32	0	0	Satisfied
-297.1	-0.8	-879.8	-33	-33	0	0	Satisfied
-305.9	-0.8	-906.1	-34	-33.9	0	0	Satisfied
-314.7	-0.8	-932.5	-35	-34.9	0	0	Satisfied
-323.5	-0.8	-958.8	-35.9	-35.9	0	0	Satisfied
-332.4	-0.9	-985.2	-36.9	-36.9	0	0	Satisfied
-341.2	-0.9	-1011.5	-37.9	-37.9	0	0	Satisfied
-350	-0.9	-1037.9	-38.9	-38.9	0	0	Satisfied
-358.8	-0.9	-1064.3	-39.9	-39.9	0	0	Satisfied
-367.6	-0.8	-1090.7	-40.9	-40.9	0	0	Satisfied
-376.5	-0.8	-1117.1	-41.9	-41.9	0	0	Satisfied
-385.3	-0.8	-1143.5	-42.9	-42.8	0	0	Satisfied
-394.1	-0.7	-1169.9	-43.9	-43.8	0	0	Satisfied
-402.9	-0.7	-1196.4	-44.8	-44.8	0	0	Satisfied
-411.8	-0.6	-1222.8	-45.8	-45.8	0	0	Satisfied
-420.6	-0.6	-1249.3	-46.8	-46.8	0	0	Satisfied
-429.4	-0.5	-1275.7	-47.8	-47.8	0	0	Satisfied
-438.2	-0.4	-1302.2	-48.8	-48.8	0	0	Satisfied
-447.1	-0.3	-1328.7	-49.8	-49.8	0	0	Satisfied
-455.9	-0.2	-1355.2	-50.8	-50.8	0	0	Satisfied
-464.7	-0.1	-1381.7	-51.8	-51.8	0	0	Satisfied
-473.5	-0.1	-1408.2	-52.8	-52.8	0	0	Satisfied
-482.4	0	-1434.8	-53.8	-53.8	0	0	Satisfied
-491.2	0	-1461.3	-54.8	-54.8	0	0	Satisfied
-500	0	-1487.9	-55.8	-55.8	0	0	Satisfied

Table 5.11 Approach (1) verification state phase 1

Check the verification with VCASLU software

Verifica C.A. S.L.U. - File

File Materiali Opzioni Visualizza Progetto Sez. Rett. Sismica Normativa: NTC 2008 ?

Titolo : _____

Sezione circolare cava

Raggio esterno: 14 [cm]
 Raggio interno: 11.4 [cm]
 N° barre uguali: 45
 Diametro barre: .8 [cm]
 Copriferro (baric.): 2.6 [cm]

N° barre: 0 Zoom

Tipo Sezione

Rettan.re Trapezi
 a T Circolare
 Rettangoli Coord.

Sollecitazioni

S.L.U. Metodo n

N_{Ed}: 5.16 kN
 M_{xEd}: 12.14 kNm
 M_{yEd}: 0 kNm

P.to applicazione N

Centro Baricentro cls
 Coord.[cm] xN: 0 yN: 0

Tipo rottura

Lato calcestruzzo - Acciaio snervato

Metodo di calcolo

S.L.U.+ S.L.U.-
 Metodo n

Tipo flessione

Retta Deviata

Vertici: 52 N° rett.: 100

Calcola MRd Dominio M-N

L₀: 0 cm Col. modello

Precompresso

Materiali

S355 C25/30

ε_{su}: 67.5 ‰ ε_{c2}: 2 ‰
 f_{yd}: 308.7 N/mm² ε_{cu}: 3.5 ‰
 E_s: 200,000 N/mm² f_{cd}: 14.17
 E_s/E_c: 15 f_{cc}/f_{cd}: 0.8
 ε_{syd}: 1.544 ‰ σ_{c,adm}: 9.75
 σ_{s,adm}: 235.3 N/mm² τ_{co}: 0.6
 τ_{c1}: 1.829

M_{xRd}: 58.7 kN m

σ_c: -14.17 N/mm²
 σ_s: 308.7 N/mm²
 ε_c: 3.5 ‰
 ε_s: 4.121 ‰
 d: 25.37 cm
 x: 11.65 x/d: 0.4592
 δ: 1

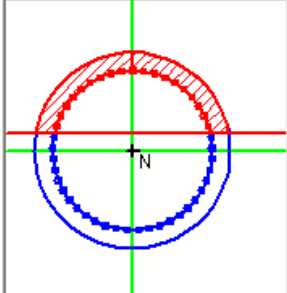


Figure 5.23 Properties definitions

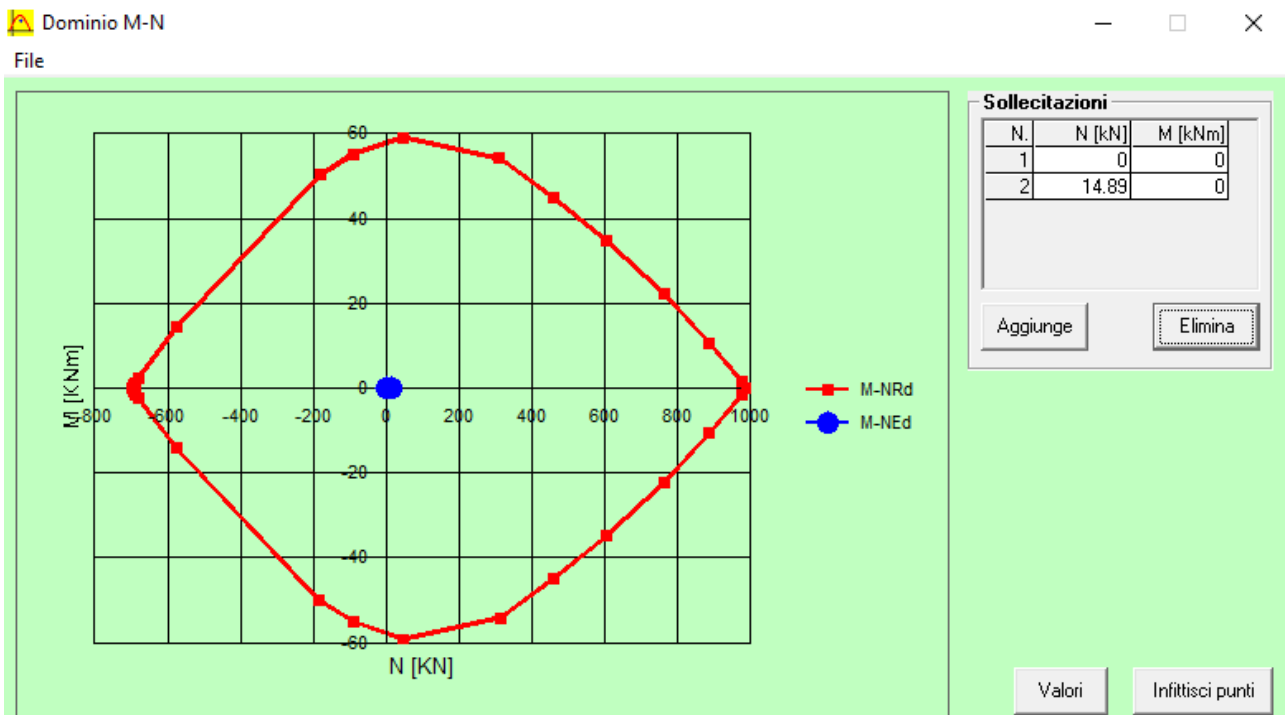


Figure 5.24 Interaction domain verification

5.6.1.2.2 Approach [1] verification Phase (2)

Acciaio (daN/cm²):
Max:3381. (3381.)

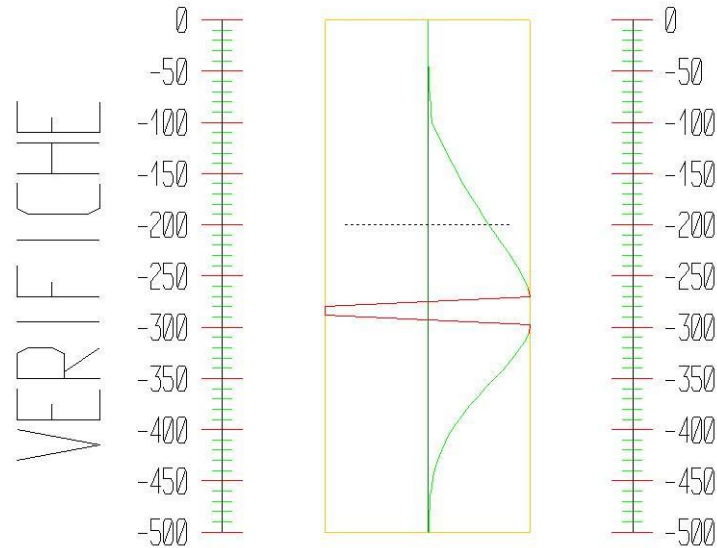


Figure 5.25 Approach (1)-Stress verification phase (2)

Phase 2 verification							
σ max = max compression stress, σ max2 = max tensile stress, ε max = max compression strain, ε max2 = max tensile strain.							
Elevation [cm]	M [daN cm]	N [daN]	σ max [daN/cm ²]	σ max2 [daN/cm ²]	ε max [%]	ε max2 [%]	Verification
0	0	0	0	0	0	0	Satisfied
-8.3	-29.3	-24.5	-1.4	-0.5	0	0	Satisfied
-16.7	-130.7	-49	-3.8	0.1	0	0	Satisfied
-25	-321.9	-73.6	-7.6	2.1	0	0	Satisfied
-33.3	-620.9	-98.1	-13.1	5.7	0	0	Satisfied
-41.7	-1045.4	-122.7	-20.5	11.3	0	0	Satisfied
-50	-1613.3	-147.3	-30	18.9	0	0	Satisfied
-58.3	-2342.5	-171.8	-42	29.1	0	0	Satisfied
-66.7	-3250.8	-196.4	-56.7	41.9	0	0	Satisfied
-75	-4356	-221	-74.3	57.8	0	0	Satisfied
-83.3	-5676	-245.6	-95.3	76.9	0	0	Satisfied
-91.7	-7228.6	-270.2	-119.7	99.5	-0.01	0	Satisfied
-100	-9031.6	-294.9	-148	125.9	-0.01	0.01	Satisfied
-108.3	-17352.9	-319.5	-275.1	251.2	-0.01	0.01	Satisfied
-116.7	-25960.4	-344.2	-406.6	380.8	-0.02	0.02	Satisfied
-125	-34871.8	-368.8	-542.6	515	-0.03	0.02	Satisfied
-133.3	-44105	-393.5	-683.6	654.1	-0.03	0.03	Satisfied
-141.7	-53677.8	-418.2	-829.6	798.3	-0.04	0.04	Satisfied

-150	-63608	-442.9	-981.1	948	-0.05	0.05	Satisfied
-158.3	-73913.5	-467.6	-1138.3	1103.3	-0.05	0.05	Satisfied
-166.7	-84612.1	-492.3	-1301.5	1264.6	-0.06	0.06	Satisfied
-175	-95721.6	-517	-1470.9	1432.1	-0.07	0.07	Satisfied
-183.3	-107259.7	-541.8	-1646.8	1606.2	-0.08	0.08	Satisfied
-191.7	-119244.4	-566.5	-1829.5	1787	-0.09	0.09	Satisfied
-200	-131693.3	-591.3	-2019.2	1974.8	-0.1	0.09	Satisfied
-208.8	-145394.7	-617.5	-2227.9	2181.6	-0.11	0.1	Satisfied
-217.6	-159239.7	-643.7	-2438.8	2390.6	-0.12	0.11	Satisfied
-226.5	-172831.6	-670	-2645.9	2595.7	-0.13	0.12	Satisfied
-235.3	-185773.5	-696.2	-2843.2	2791	-0.14	0.13	Satisfied
-244.1	-197668.7	-722.5	-3024.5	2970.4	-0.14	0.14	Satisfied
-252.9	-208120.4	-748.8	-3184	3127.9	-0.15	0.15	Satisfied
-261.8	-216731.7	-775.1	-3315.6	3257.5	-0.16	0.16	Satisfied
-270.6	-223106	-801.4	-3381	3353.2	-0.16	0.16	Satisfied
-279.4	-226846.4	-827.7	3381	-3381	-0.17	0.16	Satisfied
-288.2	-227556.2	-854	3381	-3381	-0.17	0.16	Satisfied
-297.1	-224838.7	-880.4	-3381	3376.6	-0.16	0.16	Satisfied
-305.9	-218297.1	-906.7	-3344.2	3276.3	-0.16	0.16	Satisfied
-314.7	-207652.8	-933.1	-3183.8	3113.9	-0.15	0.15	Satisfied
-323.5	-193957.3	-959.4	-2977.1	2905.2	-0.14	0.14	Satisfied
-332.4	-178100.7	-985.8	-2737.7	2663.8	-0.13	0.13	Satisfied
-341.2	-160822.1	-1012.2	-2476.6	2400.8	-0.12	0.11	Satisfied
-350	-142721.7	-1038.6	-2203.2	2125.3	-0.1	0.1	Satisfied
-358.8	-124274.5	-1065.1	-1924.4	1844.6	-0.09	0.09	Satisfied
-367.6	-106205.8	-1091.5	-1651.4	1569.6	-0.08	0.07	Satisfied
-376.5	-89077.7	-1117.9	-1392.7	1308.9	-0.07	0.06	Satisfied
-385.3	-73286	-1144.4	-1154.2	1068.4	-0.05	0.05	Satisfied
-394.1	-59052.9	-1170.9	-939.4	851.6	-0.04	0.04	Satisfied
-402.9	-46464	-1197.3	-749.5	659.7	-0.04	0.03	Satisfied
-411.8	-35558.6	-1223.8	-585.1	493.3	-0.03	0.02	Satisfied
-420.6	-26339.4	-1250.3	-446.3	352.6	-0.02	0.02	Satisfied
-429.4	-18781.3	-1276.9	-332.7	236.9	-0.02	0.01	Satisfied
-438.2	-12782.9	-1303.4	-242.7	145	-0.01	0.01	Satisfied
-447.1	-8193.7	-1329.9	-174.1	74.4	-0.01	0	Satisfied
-455.9	-4842.3	-1356.5	-124.3	22.6	-0.01	0	Satisfied
-464.7	-2544.6	-1383	-90.4	-13.2	0	0	Satisfied
-473.5	-1108.6	-1409.6	-69.6	-36	0	0	Satisfied
-482.4	-338	-1436.2	-59	-48.7	0	0	Satisfied
-491.2	-34.8	-1462.8	-55.3	-54.3	0	0	Satisfied
-500	0	-1489.4	-55.8	-55.8	0	0	Satisfied

Table 5.12 Approach (1) verification state phase 2

Check the verification with VCASLU software

Verifica C.A. S.L.U. - File

File Materiali Opzioni Visualizza Progetto Sez. Rett. Sismica Normativa: NTC 2008 ?

Titolo :

Sezione circolare cava

Raggio esterno: 14 [cm]
 Raggio interno: 11.4 [cm]
 N° barre uguali: 45
 Diametro barre: .8 [cm]
 Copriferro (baric.): 2.6 [cm]

N° barre: 0 Zoom

Tipo Sezione

Rettan.re Trapezi
 a T Circolare
 Rettangoli Coord.

Sollecitazioni

S.L.U. Metodo n

N_{Ed}: 5.16 0 kN
 M_{xEd}: 12.14 0 kNm
 M_{yEd}: 0 0

P.to applicazione N

Centro Baricentro cls
 Coord.[cm] xN: 0 yN: 0

Tipo rottura

Lato calcestruzzo - Acciaio snervato

Metodo di calcolo

S.L.U.+ S.L.U.-
 Metodo n

Tipo flessione

Retta Deviata

Vertici: 52 N° rett. 100

Calcola MRd Dominio M-N

L₀: 0 cm Col. modello

Precompresso

Materiali

S355 C25/30

ε_{su}: 67.5 ‰ ε_{c2}: 2 ‰
 f_{yd}: 308.7 N/mm² ε_{cu}: 3.5 ‰
 E_s: 200,000 N/mm² f_{cd}: 14.17
 E_s/E_c: 15 f_{cc}/f_{cd}: 0.8
 ε_{syd}: 1.544 ‰ σ_{c,adm}: 9.75
 σ_{s,adm}: 235.3 N/mm² τ_{co}: 0.6
 τ_{c1}: 1.829

M_{xRd}: 58.7 kN m

σ_c: -14.17 N/mm²
 σ_s: 308.7 N/mm²
 ε_c: 3.5 ‰
 ε_s: 4.121 ‰
 d: 25.37 cm
 x: 11.65 x/d: 0.4592
 δ: 1

Figure 5.26 Properties definitions

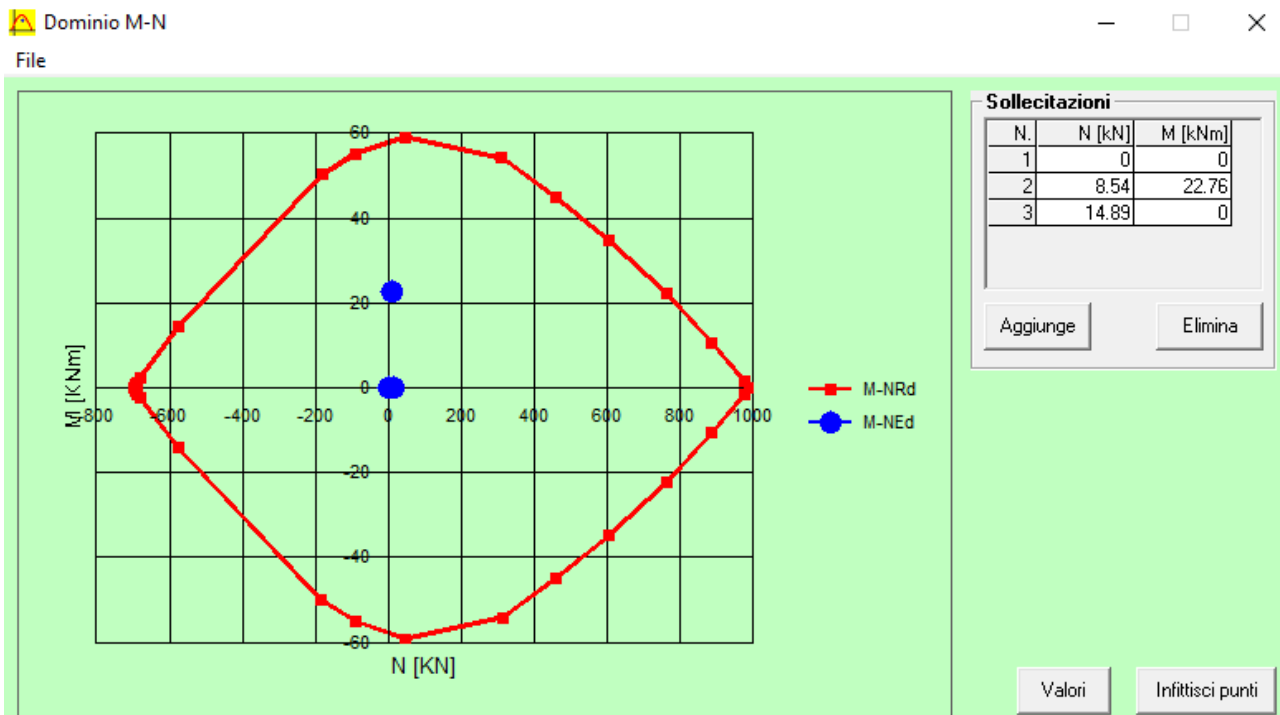


Figure 5.27 Interaction domain verification

5.6.1.3 Analysis of approach [2] combination

5.6.1.3.1 Approach [2] phase (1) results

Soil pressure along the micropiles results:

Soil pressure												
Elevation [cm]	Active pressure [daN/cm ²]						Passive pressure [daN/cm ²]					
z	σ_v	σ_h	u	σ'_v	σ'_h	τ	σ_v	σ_h	u	σ'_v	σ'_h	τ
0	0.004	0.002	0	0.004	0.002	0	0.004	0.002	0	0.004	0.002	0
-8.33	0.015	0.006	0	0.015	0.006	0	0.015	0.007	0	0.015	0.007	0
-16.67	0.03	0.012	0	0.03	0.012	0	0.03	0.014	0	0.03	0.014	0
-25	0.045	0.019	0	0.045	0.019	0	0.045	0.021	0	0.045	0.021	0
-33.33	0.06	0.025	0	0.06	0.025	0	0.06	0.028	0	0.06	0.028	0
-41.67	0.075	0.031	0	0.075	0.031	0	0.075	0.035	0	0.075	0.035	0
-50	0.09	0.037	0	0.09	0.037	0	0.09	0.042	0	0.09	0.042	0
-58.33	0.105	0.044	0	0.105	0.044	0	0.105	0.049	0	0.105	0.049	0
-66.67	0.12	0.05	0	0.12	0.05	0	0.12	0.056	0	0.12	0.056	0
-75	0.135	0.056	0	0.135	0.056	0	0.135	0.063	0	0.135	0.063	0
-83.33	0.15	0.062	0	0.15	0.062	0	0.15	0.07	0	0.15	0.07	0
-91.67	0.165	0.069	0	0.165	0.069	0	0.165	0.077	0	0.165	0.077	0
-100	0.18	0.075	0	0.18	0.075	0	0.18	0.084	0	0.18	0.084	0
-108.33	0.195	0.081	0	0.195	0.081	0	0.195	0.091	0	0.195	0.091	0
-116.67	0.21	0.087	0	0.21	0.087	0	0.21	0.097	0	0.21	0.097	0
-125	0.225	0.094	0	0.225	0.094	0	0.225	0.104	0	0.225	0.104	0
-133.33	0.24	0.1	0	0.24	0.1	0	0.24	0.111	0	0.24	0.111	0
-141.67	0.255	0.106	0	0.255	0.106	0	0.255	0.118	0	0.255	0.118	0
-150	0.27	0.112	0	0.27	0.112	0	0.27	0.125	0	0.27	0.125	0
-158.33	0.285	0.118	0	0.285	0.118	0	0.285	0.132	0	0.285	0.132	0
-166.67	0.3	0.125	0	0.3	0.125	0	0.3	0.139	0	0.3	0.139	0
-175	0.315	0.131	0	0.315	0.131	0	0.315	0.146	0	0.315	0.146	0
-183.33	0.33	0.137	0	0.33	0.137	0	0.33	0.153	0	0.33	0.153	0
-191.67	0.345	0.143	0	0.345	0.143	0	0.345	0.16	0	0.345	0.16	0
-200	0.36	0.15	0	0.36	0.15	0	0.36	0.167	0	0.36	0.167	0
-208.82	0.376	0.156	0	0.376	0.156	0	0.376	0.175	0	0.376	0.175	0
-217.65	0.392	0.163	0	0.392	0.163	0	0.392	0.182	0	0.392	0.182	0
-226.47	0.408	0.169	0	0.408	0.169	0	0.408	0.189	0	0.408	0.189	0
-235.29	0.424	0.176	0	0.424	0.176	0	0.424	0.197	0	0.424	0.197	0
-244.12	0.439	0.183	0	0.439	0.183	0	0.439	0.204	0	0.439	0.204	0
-252.94	0.455	0.189	0	0.455	0.189	0	0.455	0.211	0	0.455	0.211	0
-261.76	0.471	0.196	0	0.471	0.196	0	0.471	0.219	0	0.471	0.219	0
-270.59	0.487	0.202	0	0.487	0.202	0	0.487	0.226	0	0.487	0.226	0
-279.41	0.503	0.209	0	0.503	0.209	0	0.503	0.233	0	0.503	0.233	0
-288.24	0.519	0.216	0	0.519	0.216	0	0.519	0.241	0	0.519	0.241	0
-297.06	0.535	0.222	0	0.535	0.222	0	0.535	0.248	0	0.535	0.248	0
-305.88	0.551	0.229	0	0.551	0.229	0	0.551	0.256	0	0.551	0.256	0
-314.71	0.566	0.235	0	0.566	0.235	0	0.566	0.263	0	0.566	0.263	0
-323.53	0.582	0.242	0	0.582	0.242	0	0.582	0.27	0	0.582	0.27	0
-332.35	0.598	0.249	0	0.598	0.249	0	0.598	0.278	0	0.598	0.278	0

-341.18	0.614	0.255	0	0.614	0.255	0	0.614	0.285	0	0.614	0.285	0
-350	0.63	0.262	0	0.63	0.262	0	0.63	0.292	0	0.63	0.292	0
-358.82	0.646	0.269	0	0.646	0.269	0	0.646	0.3	0	0.646	0.3	0
-367.65	0.662	0.275	0	0.662	0.275	0	0.662	0.307	0	0.662	0.307	0
-376.47	0.678	0.282	0	0.678	0.282	0	0.678	0.315	0	0.678	0.315	0
-385.29	0.694	0.288	0	0.694	0.288	0	0.694	0.322	0	0.694	0.322	0
-394.12	0.709	0.295	0	0.709	0.295	0	0.709	0.329	0	0.709	0.329	0
-402.94	0.725	0.302	0	0.725	0.302	0	0.725	0.337	0	0.725	0.337	0
-411.76	0.741	0.308	0	0.741	0.308	0	0.741	0.344	0	0.741	0.344	0
-420.59	0.757	0.315	0	0.757	0.315	0	0.757	0.351	0	0.757	0.351	0
-429.41	0.773	0.321	0	0.773	0.321	0	0.773	0.359	0	0.773	0.359	0
-438.24	0.789	0.328	0	0.789	0.328	0	0.789	0.366	0	0.789	0.366	0
-447.06	0.805	0.335	0	0.805	0.335	0	0.805	0.374	0	0.805	0.374	0
-455.88	0.821	0.341	0	0.821	0.341	0	0.821	0.381	0	0.821	0.381	0
-464.71	0.836	0.348	0	0.836	0.348	0	0.836	0.388	0	0.836	0.388	0
-473.53	0.852	0.354	0	0.852	0.354	0	0.852	0.396	0	0.852	0.396	0
-482.35	0.868	0.361	0	0.868	0.361	0	0.868	0.403	0	0.868	0.403	0
-491.18	0.884	0.368	0	0.884	0.368	0	0.884	0.41	0	0.884	0.41	0
-500	0.896	0.372	0	0.896	0.372	0	0.896	0.416	0	0.896	0.416	0

σ_v = total vertical tension
 σ_h = total horizontal tension
 u = neutral pressure
 σ'_v = effective vertical tension
 σ'_h = effective horizontal tension

Table 5.13 Approach (2) - Phase 1 soil pressure

The accumulative pressure and the corresponding moment arm:

Results of pressures [daN] and arms [cm], micropile							
Active				Passive			
R_h	-9354.1	b_h	333.3	R_h	10445.9	b_h	333.3
R'_h	-9354.1	b'_h	333.3	R'_h	10445.9	b'_h	333.3
R_u	0	b_u	0	R_u	0	b_u	0

R = results of the thrusts, b = arms with respect to the head of the micropile.
subscript h = resulting from the total pressures on the micropile.
subscript $'h$ = resulting from the effective pressures on the micropile.
subscript u = resultant of the neutral pressures on the micropile.

Table 5.14 Approach (2) - Phase 1 accumulative soil pressure

Internal actions:

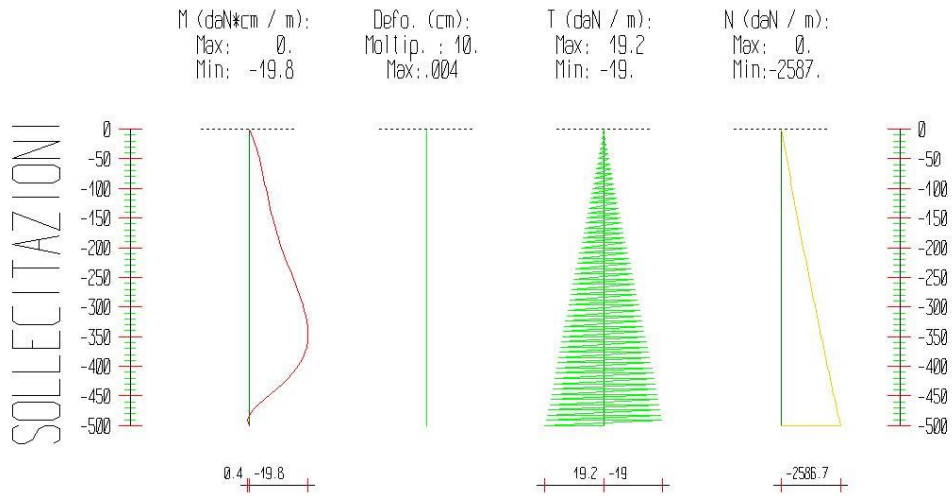


Figure 5.28 Approach (2)-phase (1) internal actions

Phase 1: Internal actions					
Elevation [cm]	Horizontal Deformation [cm]	Vertical Deformation [cm]	Bending Moment [daN cm]	Shear Forces [daN]	Axial Forces [daN]
-8.3	-0.0001	-0.001	-0.786	0.3	-37.8
-16.7	-0.0001	-0.001	-1.472	0.6	-75.8
-25	-0.0002	-0.001	-2.075	0.9	-113.9
-33.3	-0.0003	-0.001	-2.608	1.2	-152.3
-41.7	-0.0004	-0.001	-3.084	1.5	-190.8
-50	-0.0004	-0.001	-3.516	1.8	-229.5
-58.3	-0.0005	-0.001	-3.913	2.1	-268.4
-66.7	-0.0006	-0.001	-4.285	2.4	-307.4
-75	-0.0007	-0.001	-4.64	2.7	-346.7
-83.3	-0.0007	-0.001	-4.987	3	-386.1
-91.7	-0.0008	-0.001	-5.33	3.3	-425.7
-100	-0.0009	-0.001	-5.674	3.6	-465.5
-108.3	-0.0009	-0.001	-6.025	3.9	-505.4
-116.7	-0.001	-0.001	-6.386	4.2	-545.6
-125	-0.0011	-0.001	-6.759	4.5	-585.9
-133.3	-0.0012	-0.001	-7.147	4.8	-626.4
-141.7	-0.0012	-0.001	-7.551	5.1	-667.1
-150	-0.0013	-0.001	-7.972	5.4	-707.9
-158.3	-0.0014	-0.001	-8.412	5.7	-749
-166.7	-0.0015	-0.001	-8.869	6	-790.2
-175	-0.0015	-0.001	-9.345	6.3	-831.6
-183.3	-0.0016	-0.001	-9.838	6.6	-873.2
-191.7	-0.0017	-0.001	-10.346	6.9	-914.9
-200	-0.0017	-0.001	-10.868	7.2	-956.9
-208.8	-0.0018	-0.001	-11.54	8	-1001.5
-217.6	-0.0019	-0.001	-12.219	8.4	-1046.3

-226.5	-0.002	-0.001	-12.902	8.7	-1091.3
-235.3	-0.0021	-0.001	-13.587	9	-1136.5
-244.1	-0.0021	-0.001	-14.269	9.4	-1181.9
-252.9	-0.0022	-0.001	-14.946	9.7	-1227.5
-261.8	-0.0023	-0.001	-15.612	10	-1273.3
-270.6	-0.0024	-0.001	-16.263	10.4	-1319.3
-279.4	-0.0024	-0.001	-16.892	10.7	-1365.6
-288.2	-0.0025	-0.001	-17.49	11.1	-1412
-297.1	-0.0026	-0.001	-18.049	11.4	-1458.6
-305.9	-0.0027	-0.001	-18.557	11.7	-1505.4
-314.7	-0.0027	-0.001	-19.001	12.1	-1552.5
-323.5	-0.0028	-0.001	-19.365	12.4	-1599.7
-332.4	-0.0029	-0.001	-19.632	12.7	-1647.1
-341.2	-0.003	-0.001	-19.785	13.1	-1694.8
-350	-0.0031	-0.001	-19.802	13.4	-1742.6
-358.8	-0.0031	-0.001	-19.664	13.7	-1790.6
-367.6	-0.0032	-0.001	-19.351	14	-1838.9
-376.5	-0.0033	0	-18.842	14.3	-1887.3
-385.3	-0.0034	0	-18.122	14.7	-1935.9
-394.1	-0.0034	0	-17.177	15	-1984.8
-402.9	-0.0035	0	-16	15.3	-2033.8
-411.8	-0.0036	0	-14.592	15.6	-2083.1
-420.6	-0.0037	0	-12.965	15.9	-2132.5
-429.4	-0.0038	0	-11.144	16.2	-2182.2
-438.2	-0.0038	0	-9.172	16.6	-2232
-447.1	-0.0039	0	-7.111	16.9	-2282.1
-455.9	-0.004	0	-5.05	17.2	-2332.3
-464.7	-0.0041	0	-3.104	17.6	-2382.8
-473.5	-0.0041	0	-1.421	17.9	-2433.5
-482.4	-0.0042	0	-0.187	18.3	-2484.3
-491.2	-0.0043	0	0.376	18.8	-2535.4
-500	-0.0044	0	0	19.2	-2586.7

Table 5.15 Approach (2) - Phase 1 internal actions

5.6.1.3.2 Approach [2] phase (2) results

Soil pressure along the micropiles results:

Soil pressure												
Elevation [cm]	Active pressure [daN/cm ²]						Passive pressure [daN/cm ²]					
Z	σ_v	σ_h	u	σ'_v	σ'_h	τ	σ_v	σ_h	u	σ'_v	σ'_h	τ
0	0.056	0.014	0	0.056	0.014	0	0	0	0	0	0	0
-8.33	0.067	0.017	0	0.067	0.017	0	0	0	0	0	0	0
-16.67	0.082	0.021	0	0.082	0.021	0	0	0	0	0	0	0
-25	0.097	0.025	0	0.097	0.025	0	0	0	0	0	0	0
-33.33	0.112	0.029	0	0.112	0.029	0	0	0	0	0	0	0
-41.67	0.127	0.033	0	0.127	0.033	0	0	0	0	0	0	0
-50	0.142	0.037	0	0.142	0.037	0	0	0	0	0	0	0
-58.33	0.157	0.041	0	0.157	0.041	0	0	0	0	0	0	0
-66.67	0.172	0.045	0	0.172	0.045	0	0	0	0	0	0	0
-75	0.187	0.049	0	0.187	0.049	0	0	0	0	0	0	0
-83.33	0.202	0.053	0	0.202	0.053	0	0	0	0	0	0	0
-91.67	0.217	0.056	0	0.217	0.056	0	0	0	0	0	0	0
-100	0.232	0.06	0	0.232	0.06	0	0	0	0	0	0	0
-108.33	0.247	0.064	0	0.247	0.064	0	0	0	0	0	0	0
-116.67	0.262	0.068	0	0.262	0.068	0	0	0	0	0	0	0
-125	0.277	0.072	0	0.277	0.072	0	0	0	0	0	0	0
-133.33	0.292	0.076	0	0.292	0.076	0	0	0	0	0	0	0
-141.67	0.307	0.08	0	0.307	0.08	0	0	0	0	0	0	0
-150	0.322	0.084	0	0.322	0.084	0	0	0	0	0	0	0
-158.33	0.337	0.088	0	0.337	0.088	0	0	0	0	0	0	0
-166.67	0.352	0.092	0	0.352	0.092	0	0	0	0	0	0	0
-175	0.367	0.095	0	0.367	0.095	0	0	0	0	0	0	0
-183.33	0.382	0.099	0	0.382	0.099	0	0	0	0	0	0	0
-191.67	0.397	0.103	0	0.397	0.103	0	0	0	0	0	0	0
-200	0.412	0.107	0	0.412	0.107	0	0	0.001	0	0	0.001	0
-208.82	0.428	0.111	0	0.428	0.111	0	0.016	0.083	0	0.016	0.083	0
-217.65	0.444	0.115	0	0.444	0.115	0	0.032	0.165	0	0.032	0.165	0
-226.47	0.46	0.12	0	0.46	0.12	0	0.048	0.248	0	0.048	0.248	0
-235.29	0.476	0.124	0	0.476	0.124	0	0.064	0.33	0	0.064	0.33	0
-244.12	0.491	0.128	0	0.491	0.128	0	0.079	0.413	0	0.079	0.413	0
-252.94	0.507	0.132	0	0.507	0.132	0	0.095	0.496	0	0.095	0.496	0
-261.76	0.523	0.136	0	0.523	0.136	0	0.111	0.578	0	0.111	0.578	0
-270.59	0.539	0.14	0	0.539	0.14	0	0.127	0.661	0	0.127	0.661	0
-279.41	0.555	0.144	0	0.555	0.144	0	0.143	0.743	0	0.143	0.743	0
-288.24	0.571	0.148	0	0.571	0.148	0	0.159	0.826	0	0.159	0.826	0
-297.06	0.587	0.153	0	0.587	0.153	0	0.175	0.908	0	0.175	0.908	0
-305.88	0.603	0.157	0	0.603	0.157	0	0.191	0.991	0	0.191	0.991	0
-314.71	0.618	0.161	0	0.618	0.161	0	0.206	1.074	0	0.206	1.074	0
-323.53	0.634	0.165	0	0.634	0.165	0	0.222	0.969	0	0.222	0.969	0
-332.35	0.65	0.169	0	0.65	0.169	0	0.238	0.753	0	0.238	0.753	0
-341.18	0.666	0.173	0	0.666	0.173	0	0.254	0.573	0	0.254	0.573	0
-350	0.682	0.177	0	0.682	0.177	0	0.27	0.427	0	0.27	0.427	0

-358.82	0.698	0.181	0	0.698	0.181	0	0.286	0.311	0	0.286	0.311	0
-367.65	0.714	0.225	0	0.714	0.225	0	0.302	0.222	0	0.302	0.222	0
-376.47	0.73	0.304	0	0.73	0.304	0	0.318	0.157	0	0.318	0.157	0
-385.29	0.746	0.363	0	0.746	0.363	0	0.334	0.112	0	0.334	0.112	0
-394.12	0.761	0.405	0	0.761	0.405	0	0.349	0.091	0	0.349	0.091	0
-402.94	0.777	0.432	0	0.777	0.432	0	0.365	0.095	0	0.365	0.095	0
-411.76	0.793	0.448	0	0.793	0.448	0	0.381	0.099	0	0.381	0.099	0
-420.59	0.809	0.455	0	0.809	0.455	0	0.397	0.103	0	0.397	0.103	0
-429.41	0.825	0.454	0	0.825	0.454	0	0.413	0.107	0	0.413	0.107	0
-438.24	0.841	0.449	0	0.841	0.449	0	0.429	0.111	0	0.429	0.111	0
-447.06	0.857	0.439	0	0.857	0.439	0	0.445	0.134	0	0.445	0.134	0
-455.88	0.873	0.427	0	0.873	0.427	0	0.461	0.16	0	0.461	0.16	0
-464.71	0.888	0.413	0	0.888	0.413	0	0.476	0.187	0	0.476	0.187	0
-473.53	0.904	0.399	0	0.904	0.399	0	0.492	0.216	0	0.492	0.216	0
-482.35	0.92	0.383	0	0.92	0.383	0	0.508	0.245	0	0.508	0.245	0
-491.18	0.936	0.368	0	0.936	0.368	0	0.524	0.274	0	0.524	0.274	0
-500	0.948	0.351	0	0.948	0.351	0	0.536	0.302	0	0.536	0.302	0

σ_v = total vertical tension
 σ_h = total horizontal tension
 u = neutral pressure
 σ'_v = effective vertical tension
 σ'_h = effective horizontal tension

Table 5.16 Approach (2) - Phase 2 soil pressure

The accumulative pressure and the corresponding moment arm:

Results of pressures [daN] and arms [cm], micropile							
Active				Passive			
R_h	-8995.7	b_h	354.2	R_h	11482.6	b_h	323.3
R'_h	-8995.7	b'_h	354.2	R'_h	11482.6	b'_h	323.3
R_u	0	b_u	0	R_u	0	b_u	0

R = results of the thrusts, b = arms with respect to the head of the micropile.
subscript h = resulting from the total pressures on the micropile.
subscript $'h$ = resulting from the effective pressures on the micropile.
subscript u = resultant of the neutral pressures on the micropile.

Table 5.17 Approach (2) - Phase 2 accumulative soil pressure

Internal actions:

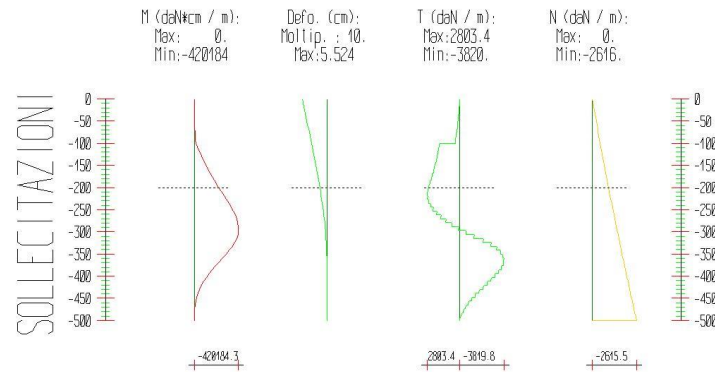


Figure 5.29 Approach (2)- phase (2) internal actions

Phase 2: Internal actions					
Elevation [cm]	Horizontal Deformation [cm]	Vertical Deformation [cm]	Bending Moment [daN cm]	Shear Forces [daN]	Axial Forces [daN]
-8.3	-5.3566	-0.001	-51.262	6.4	-37.8
-16.7	-5.1891	-0.001	-229.033	21.9	-75.8
-25	-5.0217	-0.001	-565.904	41.3	-114
-33.3	-4.8542	-0.001	-1094.467	64.6	-152.4
-41.7	-4.6867	-0.001	-1847.312	91.9	-191
-50	-4.5193	-0.001	-2857.029	123	-229.8
-58.3	-4.3519	-0.001	-4156.209	158.1	-268.8
-66.7	-4.1846	-0.001	-5777.439	197.1	-307.9
-75	-4.0174	-0.001	-7753.309	240	-347.3
-83.3	-3.8504	-0.001	-10116.405	286.8	-386.9
-91.7	-3.6835	-0.001	-12899.311	337.5	-426.7
-100	-3.5169	-0.001	-16134.608	392.1	-466.6
-108.3	-3.3505	-0.001	-30688.209	1750.6	-506.8
-116.7	-3.1848	-0.001	-45759.356	1813.1	-547.1
-125	-3.0198	-0.001	-61380.62	1879.4	-587.7
-133.3	-2.856	-0.001	-77584.565	1949.6	-628.4
-141.7	-2.6935	-0.001	-94403.753	2023.8	-669.4
-150	-2.5327	-0.001	-111870.736	2101.9	-710.5
-158.3	-2.374	-0.001	-130018.061	2183.8	-751.9
-166.7	-2.2175	-0.001	-148878.268	2269.7	-793.4
-175	-2.0637	-0.001	-168483.886	2359.5	-835.1
-183.3	-1.913	-0.001	-188867.44	2453.2	-877
-191.7	-1.7656	-0.001	-210061.444	2550.8	-919.2
-200	-1.6219	-0.001	-232098.406	2652.3	-961.5
-208.8	-1.4744	-0.001	-256377.75	2760.3	-1006.5
-217.6	-1.332	-0.001	-281034.165	2803.4	-1051.7
-226.5	-1.1952	-0.001	-305463.234	2778	-1097.2
-235.3	-1.0646	-0.001	-329060.542	2684.1	-1142.9
-244.1	-0.9405	-0.001	-351221.678	2521.7	-1188.8

-252.9	-0.8234	-0.001	-371342.246	2290.8	-1234.9
-261.8	-0.7138	-0.001	-388817.867	1991.4	-1281.2
-270.6	-0.612	-0.001	-403044.19	1623.5	-1327.8
-279.4	-0.5183	-0.001	-413416.891	1187.2	-1374.6
-288.2	-0.4328	-0.001	-419331.673	682.3	-1421.6
-297.1	-0.3557	-0.001	-420184.268	109	-1468.8
-305.9	-0.287	-0.001	-415370.431	-532.9	-1516.2
-314.7	-0.2266	-0.001	-404285.936	-1243.2	-1563.9
-323.5	-0.1742	-0.001	-386326.573	-2021.9	-1611.8
-332.4	-0.1296	-0.001	-362345.997	-2704	-1659.9
-341.2	-0.0923	-0.001	-334064.671	-3191	-1708.2
-350	-0.0616	-0.001	-302920.958	-3515.1	-1756.7
-358.8	-0.037	-0.001	-270092.997	-3705.6	-1805.5
-367.6	-0.0178	-0.001	-236522.844	-3789.3	-1854.4
-376.5	-0.0034	0	-203248.52	-3755.4	-1903.6
-385.3	0.007	0	-171401.759	-3593.3	-1953.1
-394.1	0.0139	0	-141796.843	-3338.8	-2002.7
-402.9	0.018	0	-114927.18	-3028.4	-2052.5
-411.8	0.0198	0	-90980.516	-2696.8	-2102.6
-420.6	0.0197	0	-70054.579	-2354.1	-2152.9
-429.4	0.0183	0	-52175.742	-2008.4	-2203.4
-438.2	0.0157	0	-37315.348	-1665.9	-2254.2
-447.1	0.0124	0	-25403.66	-1331.4	-2305.1
-455.9	0.0086	0	-16202.108	-1023.8	-2356.3
-464.7	0.0045	0	-9420.902	-749.2	-2407.7
-473.5	0.0002	0	-4744.39	-510.3	-2459.3
-482.4	-0.0043	0	-1841.717	-308.9	-2511.1
-491.2	-0.0088	0	-374.211	-145.8	-2563.2
-500	-0.0132	0	0	-21.6	-2615.5

Table 5.18 Approach (2) - Phase 2 internal actions

5.6.1.3.3 Approach [2] internal actions envelope

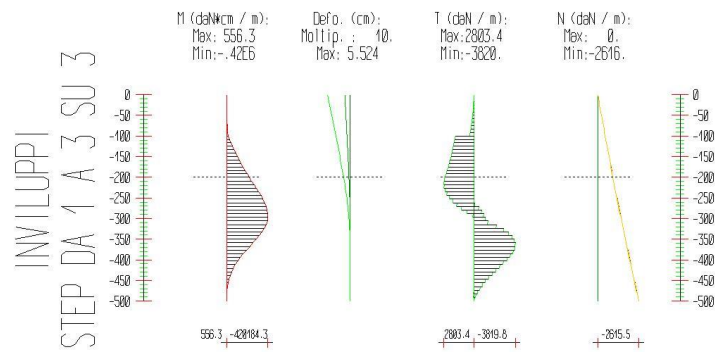


Figure 5.30 Approach (2)- envelope of internal actions.

Internal actions envelope						
Elevation [cm]	Bending moment [daN cm]		Shear forces [daN]		Axial forces [daN]	
	Min.	Max	Min.	Max	Min.	Max
z						
-8.3	-51.3	-8	.3	6.4	-37.8	-37.8
-16.7	-229.	-1.5	.6	21.9	-75.8	-75.8
-25.	-565.9	-2.1	.9	41.3	-114.	-113.9
-33.3	-1095.	-2.6	1.2	64.6	-152.4	-152.3
-41.7	-1847.	-3.1	1.5	91.9	-191.	-190.8
-50.	-2857.	-3.5	1.8	123.	-229.8	-229.5
-58.3	-4156.	-3.9	2.1	158.1	-268.8	-268.4
-66.7	-5777.	-4.3	2.4	197.1	-307.9	-307.4
-75.	-7753.	-4.6	2.7	240.	-347.3	-346.7
-83.3	-10116	-5.	3.	286.8	-386.9	-386.1
-91.7	-12899	-5.3	3.3	337.5	-426.7	-425.7
-100.	-16135	-5.7	3.6	392.1	-466.6	-465.5
-108.3	-30688	-6.	3.9	1750.6	-506.8	-505.4
-116.7	-45759	-6.4	4.2	1813.1	-547.1	-545.6
-125.	-61381	-6.8	4.5	1879.4	-587.7	-585.9
-133.3	-77585	-7.1	4.8	1949.6	-628.4	-626.4
-141.7	-94404	-7.6	5.1	2023.8	-669.4	-667.1
-150.	-.11E6	-8.	5.4	2101.9	-710.5	-707.9
-158.3	-.13E6	-8.4	5.7	2183.8	-751.9	-749.
-166.7	-.15E6	-8.9	6.	2269.7	-793.4	-790.2
-175.	-.17E6	-9.3	6.3	2359.5	-835.1	-831.6
-183.3	-.19E6	-9.8	6.6	2453.2	-877.	-873.2
-191.7	-.21E6	-10.3	6.9	2550.8	-919.2	-914.9
-200.	-.23E6	-10.9	7.2	2652.3	-961.5	-956.9
-208.8	-.26E6	-11.5	8.	2760.3	-1007.	-1002.
-217.6	-.28E6	-12.2	8.4	2803.4	-1052.	-1046.
-226.5	-.31E6	-12.9	8.7	2778.	-1097.	-1091.
-235.3	-.33E6	-13.6	9.	2684.1	-1143.	-1137.
-244.1	-.35E6	-14.3	9.4	2521.7	-1189.	-1182.
-252.9	-.37E6	-14.9	9.7	2290.8	-1235.	-1228.
-261.8	-.39E6	-15.6	10.	1991.4	-1281.	-1273.
-270.6	-.4E6	-16.3	-64.2	1623.5	-1328.	-1319.

-279.4	-.41E6	-16.9	-408.8	1187.2	-1375.	-1366.
-288.2	-.42E6	-17.5	-674.6	682.3	-1422.	-1412.
-297.1	-.42E6	-18.	-872.8	109.	-1469.	-1459.
-305.9	-.42E6	-18.6	-1014.	11.7	-1516.	-1505.
-314.7	-.4E6	-19.	-1243.	12.1	-1564.	-1553.
-323.5	-.39E6	-19.4	-2022.	12.4	-1612.	-1600.
-332.4	-.36E6	-19.6	-2704.	12.7	-1660.	-1647.
-341.2	-.33E6	-19.8	-3191.	13.1	-1708.	-1695.
-350.	-.3E6	-19.8	-3515.	13.4	-1757.	-1743.
-358.8	-.27E6	-19.7	-3706.	13.7	-1806.	-1791.
-367.6	-.24E6	-19.4	-3789.	14.	-1854.	-1839.
-376.5	-.2E6	-18.8	-3755.	14.3	-1904.	-1887.
-385.3	-.17E6	-18.1	-3593.	14.7	-1953.	-1936.
-394.1	-.14E6	-17.2	-3339.	15.	-2003.	-1985.
-402.9	-.11E6	-16.	-3028.	15.3	-2053.	-2034.
-411.8	-90981	-14.6	-2697.	15.6	-2103.	-2083.
-420.6	-70055	-13.	-2354.	15.9	-2153.	-2133.
-429.4	-52176	-11.1	-2008.	16.2	-2203.	-2182.
-438.2	-37315	-9.2	-1666.	16.6	-2254.	-2232.
-447.1	-25404	-7.1	-1331.	16.9	-2305.	-2282.
-455.9	-16202	426.9	-1024.	17.2	-2356.	-2332.
-464.7	-9421.	556.3	-749.2	17.6	-2408.	-2383.
-473.5	-4744.	477.1	-510.3	27.1	-2459.	-2434.
-482.4	-1842.	290.7	-308.9	39.6	-2511.	-2484.
-491.2	-374.2	98.2	-145.8	40.6	-2563.	-2535.
-500.	0.	0.	-21.6	30.3	-2616.	-2587.

Table 5.19 Approach (2) Internal actions envelope along the pile group

5.6.1.4 Verification state approach [2] combination

5.6.1.4.1 Approach [2] verification phase (1)

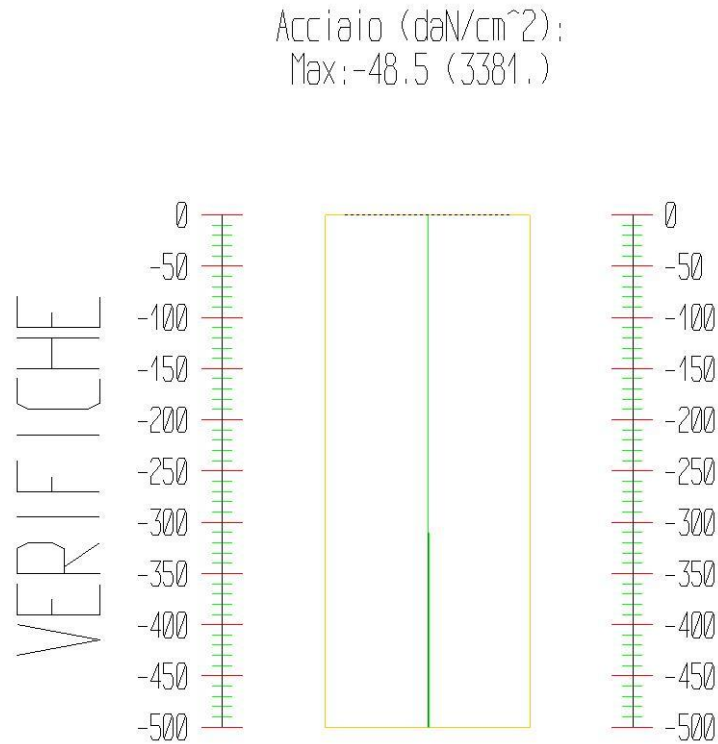


Figure 5.31 Approach (2)- Stress verification phase 1

Phase 1 verification							
σ max = max compression stress, σ max2 = max tensile stress, ε max = max compression strain, ε max2 = max tensile strain.							
Elevation [cm]	M [daN cm]	N [daN]	σ max [daN/cm ²]	σ max2 [daN/cm ²]	ε max [%]	ε max2 [%]	Verification
0	0	0	0	0	0	0	Satisfied
-8.3	-0.4	-18.9	-0.7	-0.7	0	0	Satisfied
-16.7	-0.7	-37.9	-1.4	-1.4	0	0	Satisfied
-25	-1	-57	-2.2	-2.1	0	0	Satisfied
-33.3	-1.3	-76.1	-2.9	-2.8	0	0	Satisfied
-41.7	-1.5	-95.4	-3.6	-3.6	0	0	Satisfied
-50	-1.8	-114.7	-4.3	-4.3	0	0	Satisfied
-58.3	-2	-134.2	-5.1	-5	0	0	Satisfied
-66.7	-2.1	-153.7	-5.8	-5.7	0	0	Satisfied
-75	-2.3	-173.3	-6.5	-6.5	0	0	Satisfied
-83.3	-2.5	-193	-7.3	-7.2	0	0	Satisfied
-91.7	-2.7	-212.8	-8	-7.9	0	0	Satisfied
-100	-2.8	-232.7	-8.8	-8.7	0	0	Satisfied
-108.3	-3	-252.7	-9.5	-9.4	0	0	Satisfied
-116.7	-3.2	-272.8	-10.3	-10.2	0	0	Satisfied

-125	-3.4	-292.9	-11	-10.9	0	0	Satisfied
-133.3	-3.6	-313.2	-11.8	-11.7	0	0	Satisfied
-141.7	-3.8	-333.5	-12.6	-12.4	0	0	Satisfied
-150	-4	-354	-13.3	-13.2	0	0	Satisfied
-158.3	-4.2	-374.5	-14.1	-14	0	0	Satisfied
-166.7	-4.4	-395.1	-14.9	-14.7	0	0	Satisfied
-175	-4.7	-415.8	-15.7	-15.5	0	0	Satisfied
-183.3	-4.9	-436.6	-16.4	-16.3	0	0	Satisfied
-191.7	-5.2	-457.5	-17.2	-17.1	0	0	Satisfied
-200	-5.4	-478.4	-18	-17.8	0	0	Satisfied
-208.8	-5.8	-500.7	-18.9	-18.7	0	0	Satisfied
-217.6	-6.1	-523.1	-19.7	-19.5	0	0	Satisfied
-226.5	-6.5	-545.6	-20.5	-20.4	0	0	Satisfied
-235.3	-6.8	-568.2	-21.4	-21.2	0	0	Satisfied
-244.1	-7.1	-591	-22.3	-22	0	0	Satisfied
-252.9	-7.5	-613.8	-23.1	-22.9	0	0	Satisfied
-261.8	-7.8	-636.7	-24	-23.7	0	0	Satisfied
-270.6	-8.1	-659.7	-24.8	-24.6	0	0	Satisfied
-279.4	-8.4	-682.8	-25.7	-25.5	0	0	Satisfied
-288.2	-8.7	-706	-26.6	-26.3	0	0	Satisfied
-297.1	-9	-729.3	-27.5	-27.2	0	0	Satisfied
-305.9	-9.3	-752.7	-28.4	-28.1	0	0	Satisfied
-314.7	-9.5	-776.2	-29.2	-28.9	0	0	Satisfied
-323.5	-9.7	-799.8	-30.1	-29.8	0	0	Satisfied
-332.4	-9.8	-823.6	-31	-30.7	0	0	Satisfied
-341.2	-9.9	-847.4	-31.9	-31.6	0	0	Satisfied
-350	-9.9	-871.3	-32.8	-32.5	0	0	Satisfied
-358.8	-9.8	-895.3	-33.7	-33.4	0	0	Satisfied
-367.6	-9.7	-919.4	-34.6	-34.3	0	0	Satisfied
-376.5	-9.4	-943.7	-35.5	-35.2	0	0	Satisfied
-385.3	-9.1	-968	-36.4	-36.1	0	0	Satisfied
-394.1	-8.6	-992.4	-37.3	-37.1	0	0	Satisfied
-402.9	-8	-1016.9	-38.2	-38	0	0	Satisfied
-411.8	-7.3	-1041.5	-39.1	-38.9	0	0	Satisfied
-420.6	-6.5	-1066.3	-40.1	-39.9	0	0	Satisfied
-429.4	-5.6	-1091.1	-41	-40.8	0	0	Satisfied
-438.2	-4.6	-1116	-41.9	-41.8	0	0	Satisfied
-447.1	-3.6	-1141	-42.8	-42.7	0	0	Satisfied
-455.9	-2.5	-1166.2	-43.7	-43.7	0	0	Satisfied
-464.7	-1.6	-1191.4	-44.7	-44.6	0	0	Satisfied
-473.5	-0.7	-1216.7	-45.6	-45.6	0	0	Satisfied
-482.4	-0.1	-1242.2	-46.6	-46.6	0	0	Satisfied
-491.2	0.2	-1267.7	-47.5	-47.5	0	0	Satisfied
-500	0	-1293.3	-48.5	-48.5	0	0	Satisfied

Table 5.20 Approach (2) verification state phase 1

Check the verification with VCASLU software

Verifica C.A. S.L.U. - File

File Materiali Opzioni Visualizza Progetto Sez. Rett. Sismica Normativa: NTC 2008 ?

Titolo : _____

Sezione circolare cava

Raggio esterno: 14 [cm]
 Raggio interno: 11.4 [cm]
 N° barre uguali: 45
 Diametro barre: .8 [cm]
 Copriferro (baric.): 2.6 [cm]

N° barre: 0 Zoom

Tipo Sezione

Rettan.re Trapezi
 a T Circolare
 Rettangoli Coord.

Sollecitazioni

S.L.U. Metodo n

N_{Ed}: 5.16 0 kN
 M_{xEd}: 12.14 0 kNm
 M_{yEd}: 0 0

P.to applicazione N

Centro Baricentro cls
 Coord.[cm] xN: 0 yN: 0

Tipo rottura

Lato calcestruzzo - Acciaio snervato

Metodo di calcolo

S.L.U.+ S.L.U.-
 Metodo n

Tipo flessione

Retta Deviata

Vertici: 52 N° rett.: 100

Calcola MRd Dominio M-N

L₀: 0 cm Col. modello

Precompresso

Materiali

S355 C25/30

E_{su}: 67.5 ‰ E_{c2}: 2 ‰
 f_{yd}: 308.7 N/mm² E_{cu}: 3.5 ‰
 E_s: 200,000 N/mm² f_{cd}: 14.17
 E_s/E_c: 15 f_{cc}/f_{cd}: 0.8 [?]
 E_{syd}: 1.544 ‰ σ_{c,adm}: 9.75
 σ_{s,adm}: 235.3E N/mm² τ_{co}: 0.6
 τ_{c1}: 1.829

M_{xRd}: 58.7 kN m

σ_c: -14.17 N/mm²
 σ_s: 308.7 N/mm²
 ε_c: 3.5 ‰
 ε_s: 4.121 ‰
 d: 25.37 cm
 x: 11.65 x/d: 0.4592
 δ: 1

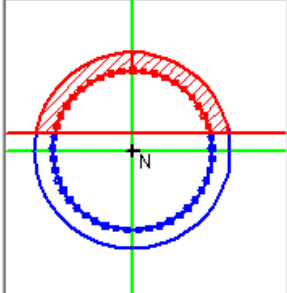


Figure 5.32 Properties definitions

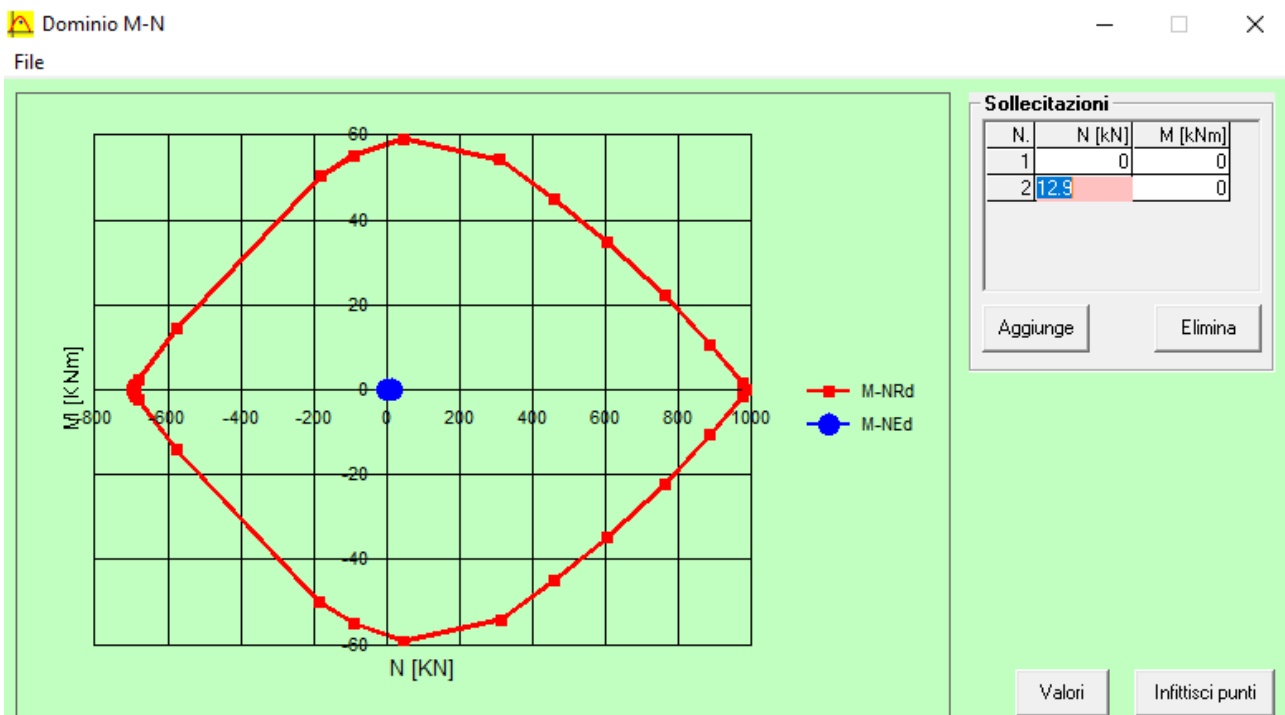


Figure 5.33 Interaction domain verification

5.6.1.4.2 Approach [2] verification Phase (2)

Acciaio (daN/cm²):
Max: -3213. (3381.)

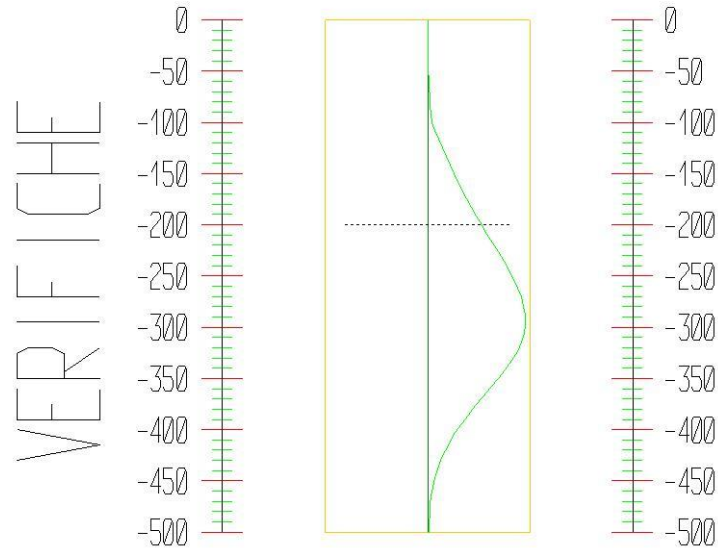


Figure 5.34 Approach (2)-Stress verification phase 2

Phase 2 verification							
σ max = max compression stress, σ max2 = max tensile stress, ε max = max compression strain, ε max2 = max tensile strain.							
Elevation [cm]	M [daN cm]	N [daN]	σ max [daN/cm ²]	σ max2 [daN/cm ²]	ε max [%]	ε max2 [%]	Verification
0	0	0	0	0	0	0	Satisfied
-8.3	-25.6	-18.9	-1.1	-0.3	0	0	Satisfied
-16.7	-114.5	-37.9	-3.2	0.3	0	0	Satisfied
-25	-283	-57	-6.4	2.2	0	0	Satisfied
-33.3	-547.2	-76.2	-11.2	5.4	0	0	Satisfied
-41.7	-923.7	-95.5	-17.6	10.4	0	0	Satisfied
-50	-1428.5	-114.9	-26	17.4	0	0	Satisfied
-58.3	-2078.1	-134.4	-36.5	26.5	0	0	Satisfied
-66.7	-2888.7	-154	-49.6	38	0	0	Satisfied
-75	-3876.7	-173.7	-65.3	52.3	0	0	Satisfied
-83.3	-5058.2	-193.4	-84	69.5	0	0	Satisfied
-91.7	-6449.7	-213.3	-105.8	89.8	-0.01	0	Satisfied
-100	-8067.3	-233.3	-131.1	113.6	-0.01	0.01	Satisfied
-108.3	-15344.1	-253.4	-242.2	223.2	-0.01	0.01	Satisfied
-116.7	-22879.7	-273.6	-357.2	336.7	-0.02	0.02	Satisfied
-125	-30690.3	-293.8	-476.4	454.4	-0.02	0.02	Satisfied
-133.3	-38792.3	-314.2	-600	576.5	-0.03	0.03	Satisfied
-141.7	-47201.9	-334.7	-728.3	703.2	-0.03	0.03	Satisfied

-150	-55935.4	-355.3	-861.5	834.9	-0.04	0.04	Satisfied
-158.3	-65009	-375.9	-999.9	971.7	-0.05	0.05	Satisfied
-166.7	-74439.1	-396.7	-1143.7	1113.9	-0.05	0.05	Satisfied
-175	-84241.9	-417.6	-1293.1	1261.8	-0.06	0.06	Satisfied
-183.3	-94433.7	-438.5	-1448.4	1415.6	-0.07	0.07	Satisfied
-191.7	-105030.7	-459.6	-1609.9	1575.5	-0.08	0.08	Satisfied
-200	-116049.2	-480.7	-1777.8	1741.8	-0.08	0.08	Satisfied
-208.8	-128188.9	-503.2	-1962.7	1925	-0.09	0.09	Satisfied
-217.6	-140517.1	-525.9	-2150.5	2111.1	-0.1	0.1	Satisfied
-226.5	-152731.6	-548.6	-2336.6	2295.5	-0.11	0.11	Satisfied
-235.3	-164530.3	-571.4	-2516.4	2473.5	-0.12	0.12	Satisfied
-244.1	-175610.8	-594.4	-2685.2	2640.7	-0.13	0.13	Satisfied
-252.9	-185671.1	-617.4	-2838.7	2792.4	-0.14	0.13	Satisfied
-261.8	-194408.9	-640.6	-2972	2924	-0.14	0.14	Satisfied
-270.6	-201522.1	-663.9	-3080.8	3031	-0.15	0.14	Satisfied
-279.4	-206708.4	-687.3	-3160.3	3108.8	-0.15	0.15	Satisfied
-288.2	-209665.8	-710.8	-3206	3152.7	-0.15	0.15	Satisfied
-297.1	-210092.1	-734.4	-3213.4	3158.3	-0.15	0.15	Satisfied
-305.9	-207685.2	-758.1	-3177.7	3120.9	-0.15	0.15	Satisfied
-314.7	-202143	-781.9	-3094.6	3036	-0.15	0.14	Satisfied
-323.5	-193163.3	-805.9	-2959.3	2898.9	-0.14	0.14	Satisfied
-332.4	-181173	-829.9	-2778.4	2716.2	-0.13	0.13	Satisfied
-341.2	-167032.3	-854.1	-2564.9	2500.9	-0.12	0.12	Satisfied
-350	-151460.5	-878.4	-2329.7	2263.8	-0.11	0.11	Satisfied
-358.8	-135046.5	-902.7	-2081.7	2014	-0.1	0.1	Satisfied
-367.6	-118261.4	-927.2	-1828.1	1758.6	-0.09	0.08	Satisfied
-376.5	-101624.3	-951.8	-1576.7	1505.4	-0.08	0.07	Satisfied
-385.3	-85700.9	-976.5	-1336.2	1263	-0.06	0.06	Satisfied
-394.1	-70898.4	-1001.3	-1112.6	1037.6	-0.05	0.05	Satisfied
-402.9	-57463.6	-1026.3	-909.8	832.9	-0.04	0.04	Satisfied
-411.8	-45490.3	-1051.3	-729.2	650.4	-0.03	0.03	Satisfied
-420.6	-35027.3	-1076.5	-571.5	490.8	-0.03	0.02	Satisfied
-429.4	-26087.9	-1101.7	-436.9	354.3	-0.02	0.02	Satisfied
-438.2	-18657.7	-1127.1	-325.2	240.7	-0.02	0.01	Satisfied
-447.1	-12701.8	-1152.6	-235.8	149.4	-0.01	0.01	Satisfied
-455.9	-8101.1	-1178.1	-167	78.7	-0.01	0	Satisfied
-464.7	-4710.5	-1203.8	-116.5	26.3	-0.01	0	Satisfied
-473.5	-2372.2	-1229.7	-82.1	-10.1	0	0	Satisfied
-482.4	-920.9	-1255.6	-61	-33.1	0	0	Satisfied
-491.2	-187.1	-1281.6	-50.9	-45.2	0	0	Satisfied
-500	0	-1307.7	-49	-49	0	0	Satisfied

Table 5.21 Approach (2) verification state phase 2

Check the verification with VCA SLU software

Verifica C.A. S.L.U. - File

File Materiali Opzioni Visualizza Progetto Sez. Rett. Sismica Normativa: NTC 2008 ?

Titolo : _____

Sezione circolare cava

Raggio esterno: 14 [cm]
 Raggio interno: 11.4 [cm]
 N° barre uguali: 45
 Diametro barre: .8 [cm]
 Copriferro (baric.): 2.6 [cm]

N° barre: 0 Zoom

Tipo Sezione

Rettan.re Trapezi
 a T Circolare
 Rettangoli Coord.

Sollecitazioni

S.L.U. Metodo n

N_{Ed}: 5.16 0 kN
 M_{xEd}: 12.14 0 kNm
 M_{yEd}: 0 0

P.to applicazione N

Centro Baricentro cls
 Coord.[cm] xN: 0 yN: 0

Tipo rottura

Lato calcestruzzo - Acciaio snervato

Metodo di calcolo

S.L.U.+ S.L.U.-
 Metodo n

Tipo flessione

Retta Deviata

Vertici: 52 N° rett. 100

Calcola MRd Dominio M-N

L₀: 0 cm Col. modello

Precompresso

Materiali

S355 C25/30

ε_{su}: 67.5 ‰ ε_{c2}: 2 ‰
 f_{yd}: 308.7 N/mm² ε_{cu}: 3.5 ‰
 E_s: 200,000 N/mm² f_{cd}: 14.17
 E_s/E_c: 15 f_{cc}/f_{cd}: 0.8 ?
 ε_{syd}: 1.544 ‰ σ_{c,adm}: 9.75
 σ_{s,adm}: 235.3 N/mm² τ_{co}: 0.6
 τ_{c1}: 1.829

M_{xRd}: 58.7 kN m

σ_c: -14.17 N/mm²
 σ_s: 308.7 N/mm²
 ε_c: 3.5 ‰
 ε_s: 4.121 ‰
 d: 25.37 cm
 x: 11.65 x/d: 0.4592
 δ: 1

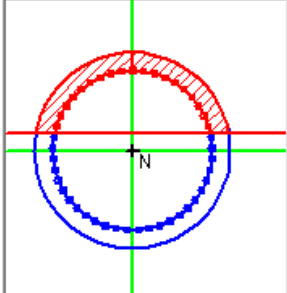


Figure 5.35 Properties definitions

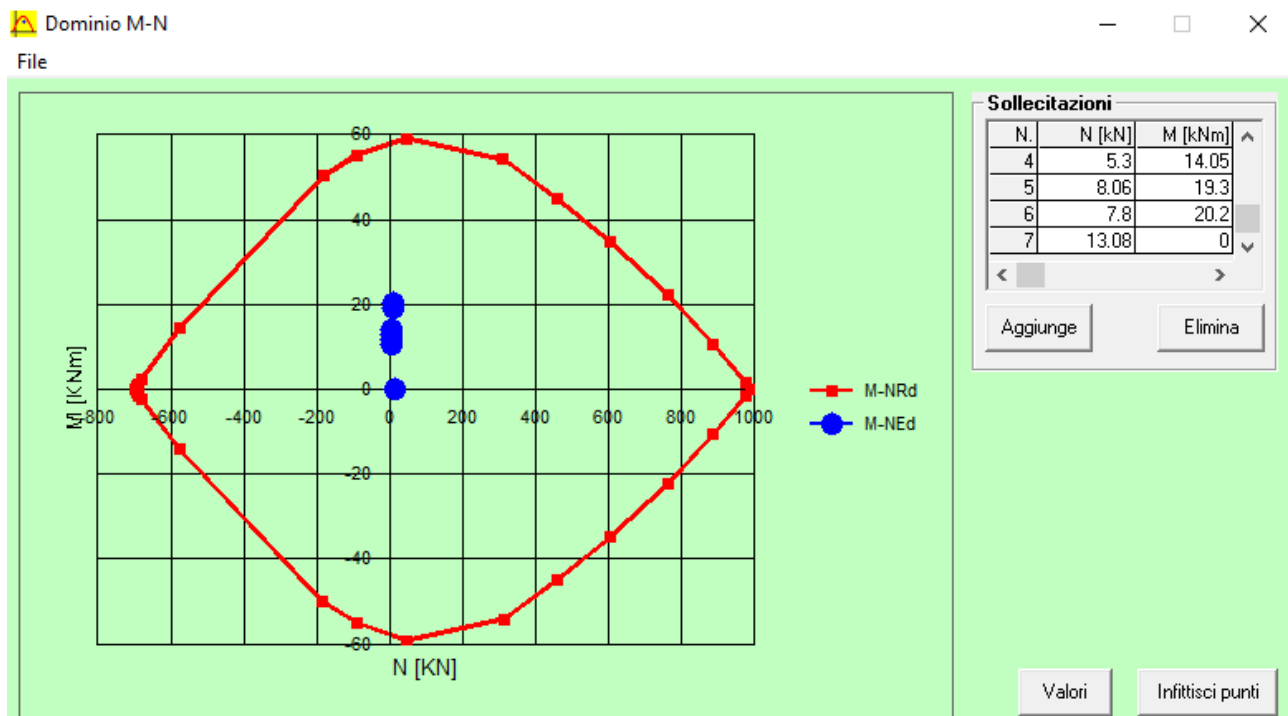


Figure 5.36 Interaction domain verification

5.6.1.5 Analysis SLV combination

5.6.1.5.1 SLV combination-Phase (1) results

Soil pressure along the micropiles results:

SLV combination soil pressure phase (2)												
Elevation [cm]	Active pressure [daN/cm ²]						Passive pressure [daN/cm ²]					
z	σ_v	σ_h	u	σ'_v	σ'_h	τ	σ_v	σ_h	u	σ'_v	σ'_h	τ
0	0.004	0.002	0	0.004	0.002	0	0.004	0.002	0	0.004	0.002	0
-8.33	0.015	0.007	0	0.015	0.007	0	0.015	0.007	0	0.015	0.007	0
-16.67	0.03	0.013	0	0.03	0.013	0	0.03	0.013	0	0.03	0.013	0
-25	0.045	0.02	0	0.045	0.02	0	0.045	0.02	0	0.045	0.02	0
-33.33	0.06	0.026	0	0.06	0.026	0	0.06	0.027	0	0.06	0.027	0
-41.67	0.075	0.033	0	0.075	0.033	0	0.075	0.033	0	0.075	0.033	0
-50	0.09	0.039	0	0.09	0.039	0	0.09	0.04	0	0.09	0.04	0
-58.33	0.105	0.046	0	0.105	0.046	0	0.105	0.046	0	0.105	0.046	0
-66.67	0.12	0.053	0	0.12	0.053	0	0.12	0.053	0	0.12	0.053	0
-75	0.135	0.059	0	0.135	0.059	0	0.135	0.06	0	0.135	0.06	0
-83.33	0.15	0.066	0	0.15	0.066	0	0.15	0.066	0	0.15	0.066	0
-91.67	0.165	0.072	0	0.165	0.072	0	0.165	0.073	0	0.165	0.073	0
-100	0.18	0.079	0	0.18	0.079	0	0.18	0.08	0	0.18	0.08	0
-108.33	0.195	0.085	0	0.195	0.085	0	0.195	0.086	0	0.195	0.086	0
-116.67	0.21	0.092	0	0.21	0.092	0	0.21	0.093	0	0.21	0.093	0
-125	0.225	0.099	0	0.225	0.099	0	0.225	0.099	0	0.225	0.099	0
-133.33	0.24	0.105	0	0.24	0.105	0	0.24	0.106	0	0.24	0.106	0
-141.67	0.255	0.112	0	0.255	0.112	0	0.255	0.113	0	0.255	0.113	0
-150	0.27	0.118	0	0.27	0.118	0	0.27	0.119	0	0.27	0.119	0
-158.33	0.285	0.125	0	0.285	0.125	0	0.285	0.126	0	0.285	0.126	0
-166.67	0.3	0.131	0	0.3	0.131	0	0.3	0.133	0	0.3	0.133	0
-175	0.315	0.138	0	0.315	0.138	0	0.315	0.139	0	0.315	0.139	0
-183.33	0.33	0.145	0	0.33	0.145	0	0.33	0.146	0	0.33	0.146	0
-191.67	0.345	0.151	0	0.345	0.151	0	0.345	0.153	0	0.345	0.153	0
-200	0.36	0.158	0	0.36	0.158	0	0.36	0.159	0	0.36	0.159	0
-208.82	0.376	0.165	0	0.376	0.165	0	0.376	0.166	0	0.376	0.166	0
-217.65	0.392	0.172	0	0.392	0.172	0	0.392	0.173	0	0.392	0.173	0
-226.47	0.408	0.179	0	0.408	0.179	0	0.408	0.18	0	0.408	0.18	0
-235.29	0.424	0.185	0	0.424	0.185	0	0.424	0.187	0	0.424	0.187	0
-244.12	0.439	0.192	0	0.439	0.192	0	0.439	0.194	0	0.439	0.194	0
-252.94	0.455	0.199	0	0.455	0.199	0	0.455	0.201	0	0.455	0.201	0
-261.76	0.471	0.206	0	0.471	0.206	0	0.471	0.208	0	0.471	0.208	0
-270.59	0.487	0.213	0	0.487	0.213	0	0.487	0.215	0	0.487	0.215	0
-279.41	0.503	0.22	0	0.503	0.22	0	0.503	0.222	0	0.503	0.222	0
-288.24	0.519	0.227	0	0.519	0.227	0	0.519	0.229	0	0.519	0.229	0
-297.06	0.535	0.234	0	0.535	0.234	0	0.535	0.236	0	0.535	0.236	0
-305.88	0.551	0.241	0	0.551	0.241	0	0.551	0.243	0	0.551	0.243	0
-314.71	0.566	0.248	0	0.566	0.248	0	0.566	0.25	0	0.566	0.25	0
-323.53	0.582	0.255	0	0.582	0.255	0	0.582	0.257	0	0.582	0.257	0

-332.35	0.598	0.262	0	0.598	0.262	0	0.598	0.264	0	0.598	0.264	0
-341.18	0.614	0.269	0	0.614	0.269	0	0.614	0.272	0	0.614	0.272	0
-350	0.63	0.276	0	0.63	0.276	0	0.63	0.279	0	0.63	0.279	0
-358.82	0.646	0.283	0	0.646	0.283	0	0.646	0.286	0	0.646	0.286	0
-367.65	0.662	0.29	0	0.662	0.29	0	0.662	0.293	0	0.662	0.293	0
-376.47	0.678	0.297	0	0.678	0.297	0	0.678	0.3	0	0.678	0.3	0
-385.29	0.694	0.304	0	0.694	0.304	0	0.694	0.307	0	0.694	0.307	0
-394.12	0.709	0.311	0	0.709	0.311	0	0.709	0.314	0	0.709	0.314	0
-402.94	0.725	0.318	0	0.725	0.318	0	0.725	0.321	0	0.725	0.321	0
-411.76	0.741	0.325	0	0.741	0.325	0	0.741	0.328	0	0.741	0.328	0
-420.59	0.757	0.332	0	0.757	0.332	0	0.757	0.335	0	0.757	0.335	0
-429.41	0.773	0.338	0	0.773	0.338	0	0.773	0.342	0	0.773	0.342	0
-438.24	0.789	0.345	0	0.789	0.345	0	0.789	0.349	0	0.789	0.349	0
-447.06	0.805	0.352	0	0.805	0.352	0	0.805	0.356	0	0.805	0.356	0
-455.88	0.821	0.359	0	0.821	0.359	0	0.821	0.363	0	0.821	0.363	0
-464.71	0.836	0.366	0	0.836	0.366	0	0.836	0.37	0	0.836	0.37	0
-473.53	0.852	0.373	0	0.852	0.373	0	0.852	0.377	0	0.852	0.377	0
-482.35	0.868	0.38	0	0.868	0.38	0	0.868	0.384	0	0.868	0.384	0
-491.18	0.884	0.387	0	0.884	0.387	0	0.884	0.391	0	0.884	0.391	0
-500	0.896	0.392	0	0.896	0.392	0	0.896	0.396	0	0.896	0.396	0

σ_v = total vertical tension
 σ_h = total horizontal tension
 u = neutral pressure
 σ'_v = effective vertical tension
 σ'_h = effective horizontal tension

Table 5.22 SLV Approach - Phase 1 soil pressure

The accumulative pressure and the corresponding moment arm:

Results of pressures [daN] and arms [cm], micropile							
Active				Passive			
R_h	-9852.6	b_h	333.3	R_h	9947.4	b_h	333.3
R'_h	-9852.6	b'_h	333.3	R'_h	9947.4	b'_h	333.3
R_u	0	b_u	0	R_u	0	b_u	0

R = results of the thrusts, b = arms with respect to the head of the micropile.
subscript h = resulting from the total pressures on the micropile.
subscript $'h$ = resulting from the effective pressures on the micropile.
subscript u = resultant of the neutral pressures on the micropile.

Table 5.23 SLV Approach - Phase 1 accumulative soil pressure

Internal actions:

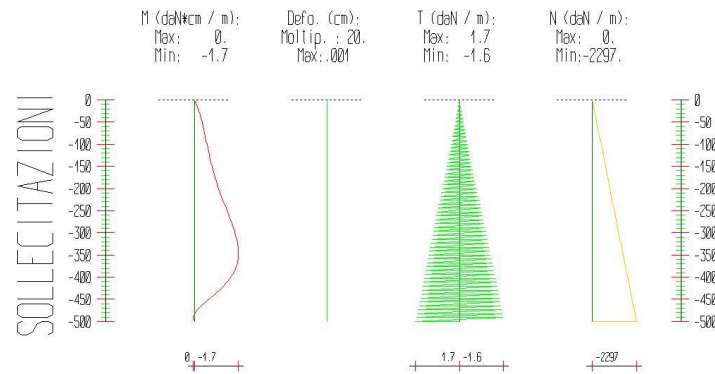


Figure 5.37 SLV-Phase (1) internal actions.

SLV-Phase (1) internal action.					
Elevation [cm]	Horizontal deformation [cm]	Vertical deformation [cm]	Bending moment [daN cm]	Shear forces [daN]	Axial forces [daN]
-8.3	0	-0.001	-0.068	0	-37.7
-16.7	0	-0.001	-0.128	0.1	-75.5
-25	0	-0.001	-0.18	0.1	-113.2
-33.3	0	-0.001	-0.226	0.1	-151
-41.7	0	-0.001	-0.268	0.1	-188.8
-50	0	-0.001	-0.305	0.2	-226.6
-58.3	0	-0.001	-0.339	0.2	-264.4
-66.7	-0.0001	-0.001	-0.372	0.2	-302.3
-75	-0.0001	-0.001	-0.403	0.2	-340.2
-83.3	-0.0001	-0.001	-0.433	0.3	-378
-91.7	-0.0001	-0.001	-0.462	0.3	-416
-100	-0.0001	-0.001	-0.492	0.3	-453.9
-108.3	-0.0001	-0.001	-0.523	0.3	-491.8
-116.7	-0.0001	-0.001	-0.554	0.4	-529.8
-125	-0.0001	-0.001	-0.586	0.4	-567.8
-133.3	-0.0001	-0.001	-0.62	0.4	-605.8
-141.7	-0.0001	-0.001	-0.655	0.4	-643.8
-150	-0.0001	-0.001	-0.692	0.5	-681.9
-158.3	-0.0001	-0.001	-0.73	0.5	-719.9
-166.7	-0.0001	-0.001	-0.769	0.5	-758
-175	-0.0001	-0.001	-0.811	0.5	-796.1
-183.3	-0.0001	-0.001	-0.853	0.6	-834.2
-191.7	-0.0001	-0.001	-0.898	0.6	-872.4
-200	-0.0002	-0.001	-0.943	0.6	-910.5
-208.8	-0.0002	-0.001	-1.001	0.7	-950.9
-217.6	-0.0002	-0.001	-1.06	0.7	-991.4
-226.5	-0.0002	-0.001	-1.119	0.8	-1031.9
-235.3	-0.0002	-0.001	-1.179	0.8	-1072.3
-244.1	-0.0002	-0.001	-1.238	0.8	-1112.9
-252.9	-0.0002	-0.001	-1.297	0.8	-1153.4
-261.8	-0.0002	-0.001	-1.354	0.9	-1193.9
-270.6	-0.0002	-0.001	-1.411	0.9	-1234.5

-279.4	-0.0002	-0.001	-1.465	0.9	-1275.1
-288.2	-0.0002	-0.001	-1.517	1	-1315.7
-297.1	-0.0002	-0.001	-1.566	1	-1356.4
-305.9	-0.0002	-0.001	-1.61	1	-1397
-314.7	-0.0002	-0.001	-1.648	1	-1437.7
-323.5	-0.0002	-0.001	-1.68	1.1	-1478.4
-332.4	-0.0003	-0.001	-1.703	1.1	-1519.1
-341.2	-0.0003	-0.001	-1.716	1.1	-1559.9
-350	-0.0003	-0.001	-1.718	1.2	-1600.7
-358.8	-0.0003	0	-1.706	1.2	-1641.4
-367.6	-0.0003	0	-1.679	1.2	-1682.3
-376.5	-0.0003	0	-1.635	1.2	-1723.1
-385.3	-0.0003	0	-1.572	1.3	-1763.9
-394.1	-0.0003	0	-1.49	1.3	-1804.8
-402.9	-0.0003	0	-1.388	1.3	-1845.7
-411.8	-0.0003	0	-1.266	1.4	-1886.6
-420.6	-0.0003	0	-1.125	1.4	-1927.6
-429.4	-0.0003	0	-0.967	1.4	-1968.5
-438.2	-0.0003	0	-0.796	1.4	-2009.5
-447.1	-0.0003	0	-0.617	1.5	-2050.5
-455.9	-0.0003	0	-0.438	1.5	-2091.5
-464.7	-0.0004	0	-0.269	1.5	-2132.6
-473.5	-0.0004	0	-0.123	1.6	-2173.7
-482.4	-0.0004	0	-0.016	1.6	-2214.7
-491.2	-0.0004	0	0.033	1.6	-2255.9
-500	-0.0004	0	0	1.7	-2297

Table 5.24 SLV Approach - Phase 1 internal actions

5.6.1.5.2 SLV combination-Phase (2) results

Soil pressure along the micropiles results:

SLV combination soil pressure phase (2)												
Elevation [cm]	Active pressure [daN/cm ²]						Passive pressure [daN/cm ²]					
z	σ_v	σ_h	u	σ'_v	σ'_h	τ	σ_v	σ_h	u	σ'_v	σ'_h	τ
0	0.044	0.011	0	0.044	0.011	0	0	0	0	0	0	0
-8.33	0.055	0.014	0	0.055	0.014	0	0	0	0	0	0	0
-16.67	0.07	0.018	0	0.07	0.018	0	0	0	0	0	0	0
-25	0.085	0.022	0	0.085	0.022	0	0	0	0	0	0	0
-33.33	0.1	0.026	0	0.1	0.026	0	0	0	0	0	0	0
-41.67	0.115	0.03	0	0.115	0.03	0	0	0	0	0	0	0
-50	0.13	0.034	0	0.13	0.034	0	0	0	0	0	0	0
-58.33	0.145	0.038	0	0.145	0.038	0	0	0	0	0	0	0
-66.67	0.16	0.042	0	0.16	0.042	0	0	0	0	0	0	0
-75	0.175	0.046	0	0.175	0.046	0	0	0	0	0	0	0
-83.33	0.19	0.049	0	0.19	0.049	0	0	0	0	0	0	0
-91.67	0.205	0.053	0	0.205	0.053	0	0	0	0	0	0	0
-100	0.22	0.057	0	0.22	0.057	0	0	0	0	0	0	0
-108.33	0.235	0.061	0	0.235	0.061	0	0	0	0	0	0	0
-116.67	0.25	0.065	0	0.25	0.065	0	0	0	0	0	0	0
-125	0.265	0.069	0	0.265	0.069	0	0	0	0	0	0	0
-133.33	0.28	0.073	0	0.28	0.073	0	0	0	0	0	0	0
-141.67	0.295	0.077	0	0.295	0.077	0	0	0	0	0	0	0
-150	0.31	0.081	0	0.31	0.081	0	0	0	0	0	0	0
-158.33	0.325	0.084	0	0.325	0.084	0	0	0	0	0	0	0
-166.67	0.34	0.088	0	0.34	0.088	0	0	0	0	0	0	0
-175	0.355	0.092	0	0.355	0.092	0	0	0	0	0	0	0
-183.33	0.37	0.096	0	0.37	0.096	0	0	0	0	0	0	0
-191.67	0.385	0.1	0	0.385	0.1	0	0	0	0	0	0	0
-200	0.4	0.104	0	0.4	0.104	0	0	0.001	0	0	0.001	0
-208.82	0.416	0.108	0	0.416	0.108	0	0.016	0.083	0	0.016	0.083	0
-217.65	0.432	0.112	0	0.432	0.112	0	0.032	0.165	0	0.032	0.165	0
-226.47	0.448	0.116	0	0.448	0.116	0	0.048	0.248	0	0.048	0.248	0
-235.29	0.464	0.121	0	0.464	0.121	0	0.064	0.33	0	0.064	0.33	0
-244.12	0.479	0.125	0	0.479	0.125	0	0.079	0.413	0	0.079	0.413	0
-252.94	0.495	0.129	0	0.495	0.129	0	0.095	0.496	0	0.095	0.496	0
-261.76	0.511	0.133	0	0.511	0.133	0	0.111	0.578	0	0.111	0.578	0
-270.59	0.527	0.137	0	0.527	0.137	0	0.127	0.661	0	0.127	0.661	0
-279.41	0.543	0.141	0	0.543	0.141	0	0.143	0.743	0	0.143	0.743	0
-288.24	0.559	0.145	0	0.559	0.145	0	0.159	0.826	0	0.159	0.826	0
-297.06	0.575	0.149	0	0.575	0.149	0	0.175	0.908	0	0.175	0.908	0
-305.88	0.591	0.154	0	0.591	0.154	0	0.191	0.804	0	0.191	0.804	0
-314.71	0.606	0.158	0	0.606	0.158	0	0.206	0.634	0	0.206	0.634	0
-323.53	0.622	0.162	0	0.622	0.162	0	0.222	0.492	0	0.222	0.492	0
-332.35	0.638	0.166	0	0.638	0.166	0	0.238	0.375	0	0.238	0.375	0
-341.18	0.654	0.17	0	0.654	0.17	0	0.254	0.283	0	0.254	0.283	0
-350	0.67	0.202	0	0.67	0.202	0	0.27	0.212	0	0.27	0.212	0

-358.82	0.686	0.268	0	0.686	0.268	0	0.286	0.159	0	0.286	0.159	0
-367.65	0.702	0.318	0	0.702	0.318	0	0.302	0.123	0	0.302	0.123	0
-376.47	0.718	0.355	0	0.718	0.355	0	0.318	0.101	0	0.318	0.101	0
-385.29	0.734	0.38	0	0.734	0.38	0	0.334	0.09	0	0.334	0.09	0
-394.12	0.749	0.396	0	0.749	0.396	0	0.349	0.091	0	0.349	0.091	0
-402.94	0.765	0.404	0	0.765	0.404	0	0.365	0.095	0	0.365	0.095	0
-411.76	0.781	0.407	0	0.781	0.407	0	0.381	0.105	0	0.381	0.105	0
-420.59	0.797	0.405	0	0.797	0.405	0	0.397	0.121	0	0.397	0.121	0
-429.41	0.813	0.4	0	0.813	0.4	0	0.413	0.14	0	0.413	0.14	0
-438.24	0.829	0.393	0	0.829	0.393	0	0.429	0.161	0	0.429	0.161	0
-447.06	0.845	0.384	0	0.845	0.384	0	0.445	0.183	0	0.445	0.183	0
-455.88	0.861	0.374	0	0.861	0.374	0	0.461	0.207	0	0.461	0.207	0
-464.71	0.876	0.364	0	0.876	0.364	0	0.476	0.231	0	0.476	0.231	0
-473.53	0.892	0.354	0	0.892	0.354	0	0.492	0.256	0	0.492	0.256	0
-482.35	0.908	0.343	0	0.908	0.343	0	0.508	0.28	0	0.508	0.28	0
-491.18	0.924	0.333	0	0.924	0.333	0	0.524	0.305	0	0.524	0.305	0
-500	0.936	0.32	0	0.936	0.32	0	0.536	0.328	0	0.536	0.328	0

σ_v = total vertical tension
 σ_h = total horizontal tension
 u = neutral pressure
 σ'_v = effective vertical tension
 σ'_h = effective horizontal tension

Table 5.25 SLV Approach - Phase 2 soil pressure

The accumulative pressure and the corresponding moment arm:

Results of pressures [daN] and arms [cm], micropile							
Active				Passive			
R_h	-8658.6	b_h	351.8	R_h	9760.5	b_h	325.8
R'_h	-8658.6	b'_h	351.8	R'_h	9760.5	b'_h	325.8
R_u	0	b_u	0	R_u	0	b_u	0

R = results of the thrusts, b = arms with respect to the head of the micropile.
subscript h = resulting from the total pressures on the micropile.
subscript $'h$ = resulting from the effective pressures on the micropile.
subscript u = resultant of the neutral pressures on the micropile.

Table 5.26 SLV Approach - Phase 2 accumulative soil pressure

Internal actions:

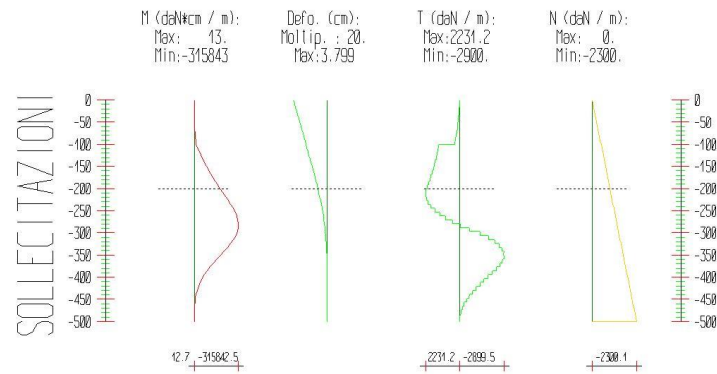


Figure 5.38 SLV-phase (2) internal actions.

SLV-Phase (2) internal action.					
Elevation [cm]	Horizontal deformation [cm]	Vertical deformation [cm]	Bending moment [daN cm]	Shear forces [daN]	Axial forces [daN]
-8.3	-3.6801	-0.001	-39.591	4.8	-37.7
-16.7	-3.5609	-0.001	-178.995	16.8	-75.5
-25	-3.4418	-0.001	-445.775	32.1	-113.2
-33.3	-3.3226	-0.001	-867.493	50.7	-151
-41.7	-3.2034	-0.001	-1471.711	72.6	-188.8
-50	-3.0843	-0.001	-2285.989	97.9	-226.6
-58.3	-2.9652	-0.001	-3337.889	126.4	-264.5
-66.7	-2.8462	-0.001	-4654.972	158.3	-302.3
-75	-2.7273	-0.001	-6264.796	193.4	-340.2
-83.3	-2.6084	-0.001	-8194.919	231.9	-378.1
-91.7	-2.4898	-0.001	-10472.898	273.7	-416.1
-100	-2.3713	-0.001	-13126.288	318.7	-454
-108.3	-2.253	-0.001	-24515.973	1367.1	-492
-116.7	-2.1353	-0.001	-36336.169	1418.8	-530
-125	-2.0181	-0.001	-48614.423	1473.8	-568
-133.3	-1.9019	-0.001	-61378.274	1532.1	-606
-141.7	-1.7867	-0.001	-74655.263	1593.7	-644.1
-150	-1.6728	-0.001	-88472.92	1658.6	-682.1
-158.3	-1.5606	-0.001	-102858.776	1726.8	-720.2
-166.7	-1.4502	-0.001	-117840.352	1798.4	-758.3
-175	-1.3419	-0.001	-133445.167	1873.2	-796.5
-183.3	-1.236	-0.001	-149700.734	1951.3	-834.6
-191.7	-1.1327	-0.001	-166634.561	2032.7	-872.8
-200	-1.0325	-0.001	-184274.152	2117.4	-911
-208.8	-0.9299	-0.001	-203742.363	2207.1	-951.5
-217.6	-0.8315	-0.001	-223422.299	2231.2	-992
-226.5	-0.7375	-0.001	-242703.618	2186	-1032.5
-235.3	-0.6483	-0.001	-260975.983	2071.7	-1073
-244.1	-0.5644	-0.001	-277629.063	1888.2	-1113.6
-252.9	-0.4861	-0.001	-292052.545	1635.6	-1154.2
-261.8	-0.4136	-0.001	-303636.131	1313.7	-1194.8

-270.6	-0.3471	-0.001	-311769.542	922.8	-1235.4
-279.4	-0.2869	-0.001	-315842.52	462.6	-1276.1
-288.2	-0.233	-0.001	-315244.823	-66.7	-1316.7
-297.1	-0.1855	-0.001	-309366.225	-665.2	-1357.4
-305.9	-0.1441	-0.001	-297596.512	-1332.8	-1398.2
-314.7	-0.1086	-0.001	-280780.945	-1904.6	-1438.9
-323.5	-0.0788	-0.001	-260278.182	-2322.5	-1479.7
-332.4	-0.0541	-0.001	-237228.315	-2611.1	-1520.5
-341.2	-0.0342	-0.001	-212568.72	-2793.5	-1561.3
-350	-0.0186	-0.001	-187051.914	-2890.6	-1602.2
-358.8	-0.0067	0	-161479.669	-2896.9	-1643
-367.6	0.0019	0	-136777.639	-2798.2	-1683.9
-376.5	0.0078	0	-113619.303	-2623.3	-1724.8
-385.3	0.0114	0	-92464.338	-2396.2	-1765.8
-394.1	0.0132	0	-73594.628	-2137.1	-1806.7
-402.9	0.0135	0	-57123.473	-1865.3	-1847.7
-411.8	0.0126	0	-43084.216	-1589.6	-1888.7
-420.6	0.0108	0	-31420.641	-1320.4	-1929.7
-429.4	0.0084	0	-21996.737	-1066.5	-1970.8
-438.2	0.0056	0	-14626.886	-833.7	-2011.9
-447.1	0.0025	0	-9090.622	-625.8	-2053
-455.9	-0.0009	0	-5144.183	-445.6	-2094.1
-464.7	-0.0043	0	-2529.216	-294.7	-2135.2
-473.5	-0.0078	0	-978.997	-174	-2176.4
-482.4	-0.0113	0	-222.582	-84	-2217.6
-491.2	-0.0148	0	12.7	-24.9	-2258.8
-500	-0.0183	0	0	3.2	-2300.1

Table 5.27 SLV Approach - Phase 2 internal actions

5.6.1.5.3 SLV combination - internal actions envelope

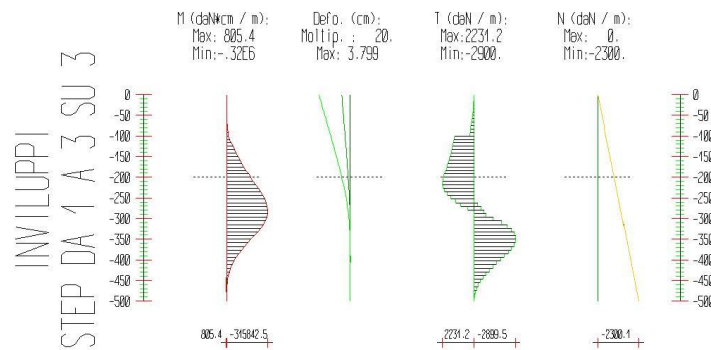


Figure 5.39 SLV envelope of internal actions.

Internal actions envelope						
Elevation (cm)	Bending momnet [daN cm]		Shear forces [daN]		Axial forces [daN]	
	Min.	Max	Min.	Max	Min.	Max
z						
-8.3	-39.6	-.1	0.	4.8	-37.7	-37.7
-16.7	-179.	-.1	.1	16.8	-75.5	-75.5
-25.	-445.8	-.2	.1	32.1	-113.2	-113.2
-33.3	-867.5	-.2	.1	50.7	-151.	-151.
-41.7	-1472.	-.3	.1	72.6	-188.8	-188.8
-50.	-2286.	-.3	.2	97.9	-226.6	-226.6
-58.3	-3338.	-.3	.2	126.4	-264.5	-264.4
-66.7	-4655.	-.4	.2	158.3	-302.3	-302.3
-75.	-6265.	-.4	.2	193.4	-340.2	-340.2
-83.3	-8195.	-.4	.3	231.9	-378.1	-378.
-91.7	-10473	-.5	.3	273.7	-416.1	-416.
-100.	-13126	-.5	.3	318.7	-454.	-453.9
-108.3	-24516	-.5	.3	1367.1	-492.	-491.8
-116.7	-36336	-.6	.4	1418.8	-530.	-529.8
-125.	-48614	-.6	.4	1473.8	-568.	-567.8
-133.3	-61378	-.6	.4	1532.1	-606.	-605.8
-141.7	-74655	-.7	.4	1593.7	-644.1	-643.8
-150.	-88473	-.7	.5	1658.6	-682.1	-681.9
-158.3	-.1E6	-.7	.5	1726.8	-720.2	-719.9
-166.7	-.12E6	-.8	.5	1798.4	-758.3	-758.
-175.	-.13E6	-.8	.5	1873.2	-796.5	-796.1
-183.3	-.15E6	-.9	.6	1951.3	-834.6	-834.2
-191.7	-.17E6	-.9	.6	2032.7	-872.8	-872.4
-200.	-.18E6	-.9	.6	2117.4	-911.	-910.5
-208.8	-.2E6	-1.	.7	2207.1	-951.5	-950.9
-217.6	-.22E6	-1.1	.7	2231.2	-992.	-991.4
-226.5	-.24E6	-1.1	.8	2186.	-1033.	-1032.
-235.3	-.26E6	-1.2	.8	2071.7	-1073.	-1072.
-244.1	-.28E6	-1.2	.8	1888.2	-1114.	-1113.
-252.9	-.29E6	-1.3	.8	1635.6	-1154.	-1153.
-261.8	-.3E6	-1.4	.9	1313.7	-1195.	-1194.

-270.6	-.31E6	-1.4	-259.3	922.8	-1235.	-1235.
-279.4	-.32E6	-1.5	-496.8	462.6	-1276.	-1275.
-288.2	-.32E6	-1.5	-677.5	1.	-1317.	-1316.
-297.1	-.31E6	-1.6	-810.2	1.	-1357.	-1356.
-305.9	-.3E6	-1.6	-1333.	1.	-1398.	-1397.
-314.7	-.28E6	-1.6	-1905.	1.	-1439.	-1438.
-323.5	-.26E6	-1.7	-2323.	1.1	-1480.	-1478.
-332.4	-.24E6	-1.7	-2611.	1.1	-1521.	-1519.
-341.2	-.21E6	-1.7	-2794.	1.1	-1561.	-1560.
-350.	-.19E6	-1.7	-2891.	1.2	-1602.	-1601.
-358.8	-.16E6	-1.7	-2897.	1.2	-1643.	-1641.
-367.6	-.14E6	-1.7	-2798.	1.2	-1684.	-1682.
-376.5	-.11E6	-1.6	-2623.	1.2	-1725.	-1723.
-385.3	-92464	-1.6	-2396.	1.3	-1766.	-1764.
-394.1	-73595	-1.5	-2137.	1.3	-1807.	-1805.
-402.9	-57124	-1.4	-1865.	1.3	-1848.	-1846.
-411.8	-43084	-1.3	-1590.	1.4	-1889.	-1887.
-420.6	-31421	-1.1	-1320.	1.4	-1930.	-1928.
-429.4	-21997	-1.	-1067.	1.4	-1971.	-1969.
-438.2	-14627	256.2	-833.7	1.4	-2012.	-2010.
-447.1	-9091.	673.2	-625.8	1.5	-2053.	-2051.
-455.9	-5144.	805.4	-445.6	1.5	-2094.	-2092.
-464.7	-2529.	734.1	-294.7	9.6	-2135.	-2133.
-473.5	-979.	539.4	-174.	23.6	-2176.	-2174.
-482.4	-222.6	300.1	-84.	28.7	-2218.	-2215.
-491.2	0.	94.4	-24.9	24.9	-2259.	-2256.
-500.	0.	0.	1.7	12.4	-2300.	-2297.

Table 5.28 SLV Approach - Internal actions envelope along the pile group

5.6.1.6 Verification state SLV combination

5.6.1.6.1 SLV combination - verification Phase (1)

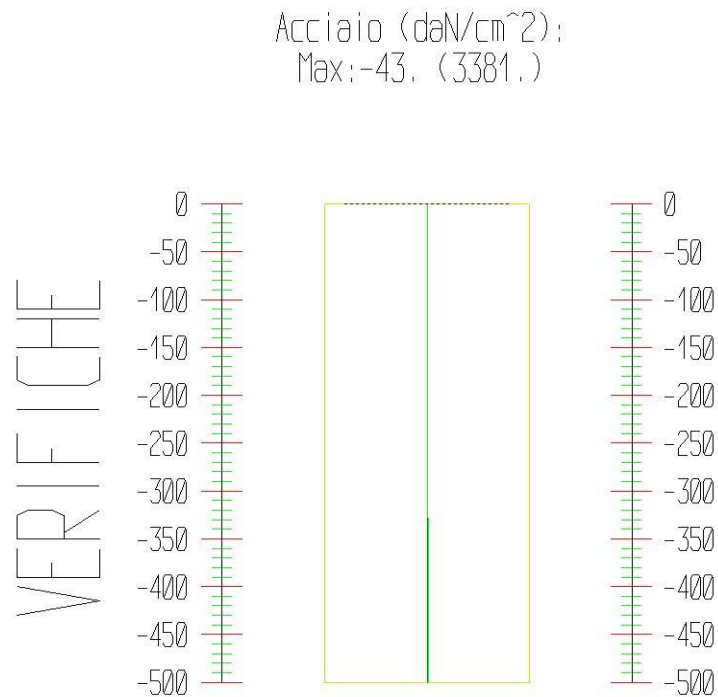


Figure 5.40 SLV- Phase (1) Verification

Phase (1) verification							
σ max = max compression stress, σ max2 = max tensile stress, ε max = max compression strain, ε max2 = max tensile strain							
Elevation [cm]	M [daN cm]	N [daN]	σ max [daN/cm ²]	σ max2 [daN/cm ²]	ε max [%]	ε max2 [%]	Verification
0	0	0	0	0	0	0	Satisfied
-8.3	0	-18.9	-0.7	-0.7	0	0	Satisfied
-16.7	-0.1	-37.7	-1.4	-1.4	0	0	Satisfied
-25	-0.1	-56.6	-2.1	-2.1	0	0	Satisfied
-33.3	-0.1	-75.5	-2.8	-2.8	0	0	Satisfied
-41.7	-0.1	-94.4	-3.5	-3.5	0	0	Satisfied
-50	-0.2	-113.3	-4.2	-4.2	0	0	Satisfied
-58.3	-0.2	-132.2	-5	-5	0	0	Satisfied
-66.7	-0.2	-151.1	-5.7	-5.7	0	0	Satisfied
-75	-0.2	-170.1	-6.4	-6.4	0	0	Satisfied
-83.3	-0.2	-189	-7.1	-7.1	0	0	Satisfied
-91.7	-0.2	-208	-7.8	-7.8	0	0	Satisfied
-100	-0.2	-226.9	-8.5	-8.5	0	0	Satisfied
-108.3	-0.3	-245.9	-9.2	-9.2	0	0	Satisfied
-116.7	-0.3	-264.9	-9.9	-9.9	0	0	Satisfied
-125	-0.3	-283.9	-10.6	-10.6	0	0	Satisfied
-133.3	-0.3	-302.9	-11.4	-11.3	0	0	Satisfied
-141.7	-0.3	-321.9	-12.1	-12.1	0	0	Satisfied
-150	-0.3	-340.9	-12.8	-12.8	0	0	Satisfied

-158.3	-0.4	-360	-13.5	-13.5	0	0	Satisfied
-166.7	-0.4	-379	-14.2	-14.2	0	0	Satisfied
-175	-0.4	-398.1	-14.9	-14.9	0	0	Satisfied
-183.3	-0.4	-417.1	-15.6	-15.6	0	0	Satisfied
-191.7	-0.4	-436.2	-16.4	-16.3	0	0	Satisfied
-200	-0.5	-455.3	-17.1	-17.1	0	0	Satisfied
-208.8	-0.5	-475.5	-17.8	-17.8	0	0	Satisfied
-217.6	-0.5	-495.7	-18.6	-18.6	0	0	Satisfied
-226.5	-0.6	-515.9	-19.3	-19.3	0	0	Satisfied
-235.3	-0.6	-536.2	-20.1	-20.1	0	0	Satisfied
-244.1	-0.6	-556.4	-20.9	-20.8	0	0	Satisfied
-252.9	-0.6	-576.7	-21.6	-21.6	0	0	Satisfied
-261.8	-0.7	-597	-22.4	-22.4	0	0	Satisfied
-270.6	-0.7	-617.3	-23.1	-23.1	0	0	Satisfied
-279.4	-0.7	-637.6	-23.9	-23.9	0	0	Satisfied
-288.2	-0.8	-657.9	-24.7	-24.6	0	0	Satisfied
-297.1	-0.8	-678.2	-25.4	-25.4	0	0	Satisfied
-305.9	-0.8	-698.5	-26.2	-26.2	0	0	Satisfied
-314.7	-0.8	-718.9	-27	-26.9	0	0	Satisfied
-323.5	-0.8	-739.2	-27.7	-27.7	0	0	Satisfied
-332.4	-0.9	-759.6	-28.5	-28.5	0	0	Satisfied
-341.2	-0.9	-779.9	-29.2	-29.2	0	0	Satisfied
-350	-0.9	-800.3	-30	-30	0	0	Satisfied
-358.8	-0.9	-820.7	-30.8	-30.7	0	0	Satisfied
-367.6	-0.8	-841.1	-31.5	-31.5	0	0	Satisfied
-376.5	-0.8	-861.5	-32.3	-32.3	0	0	Satisfied
-385.3	-0.8	-882	-33.1	-33	0	0	Satisfied
-394.1	-0.7	-902.4	-33.8	-33.8	0	0	Satisfied
-402.9	-0.7	-922.9	-34.6	-34.6	0	0	Satisfied
-411.8	-0.6	-943.3	-35.4	-35.3	0	0	Satisfied
-420.6	-0.6	-963.8	-36.1	-36.1	0	0	Satisfied
-429.4	-0.5	-984.3	-36.9	-36.9	0	0	Satisfied
-438.2	-0.4	-1004.8	-37.7	-37.6	0	0	Satisfied
-447.1	-0.3	-1025.3	-38.4	-38.4	0	0	Satisfied
-455.9	-0.2	-1045.8	-39.2	-39.2	0	0	Satisfied
-464.7	-0.1	-1066.3	-40	-40	0	0	Satisfied
-473.5	-0.1	-1086.8	-40.7	-40.7	0	0	Satisfied
-482.4	0	-1107.4	-41.5	-41.5	0	0	Satisfied
-491.2	0	-1127.9	-42.3	-42.3	0	0	Satisfied
-500	0	-1148.5	-43	-43	0	0	Satisfied

Table 5.29 SLV Approach - verification state phase 1

Check the verification with VCASLU software

Verifica C.A. S.L.U. - File

File Materiali Opzioni Visualizza Progetto Sez. Rett. Sismica Normativa: NTC 2008 ?

Titolo : _____

Sezione circolare cava

Raggio esterno: 14 [cm]
 Raggio interno: 11.4 [cm]
 N° barre uguali: 45
 Diametro barre: .8 [cm]
 Copriferro (baric.): 2.6 [cm]

N° barre: 0 Zoom

Tipo Sezione

Rettan.re Trapezi
 a T Circolare
 Rettangoli Coord.

Sollecitazioni

S.L.U. Metodo n

N_{Ed}: 5.16 [kN]
 M_{xEd}: 12.14 [kNm]
 M_{yEd}: 0 [kNm]

P.to applicazione N

Centro Baricentro cls
 Coord.[cm] xN: 0 yN: 0

Tipo rottura

Lato calcestruzzo - Acciaio snervato

Metodo di calcolo

S.L.U.+ S.L.U.-
 Metodo n

Tipo flessione

Retta Deviata

Vertici: 52 N° rett.: 100

Calcola MRd Dominio M-N

L₀: 0 cm Col. modello

Precompresso

Materiali

S355 C25/30

ε_{su}: 67.5 % ε_{c2}: 2 %
 f_{yd}: 308.7 N/mm² ε_{cu}: 3.5 %
 E_s: 200,000 N/mm² f_{cd}: 14.17
 E_s/E_c: 15 f_{cc}/f_{cd}: 0.8
 ε_{syd}: 1.544 % σ_{c,adm}: 9.75
 σ_{s,adm}: 235.3 N/mm² τ_{co}: 0.6
 τ_{c1}: 1.829

M_{xRd}: 58.7 [kNm]

σ_c: -14.17 N/mm²
 σ_s: 308.7 N/mm²
 ε_c: 3.5 %
 ε_s: 4.121 %
 d: 25.37 cm
 x: 11.65 x/d: 0.4592
 δ: 1

Figure 5.41 Properties definitions

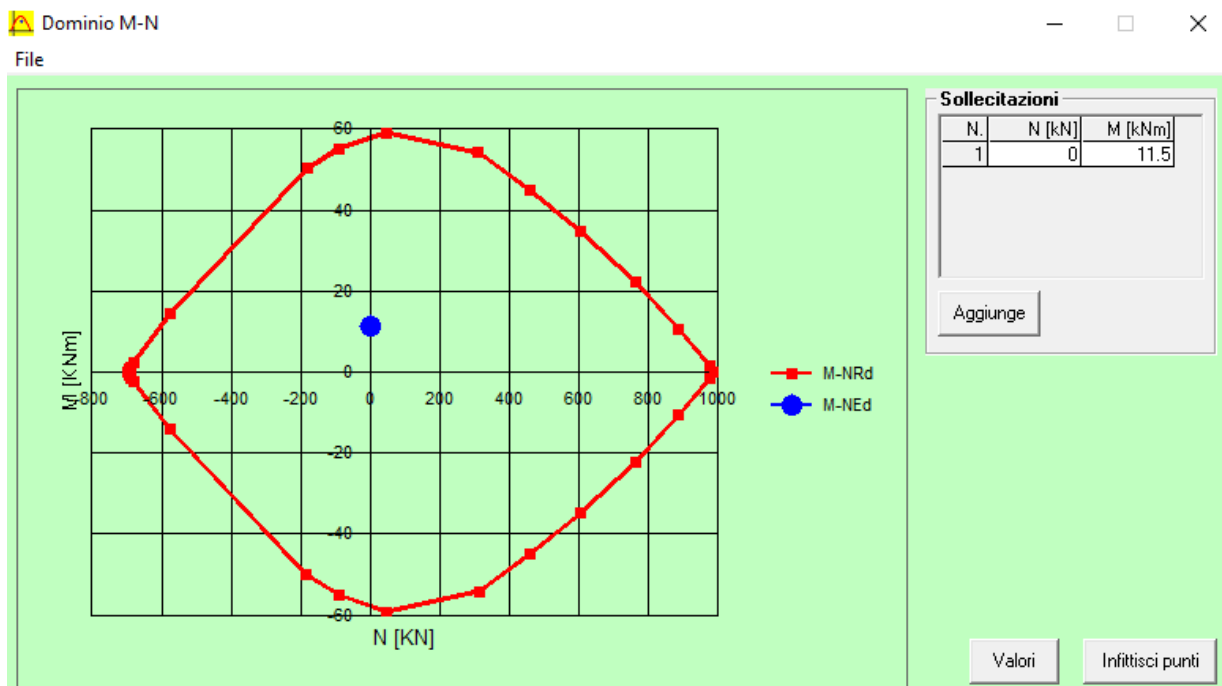


Figure 5.42 Interaction domain verification

5.6.1.6.2 SLV combination - verification Phase (2)

Acciaio (daN/cm²):
Max: -2419. (3381.)

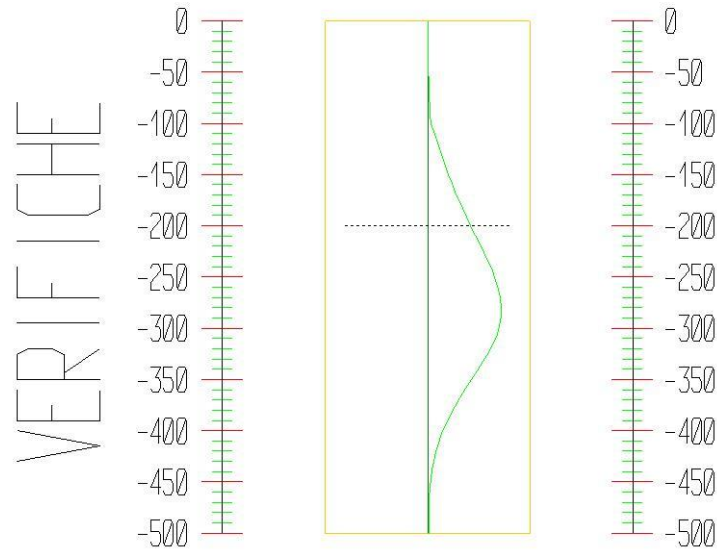


Figure 5.43 SLV-phase (2) verification

Phase (2) verification							
σ max = max compression stress, σ max2 = max tensile stress, ε max = max compression strain, ε max2 = max tensile strain							
Elevation [cm]	M [daN cm]	N [daN]	σ max [daN/cm ²]	σ max2 [daN/cm ²]	ε max [%]	ε max2 [%]	Verification
0	0	0	0	0	0	0	Satisfied
-8.3	-19.8	-18.9	-1	-0.4	0	0	Satisfied
-16.7	-89.5	-37.7	-2.8	-0.1	0	0	Satisfied
-25	-222.9	-56.6	-5.5	1.3	0	0	Satisfied
-33.3	-433.7	-75.5	-9.4	3.7	0	0	Satisfied
-41.7	-735.9	-94.4	-14.7	7.6	0	0	Satisfied
-50	-1143	-113.3	-21.6	13.1	0	0	Satisfied
-58.3	-1668.9	-132.2	-30.3	20.4	0	0	Satisfied
-66.7	-2327.5	-151.2	-41	29.6	0	0	Satisfied
-75	-3132.4	-170.1	-53.9	41.1	0	0	Satisfied
-83.3	-4097.5	-189.1	-69.2	55	0	0	Satisfied
-91.7	-5236.4	-208	-87.2	71.6	0	0	Satisfied
-100	-6563.1	-227	-108	91	-0.01	0	Satisfied
-108.3	-12258	-246	-195.1	176.7	-0.01	0.01	Satisfied
-116.7	-18168.1	-265	-285.4	265.6	-0.01	0.01	Satisfied
-125	-24307.2	-284	-379.2	358	-0.02	0.02	Satisfied
-133.3	-30689.1	-303	-476.7	454	-0.02	0.02	Satisfied
-141.7	-37327.6	-322	-578.1	554	-0.03	0.03	Satisfied
-150	-44236.5	-341.1	-683.6	658	-0.03	0.03	Satisfied

-158.3	-51429.4	-360.1	-793.4	766.4	-0.04	0.04	Satisfied
-166.7	-58920.2	-379.2	-907.7	879.3	-0.04	0.04	Satisfied
-175	-66722.6	-398.2	-1026.7	996.9	-0.05	0.05	Satisfied
-183.3	-74850.4	-417.3	-1150.7	1119.4	-0.05	0.05	Satisfied
-191.7	-83317.3	-436.4	-1279.8	1247.1	-0.06	0.06	Satisfied
-200	-92137.1	-455.5	-1414.2	1380.1	-0.07	0.07	Satisfied
-208.8	-101871.2	-475.7	-1562.6	1526.9	-0.07	0.07	Satisfied
-217.6	-111711.1	-496	-1712.6	1675.4	-0.08	0.08	Satisfied
-226.5	-121351.8	-516.2	-1859.5	1820.8	-0.09	0.09	Satisfied
-235.3	-130488	-536.5	-1998.8	1958.6	-0.1	0.09	Satisfied
-244.1	-138814.5	-556.8	-2125.8	2084.1	-0.1	0.1	Satisfied
-252.9	-146026.3	-577.1	-2236	2192.7	-0.11	0.1	Satisfied
-261.8	-151818.1	-597.4	-2324.6	2279.8	-0.11	0.11	Satisfied
-270.6	-155884.8	-617.7	-2387	2340.7	-0.11	0.11	Satisfied
-279.4	-157921.3	-638	-2418.6	2370.8	-0.12	0.11	Satisfied
-288.2	-157622.4	-658.4	-2414.9	2365.5	-0.11	0.11	Satisfied
-297.1	-154683.1	-678.7	-2371.1	2320.2	-0.11	0.11	Satisfied
-305.9	-148798.3	-699.1	-2282.6	2230.2	-0.11	0.11	Satisfied
-314.7	-140390.5	-719.5	-2155.8	2101.9	-0.1	0.1	Satisfied
-323.5	-130139.1	-739.8	-2001.2	1945.7	-0.1	0.09	Satisfied
-332.4	-118614.2	-760.2	-1827.2	1770.2	-0.09	0.08	Satisfied
-341.2	-106284.4	-780.7	-1641	1582.4	-0.08	0.08	Satisfied
-350	-93526	-801.1	-1448.2	1388.2	-0.07	0.07	Satisfied
-358.8	-80739.8	-821.5	-1255.1	1193.6	-0.06	0.06	Satisfied
-367.6	-68388.8	-842	-1068.6	1005.5	-0.05	0.05	Satisfied
-376.5	-56809.7	-862.4	-893.8	829.1	-0.04	0.04	Satisfied
-385.3	-46232.2	-882.9	-734.2	668	-0.03	0.03	Satisfied
-394.1	-36797.3	-903.4	-591.8	524.1	-0.03	0.02	Satisfied
-402.9	-28561.7	-923.9	-467.7	398.5	-0.02	0.02	Satisfied
-411.8	-21542.1	-944.4	-362.1	291.3	-0.02	0.01	Satisfied
-420.6	-15710.3	-964.9	-274.4	202.1	-0.01	0.01	Satisfied
-429.4	-10998.4	-985.4	-203.7	129.8	-0.01	0.01	Satisfied
-438.2	-7313.4	-1005.9	-148.6	73.2	-0.01	0	Satisfied
-447.1	-4545.3	-1026.5	-107.4	30.5	-0.01	0	Satisfied
-455.9	-2572.1	-1047	-78.2	-0.2	0	0	Satisfied
-464.7	-1264.6	-1067.6	-59.2	-20.8	0	0	Satisfied
-473.5	-489.5	-1088.2	-48.2	-33.4	0	0	Satisfied
-482.4	-111.3	-1108.8	-43.2	-39.9	0	0	Satisfied
-491.2	6.3	-1129.4	-42.4	-42.2	0	0	Satisfied
-500	0	-1150	-43.1	-43.1	0	0	Satisfied

Table 5.30 SLV Approach - verification state phase 2

Check the verification with VCASLU software

Verifica C.A. S.L.U. - File

File Materiali Opzioni Visualizza Progetto Sez. Rett. Sismica Normativa: NTC 2008 ?

Titolo : _____

Sezione circolare cava

Raggio esterno: 14 [cm]
 Raggio interno: 11.4 [cm]
 N° barre uguali: 45
 Diametro barre: .8 [cm]
 Copriferro (baric.): 2.6 [cm]

N° barre: 0 Zoom

Tipo Sezione

Rettan.re Trapezi
 a T Circolare
 Rettangoli Coord.

Sollecitazioni

S.L.U. Metodo n

N_{Ed}: 5.16 0 kN
 M_{xEd}: 12.14 0 kNm
 M_{yEd}: 0 0

P.to applicazione N

Centro Baricentro cls
 Coord.[cm] xN: 0 yN: 0

Tipo rottura

Lato calcestruzzo - Acciaio snervato

Metodo di calcolo

S.L.U.+ S.L.U.-
 Metodo n

Tipo flessione

Retta Deviata

Vertici: 52 N° rett.: 100

Calcola MRd Dominio M-N

L₀: 0 cm Col. modello

Precompresso

Materiali

S355 C25/30

ε_{su}: 67.5 ‰ ε_{c2}: 2 ‰
 f_{yd}: 308.7 N/mm² ε_{cu}: 3.5 ‰
 E_s: 200,000 N/mm² f_{cd}: 14.17
 E_s/E_c: 15 f_{cc}/f_{cd}: 0.8
 ε_{syd}: 1.544 ‰ σ_{c,adm}: 9.75
 σ_{s,adm}: 235.3 N/mm² τ_{co}: 0.6
 τ_{c1}: 1.829

M_{xRd}: 58.7 kN m

σ_c: -14.17 N/mm²
 σ_s: 308.7 N/mm²
 ε_c: 3.5 ‰
 ε_s: 4.121 ‰
 d: 25.37 cm
 x: 11.65 x/d: 0.4592
 δ: 1

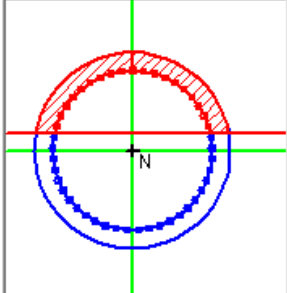


Figure 5.44 properties definitions

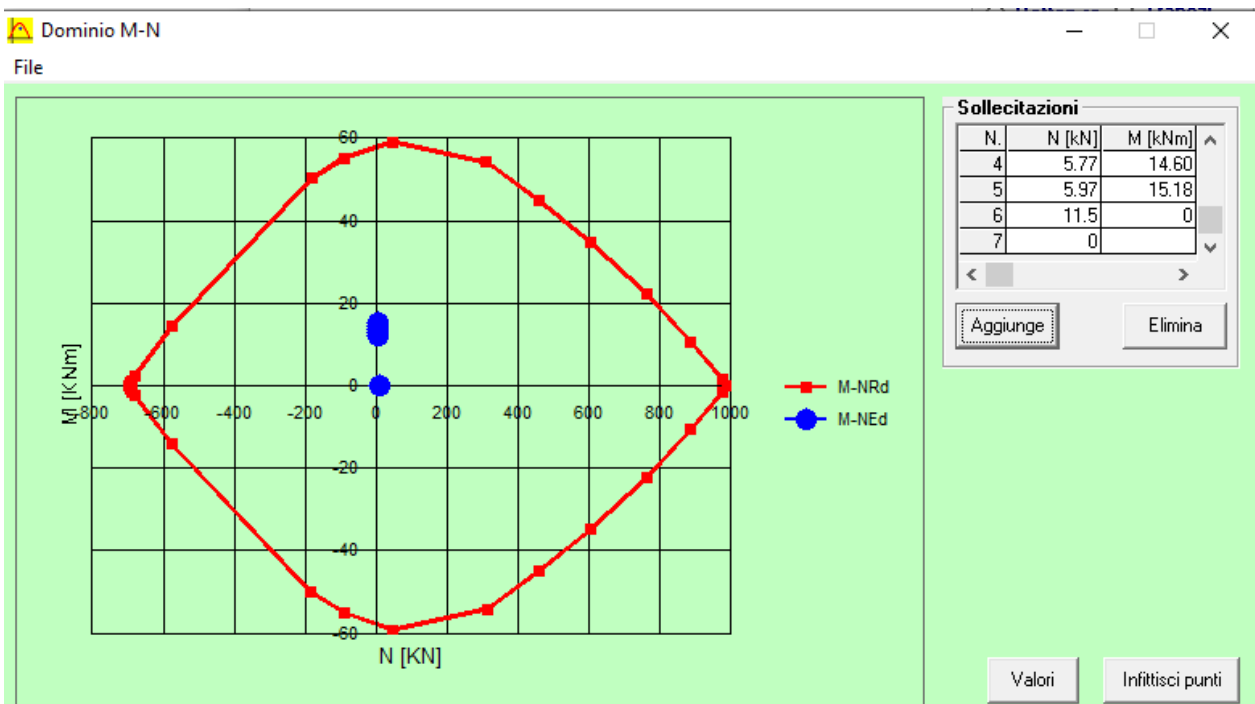


Figure 5.45 Interaction domain verification

5.6.2 GFRP micropile verification

Since all the analysis results don't depend on any of the structural components of the micropile, all the previously reported results of soil pressure, moment arm, internal actions and soil deformations are exactly the same. The verification as explained previously is the same as in the case of steel reinforced micropiles but using the properties of the GFRP. The verification is performed with the help of VCASLU software as a circular section under axial and flexural action.

The new cross section of the micropile is a circular section of a diameter of 190 mm reinforced with a GFRP tube of 160.00 mm with a thickness of 14.00 mm and a total length of 5.00 m. The chosen reinforcement element is a commercial item proposed by the ATP laboratory. The studied reinforcing element studied by ATP laboratory has the following properties as reported from the laboratory.



AZIENDA CON
SISTEMA DI GESTIONE QUALITÀ
CERTIFICATO DA DNV
ISO 9001



U n d e r g r o u n d & C i v i l W o r k s d i v i s i o n

SERIE COMMERCIALE MICROPALO IN GFRP 160/14

ϕ est (mm)	Spessore (mm)	Atubo (cm ²)	We (cm ³)	Je (cm ⁴)	E (kg/cm ²)	Peso (kg/ml)	EI (kg*cm ²)
160	14	64,21	216	1727	350000	12,8	6,0E+08

Caratteristiche Fisico-Meccaniche del Composito	
σ_{max} longitudinale a rottura (ASTM D 790)	600 MPa
τ_{max} a taglio a rottura (ASTM D 4475)	35 MPa
Modulo elastico longitudinale	35 GPa
Deformazione a rottura (ϵ_r)	1,7%
Massa volumetrica	> 1,8 gr/cm ³

Figure 5.46 GFRP reinforcement properties.

The verification follows the same order as done for the traditional steel reinforced micropile using the same obtained internal actions.

5.6.2.1 Material properties definition

The following material properties as previously mentioned are defined on the software VcasLU and will be used for all the following verifications.

Verifica C.A. S.L.U. - File: micropilesGFRP

File Materiali Opzioni Visualizza Progetto Sez. Rett. Sismica Normativa: NTC 2008 ?

TITOLO : _____

Sezione circolare cava

Raggio esterno: 19 [cm]
 Raggio interno: 0 [cm]
 N° barre uguali: 36
 Diametro barre: 1.4 [cm]
 Copriferro (baric.): 2 [cm]

N° barre: 0 Zoom

Sollecitazioni

S.L.U. Metodo n

N_{Ed}: 0 0 kN
 M_{xEd}: 0 0 kNm
 M_{yEd}: 0 0

P.to applicazione N

Centro Baricentro cls
 Coord.[cm] xN: 0 yN: 0

Tipo rottura

Lato calcestruzzo - Acciaio elastico

Metodo di calcolo

S.L.U.+ S.L.U.-
 Metodo n

Tipo flessione

Retta Deviata

Vertici: 52 N° rett.: 100

Calcola MRd Dominio M-N

L₀: 0 cm Col. modello

Precompresso

Materiali

GFRP C25/30

ε_{su}: 14.91 ‰ ε_{c2}: 2 ‰
 f_{yd}: 521.7 N/mm² ε_{cu}: 3.5 ‰
 E_s: 35,000 N/mm² f_{cd}: 14.17
 E_s/E_c: 20 f_{cc}/f_{cd}: 0.8
 ε_{syd}: 14.91 ‰ σ_{c,adm}: 9.75
 σ_{s,adm}: 300 N/mm² τ_{co}: 0.6
 τ_{c1}: 1.829

M_{xRd}: -122.5 kN m
 σ_c: -14.17 N/mm²
 σ_s: 228.4 N/mm²
 ε_c: 3.5 ‰
 ε_s: 6.525 ‰
 d: 36 cm
 x: 12.57 x/d: 0.3491
 δ: 0.8764

Figure 5.47 Material properties definition

5.6.2.2 GFRP Approach [1] combination

5.6.2.2.1 GFRP Approach [1] - phase (1) verification

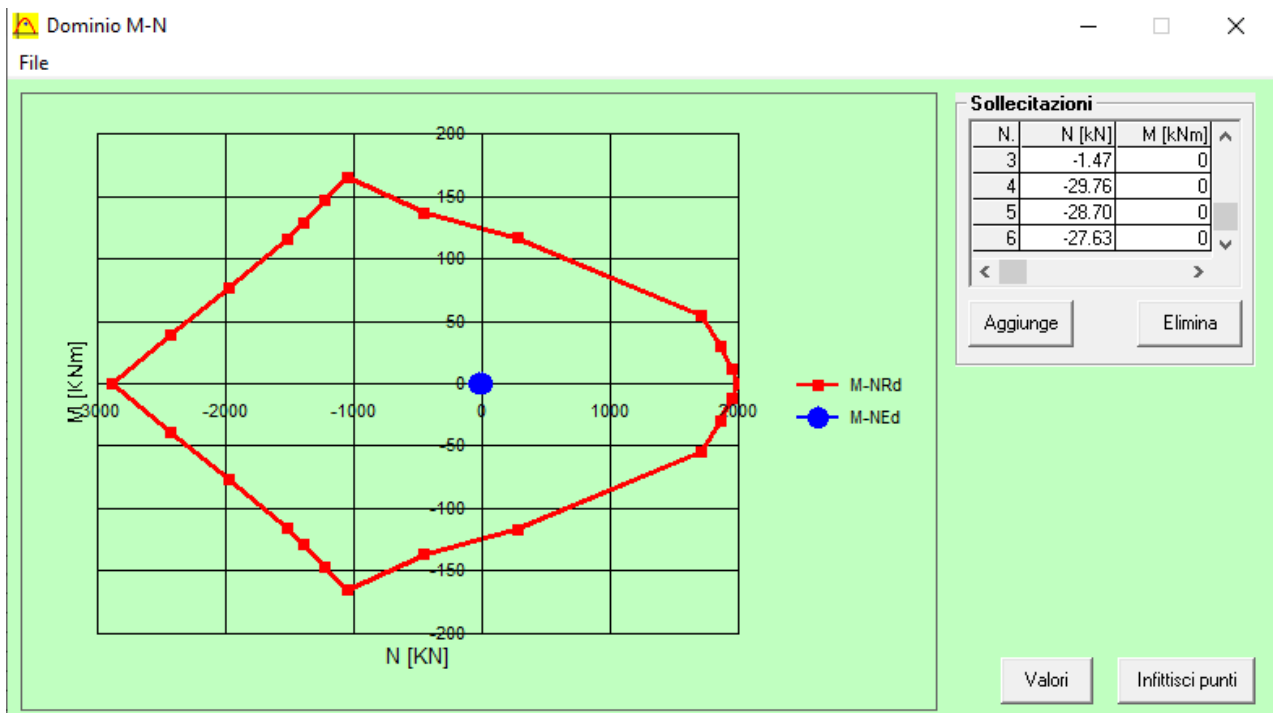


Figure 5.48 Interaction domain verification approach [1] - phase (1).

5.6.2.2.2 GFRP Approach [1] - phase (2) verification

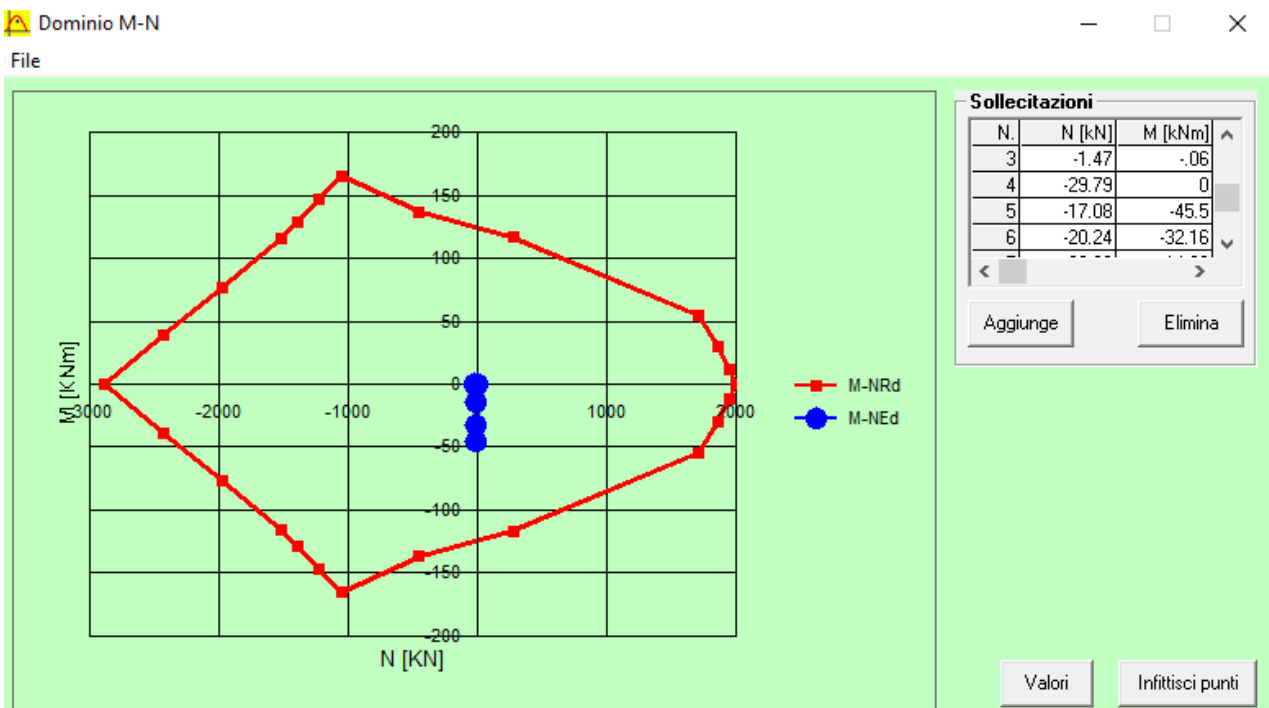


Figure 5.49 Interaction domain verification approach [1] - phase (2).

5.6.2.3 GFRP micropile approach [2] combination

5.6.2.3.1 GFRP approach [2] - phase (1) verification

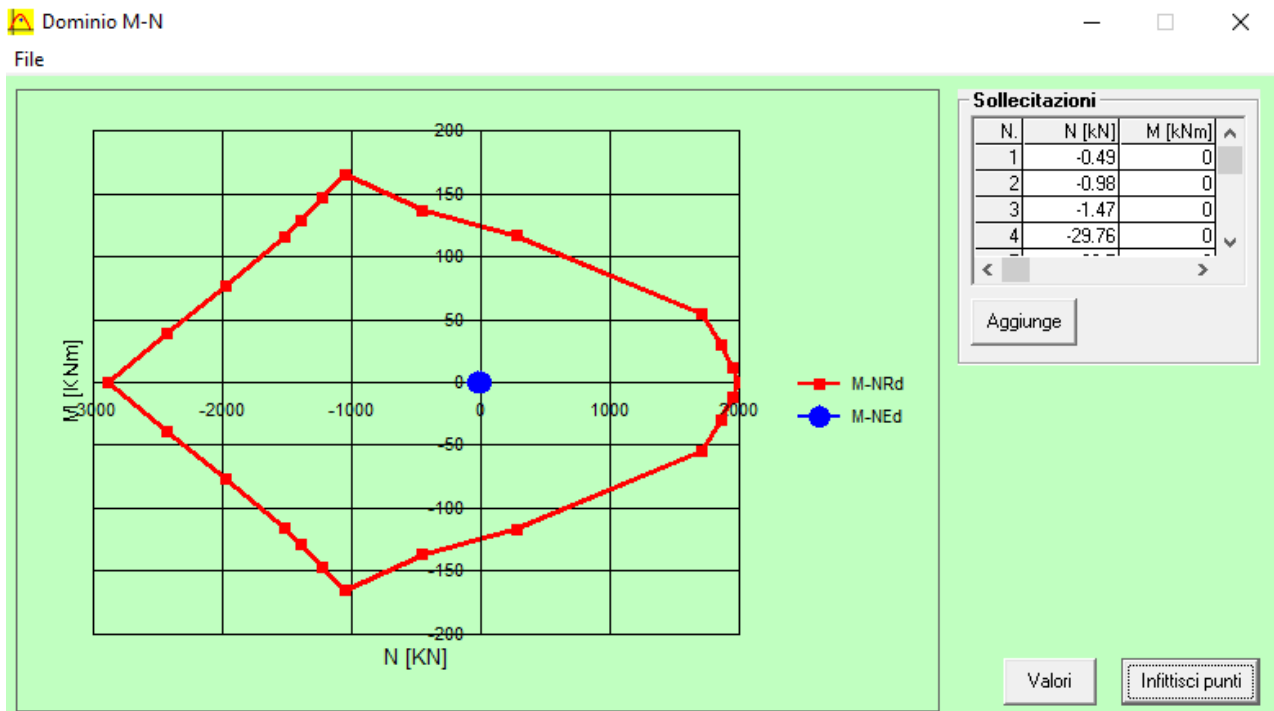


Figure 5.50 Interaction domain verification approach [2] - phase (1).

5.6.2.3.2 GFRP approach [2] - phase (2) verification

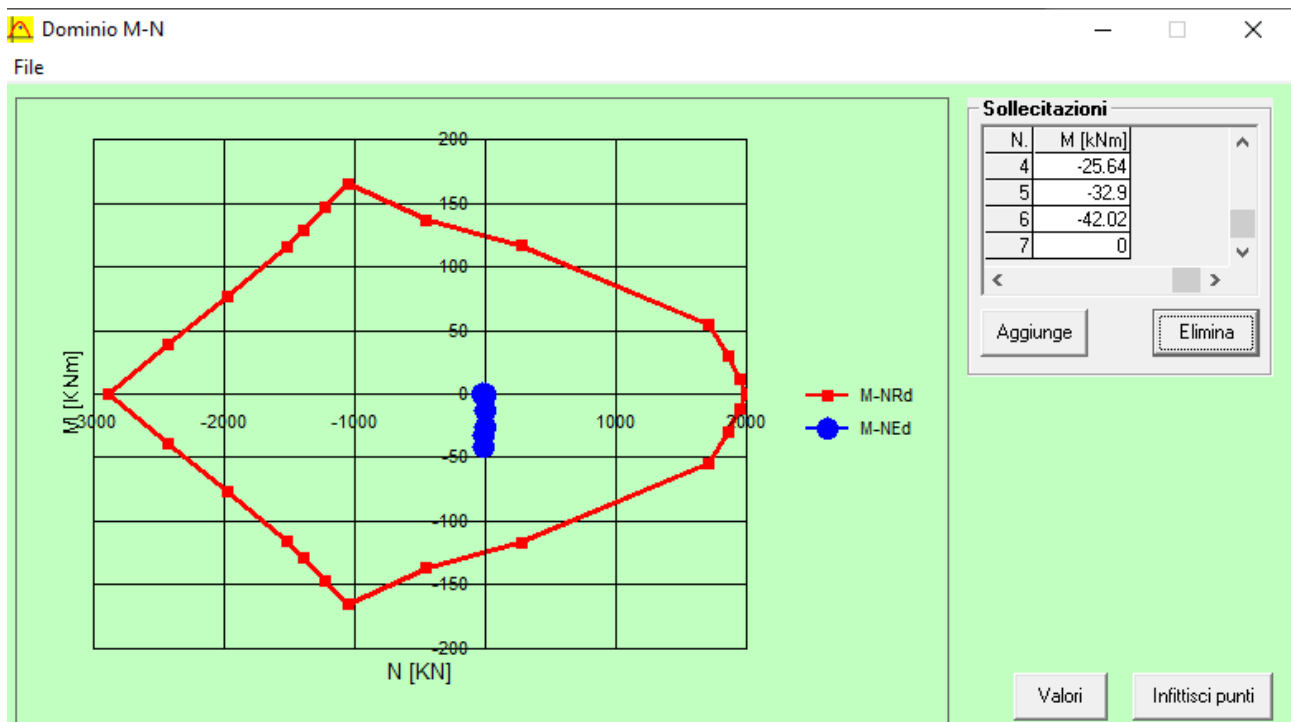


Figure 5.51 Interaction domain verification approach [2] - phase (2).

5.6.2.4 GFRP micropile SLV combination

5.6.2.4.1 GFRP SLV combination - phase (1) verification

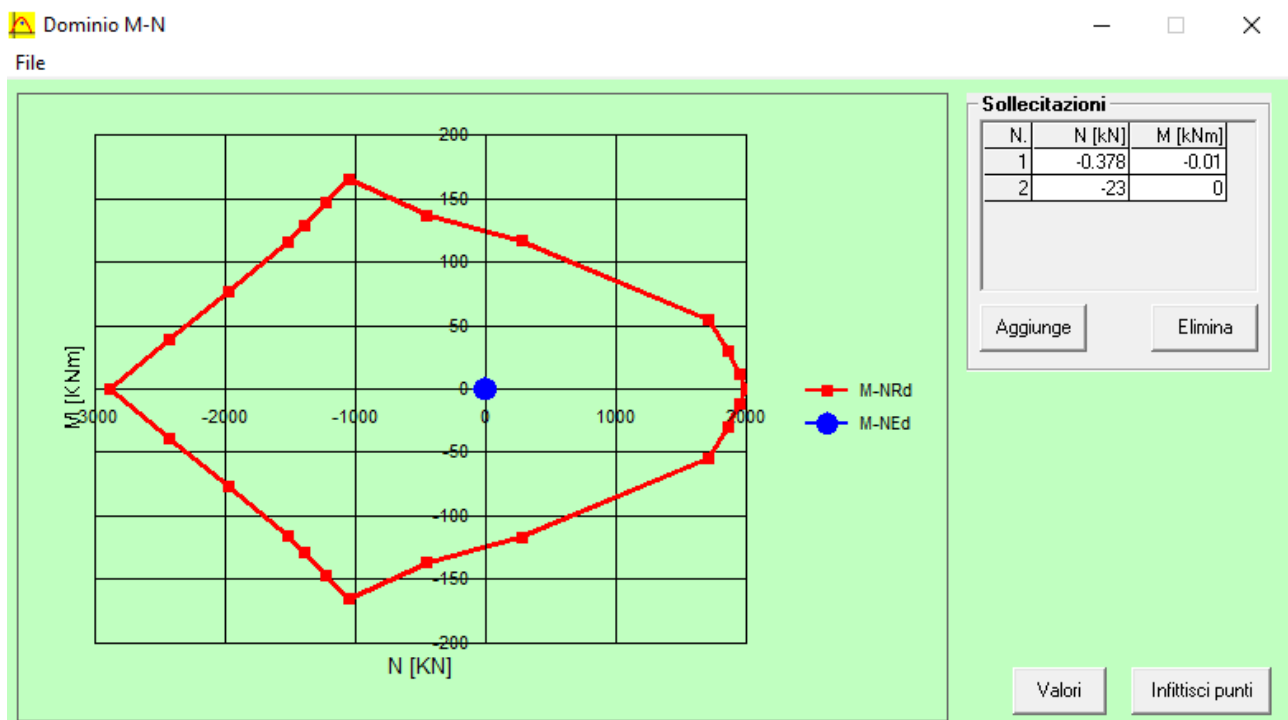


Figure 5.52 Interaction domain verification approach [SLV] - phase (1).

5.6.2.4.2 GFRP SLV combination - phase (2) verification

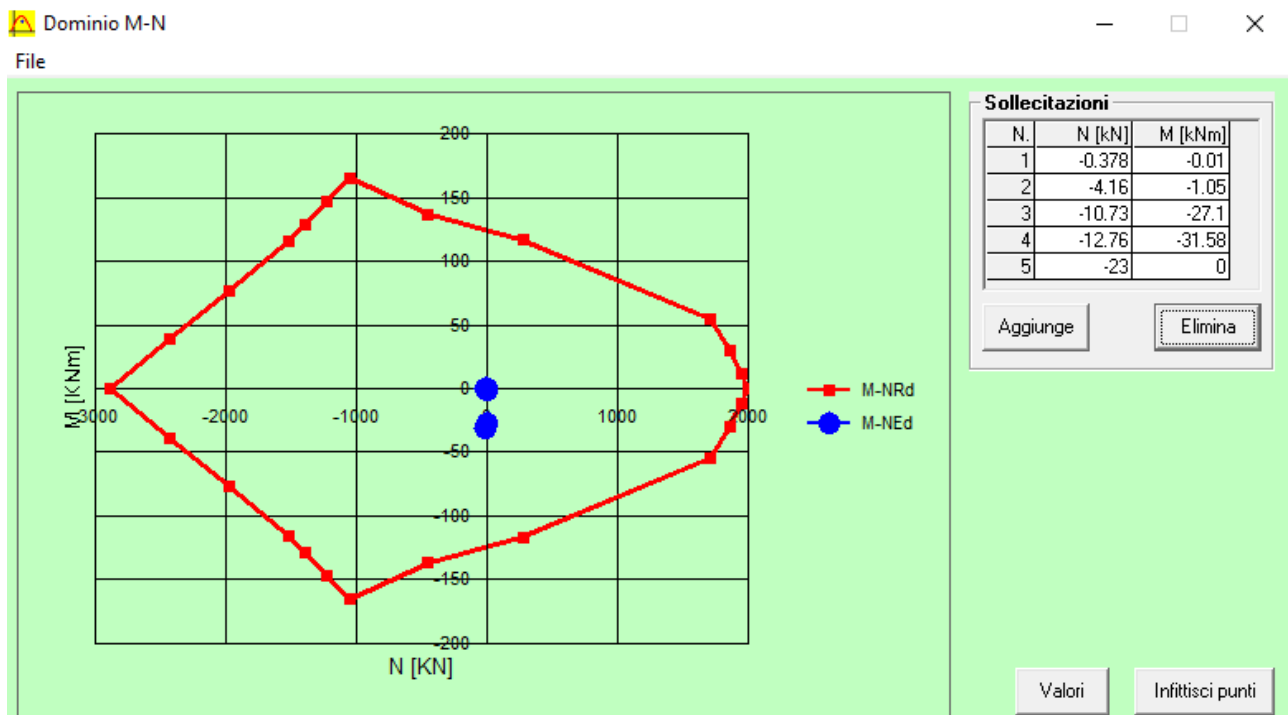


Figure 5.53 Interaction domain verification approach [SLV] - phase (2).

5.6.2.4.3 GFRP micropile verification summary

The verification considered the most extreme internal actions as seen and the verification situations are reported in the following table

Phase	Verification state
Approach [1]	
Phase (1)	Verified
Phase (2)	Verified
Approach [2]	
Phase (1)	Verified
Phase (2)	Verified
SLV approach	
Phase (1)	Verified
Phase (2)	Verified

Table 5.31 GFRP micropiles verification summary

5.7 Cost comparison:

The cost in construction industry as previously mentioned is one of the most important factors that control the whole industry. In the following paragraphs the cost is developed for a single micropile in order to evaluate the comparison between the two approaches. Since the two approaches of traditional micropiles and GFRP micropiles are almost identical at the level of construction, the develop of the cost will consider just the different activities between the two approaches. The only different activities in construction are the reinforcement activity and the concrete amount. The following cost estimation was done using the national costs published by the region of Piemonte.

Traditional steel micropile

Activity	Area [m ²]	Length [m]	γ [kg/m ³]	Total	Unit price [€]	Total price [€]
Code 01.P12.O00.005 Steel pipes type S355-EN10219 for cement injections (micropile reinforcement) [kg]	1.39x10 ⁻³	4.00	7850	43.646	1.99	86.86
Code 01.A03.B50.010 Execution of micropiles performed by drilling with special equipment through soils of any nature and consistency including cement injection up to a maximum of twice the theoretical volume, excluding the supply of tubular reinforcement to be evaluated separately. -With a diameter of 130-140 mm [m]	-	4	-	4	115.86	463.44
Total cost for each traditional micropile [€]						550.3

Table 5.32 Cost of traditional single micropile.

GFRP micropile

Activity	Area [m ²]	Length [m]	γ [kg/m ³]	Total	Unit price [€]	Total price [€]
Code 25.A01.B40.005 Fiberglass tube of a diameter of at least 65 mm for micropiles - tie rods [m]	-	4.00	-	4	16.96	67.84
Code 01.A03.B50.015 Execution of micropiles performed by drilling with special equipment through soils of any nature and consistency including cement injection up to a maximum of twice the theoretical volume, excluding the supply of tubular reinforcement to be evaluated separately. -With a diameter of 150-190 mm [m]	-	4	-	4	135.28	541.12
Total cost for each GFRP micropile [€]						608.96

Table 5.33 Cost of GFRP single micropile.

The previous tables report the cost of the main different activities of the two approaches, noting that the cost of in the case of GFRP is a bit higher than the cost of the traditional micropiles at the level of the material and construction because the diameter is a bit bigger to satisfy the safety levels and the commercial availability.

6. Chapter 6: Conclusion

The GFRP reinforcement is a valid acceptable alternative for steel reinforcement in all the fields generally and in the design of micropiles especially. Through the previous study we can notice that the design in both cases meets the safety standards paying attention to the differences between the two approaches. In the case of GFRP, the verification was satisfied applying a bit larger tube as reported in the following table:

	Traditional steel micropile	GFRP micropile
Micropile Diameter [mm]	140	190
Reinforcement diameter [mm]	114.3	160
Tube thickness [mm]	8	14

Economically, the two approaches of traditional micropiles and GFRP micropiles are almost identical in most of the activities except the previously mentioned activities that cause the differences in the cost as reported in the following table:

	Traditional steel micropile	GFRP micropile
<u>Cost of the activities</u>		
1- reinforcement	550.3 €	608.96 €
2- drilling and injection.		

The cost of the GFRP micropiles is a little higher than the traditional micropiles considering the materials as a result that the diameter for the same verification level is bigger. The previously mentioned cost did not consider the transportation cost which would be much lower in the case of GFRP because the weight is much lower than the steel weight. The previously mentioned cost also did not consider the protection cost of steel reinforcement which would cause a big difference in the cost of the traditional approach. Finally, the traditional approach would have the corrosion problem which was one of the main reasons of searching for alternatives for steel. We should as well pay attention that the commercial market of GFRP is not yet well established which means that there are few availabilities in diameter and thickness of the GFRP reinforcement tubes that may force to use an overestimated diameter or thickness. Once the market gets more availabilities, it is expected to perform the same work with lower cost.

The GFRP reinforcement is an acceptable alternative for steel reinforcement structurally and economically.

References

- Abd Elaziz and El Naggar, 2015; Long et al., (2004); Richards and Rothbauer, (2004).
Abdalla, (2002).
ACI 440.1R-06, AS/NZS 4673: 2001, fib (2007).
ACI Committee 440, (2006).
ACI222 (2001).
Bouguerra, Ahmed, El-Gamal, & Benmokrane, (2011).
D.M. 17/01/2018 .
Deitz, Harik, & Gesund, (1999).
Dulude, Hassan, Ahmed, & Benmokrane, (2013).
El-Gamal, El-Salakawy, & Benmokrane, (2007).
El-Ghandour, Pilakoutas, & Waldron, (2003).
Fam and Rizkalla, (2002).
Fardis and Khalili (1981).
FHWA. (1997).
FHWA-SA-97-070.
fib, (2007).
Fleming et al.(1992).
Guadagnini, Pilakoutas, & Waldron, (2003).
Hassan, Ahmed, & Benmokrane, (2013).
Katz, (1998).
Kocaoz, Samaranayake, & Nanni, (2005).
Masmoudi, Zaidi, & Gerard, (2005).
NTC2018.
Ospina, Alexander, & Cheng, (2003).
Piles and pile foundations by Carlo Viggiani, Alessandro Mandolini, Gianpiero Russo.
Prehistoric rubble mixes to Roman cement By Richard W. Steiger. Richard W. Steiger.
Publication-Article in E-Zbornik elektronički zbornik radova Građevinskog fakulteta · December 2019.
Renata Kotyniaa, D. S. (2017). Bond behavior of GRFP bars to concrete in beam test.
Robert, Cousin and Benmokrane . (2009).
Salgado 2008.
Section 8.16.2.3 of AASHTO. (2002).

Viggiani, C., Mandolini, A., & Russo, G . Piles and pile foundations.

Yost, Gross, & Dinehart, (2001).